論文 / 著書情報
Article / Book Information

題目(和文)	連鎖構造制御による脂肪族共重合ポリエステルの材料設計に関する研究
Title(English)	Study on material design of aliphatic copolyesters by regulation of sequential structure
著者(和文)	田端雄太
Author(English)	Yuta Tabata
出典(和文)	学位:博士（工学）, 学位授与機関:東京工業大学, 報告番号:甲第9825号, 授与年月日:2015年3月26日, 学位の種別:課程博士, 審査員:阿部　英喜,彌田　智一,原　亨和,柘植　丈治,福居　俊昭
Citation(English)	Degree:, Conferring organization: Tokyo Institute of Technology, Report number:甲第9825号, Conferred date:2015/3/26, Degree Type:Course doctor, Examiner:,,,,
学位種別(和文)	博士論文
Type(English)	Doctoral Thesis

Study on material design of aliphatic copolyesters by regulation of sequential structure

2015

Department of Innovative and Engineered Materials

Tokyo Institute of Technology

Yuta Tabata

Contents

Chapter 1

General introduction

1-1 Bio-based polymers

Polymers or polymer materials are high molecular weight compounds composed of repeating units linked to each other by covalent bonds.[1] Over many years, films and tensile made from synthetic polymers, such as nylon, polyester, and polyolefin have been used in the fields of packaging, agriculture, clothing, lubricants, medicine, and other areas as plastics. Production of plastics derived from fossil resources has resulted in the increase of the concentration of CO_2 in atmosphere. Furthermore, huge consumption of the plastics results in the declining amounts of fossil fuels which are limited resources. Consequently, many research interests have then focused on environmentally friendly functional substances, which are one of the sustainable paradigms and benefit society, not only impacting on people in our era, but also affecting next generation.

As one of possible solutions to these problems, bio-based polymers have attracted much social and industrial attention. The source of bio-based polymers is mainly CO_2 in the natural environment. It is stored in the living system of plants and microorganisms as an energy source. Thus, the use and diffusion of bio-based polymers have potential to be an alternative solution for CO_2 emission problem from the viewpoints of carbon neutral and CO_2 fixation. Bio-based polymers fundamentally originate from bio-based chemicals, which are renewable and sustainable resources.

As shown in Table 1-1, bio-based polymers are mainly classified into three groups; (i) aliphatic polyesters (poly(hydroxyalkanoates) (PHAs) such as poly(L-lactate), poly[(*R*)-3-hydroxybutyrate] etc), (ii) plant polysaccharides (cellulose, starch, chitin, chitosan, etc), (iii) animal proteins (polypeptide, gelatin, etc).[2]

Table 1-1. Chemical structure, origin, and application of typical bio-based polymer

chemical structures	origins and methods	applications (field)
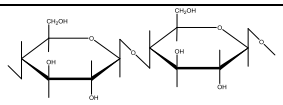 cellulose	・plants ・microorganisms (Acetobacta aceti)	fiber, filter, additive, film, coating, etc (food, construction, papermaking, etc)
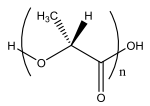 poly(L-Lactate);PLA	・condensation ・ring-opening polymerization	fiber, film, seetcasting, etc. (agriculture, medical, etc)
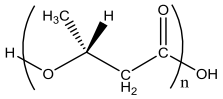 poly[(*R*)-3-hydroxybuytrate]; P[(*R*)-3HB]	・microorganisms(Ralstonia eutropha,Aeromonas caviae, etc) ・polycondensation ・ring-opening polymerization	suture, fiber, film, etc. (healthcare, food, agriculture, etc)
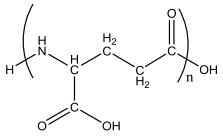 P(γ-glutamate)	・microorganisms (bacillus natto)	moisturizer, additives, etc (cosmetic, healthcare, food, etc)

Among them, aliphatic polyesters are extensively studied on the relationship between structure, morphology, properties, and biodegrabilities. Nowadays, plastic manufacturers are allured by the usefulness of bio-based polyesters since they are made from the renewable plant resources as bio-based plastic. In order to fulfill the demands in practical and specialized applications, the research on synthesis of bio-based polyesters has been established to obtain high-performance and specific functional bio-based plastic materials. Thus, to achieve this target, the present thesis has focused on construct the methodology of molecular design for bio-based plastics to predict their properties and functions, and new technology of efficient and precise bio-based plastic synthesis.

1-2 Characteristics of poly(hydroxyalkanoates) (PHAs)

Poly(hydroxyalkanoates) (PHAs) are linear aliphatic polyesters composed of hydroxyalkanoate monomer in which the carboxy group and the hydroxyl group of two monomers form an ester bond. Because of the rapid decline amounts of fossil fuels and growing concerns relating to incinerator emissions (e.g. dioxin), PHAs are attracting much social and industrial attention to be used for solving the environmental problems.

In addition, PHAs as a family of aliphatic polyesters are biodegradable, but most aromatic polyesters are not. The explanation proposed for this is that aliphatic polyesters are flexible enough to fit into the active site of the enzymes, whereas aromatic polyesters are too rigid to permit such a fit.[3] Aliphatic polyesters such as PHAs, which have structure and functional groups similar to those of natural organic materials, are expected to be degraded nonspecifically by some enzymes, such as lipase.[4] In this section, synthesis, structures, physical properties, crystallization, and comonomer sequence distribution, PHAs such as polymer of α- and β-hydroxyalkanoates are mainly described.

1-2-1 Classification of PHAs

PHAs can be classified into three groups according to type of monomers. They are classified into, α-, β-, ω-hydroxyalkanoates with respect to the bonding position of the OH groups from the COOH end groups. Three type of PHAs are listed in Table 1-2.

Table 1-2. Classification of PHAs

chemical structures		examples (trade mark)
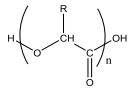	R = -H	Poly (glycolate) (PGA)
	R = $-CH_3$	Poly ($_L$-lactate) (PLLA)
poly (α-hydroxyalkanoate)		
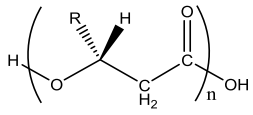	R = $-CH_3$	poly [(*R*)-3-hydroxybutyrate](P[(*R*)-3HB])
	R = $-CH_2-CH_3$	poly[(*R*)-3-hydroxybutyrate-*co*-(*R*)-hydroxyvalerate] (P[(*R*)-3HB-*co*-(*R*)-3HV])
poly (β-hydroxyalkanoate)	R = $-(CH_2)_2-CH_3$	poly[(*R*)-3-hydroxybutyrate-*co*-(*R*)-hydroxyhexanoate] (P[(*R*)-3HB-*co*-(*R*)-3HH])
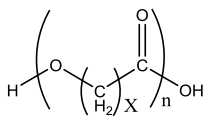	X = 3	poly (β-propiolactone) (PPL)
	X = 5	poly (ε-caprolactone) (PCL)
poly (ω-hydroxyalkanoate)		

1-2-1-1 Poly (*α*- hydroxyalkanoates)

Poly(*α*-hydroxyalkanoates) such as poly(glycolate) (PGA) (P (2-hydroxyacetate); P(2HA)) and poly (lactate) (PLA) (poly (2-hydroxypropionate); P(2HP)) are crystalline polymers with relatively high melting temperatures (see Table 1-3). PLA has been known since the 1920's as polyester for fibers.[5] Among them, PLA has been highlighted because of its availability from renewable resources such as corn. In 2010, NatureWorks was the primary producer of PLA, in US. In addition, their copolymers (PLGA), have been found rapidly increasing research interest. Because of their intrinsic biodegradability and bioassimilability, they are already used in a large range of applications from packaging and textile fibers to more sophisticated drug delivery systems, absorbable surgical fibers and stem cell scaffoldings.[6]

1-2-1-2 Poly (*β*-hydroxyalkanoate)s

Poly (*β*-hydroxyalkanoate)s such as poly[(*R*)-3-hydroxybutyrate] (P[(*R*)-3HB]) are synthesized by a wide variety of microorganisms as intracellular storage materials of carbon and energy. P[(*R*)-3HB] was discovered by the French scientist Lemoigne in 1926 from the bacterial species *Bacillus megaterium* as the inclusion bodies.[7] To meet a variety of demands for the usage of P[(*R*)-3HB] materials in a wide range of application fields, copolymerization of P[(*R*)-3HB] with other PHA monomer units has been attempted.

A copolymer of (*R*)-3HB and (*R*)-3-hydroxyvalerate ((*R*)-3HV) units, poly [(*R*)-3-hydroxybutyrate-*co*-(*R*)-3-hydroxyvalerate] (P[(*R*)-3HB-*co*-(*R*)-3HV]) is produced commercially using a fermentation process that employs glucose and propionate as carbon sources for *Ralstonia eutropha*, and was first marketed by ICI in UK. In addition, a copolymer of (*R*)-3HB and (*R*)-3-hydroxyhexanoate units (3HH), poly [(*R*)-3-hydroxybutyrate-*co*-(*R*)-3-hydroxyhexanoate] (P[(*R*)-3HB-*co*-(*R*)-3HH]) is also produced commercially using a fermentation process that employs plant oil as carbon sources for *Aeromonas caviae*, and was marketed by Kaneka in Japan. P[(*R*)-3HB-*co*-(*R*)-3HV] and P[(*R*)-3HB-*co*-(*R*)-3HH] are flexible and tough materials, while P[(*R*)-3HB] is brittle (see Table 1-3). These polymers of PHAs are can be degraded by the extracellular PHA depolymerases secreted by various microorganisms present in the natural environment.

1-2-1-3 Poly(ω-hydroxyalkanoate)s

Poly(*ω*-hydroxyalkanoate) such as poly(*ε*-caprolactone) (PCL) is prepared from the lactone of their cyclic ester monomer by a ring-opening polymerization.

High molecular weight PCL is a crystalline polymer with a moderately low T_m (60 °C), and is a tough and semi-rigid material at room temperature, having a mechanical properties between those of low- and high density polyethylenes. PCL has also been shown that it can be degraded by lipases secreted by microorganisms.

1-2-2 Synthesis of PHAs

PHAs are synthesized by chemical polymerization or bacterial fermentation. Current research activities in PHA synthesis are mainly focused on the high-molecular weight, high regularity, and/or copolymerization in order to obtain the polymer materials with desirable physical properties. They may be categorized into two groups on the basis of their occurrence or method of preparation as:

(1) Microbial synthesis of PHA

(2) Chemical synthesis of PHA

1-2-2-1 Microbial synthesis of PHAs

Microbial PHAs are energy and carbon storage materials, and accumulated intracellular by various microorganisms under unfavorable growth conditions in the presence of excess of carbon source. Of all known chiral PHAs, the hydroxyl-substituted carbon atom is always of the *R* configuration due to the stereospecificity of the polymerizing enzyme, PHA synthase.[8] Various studies have shown that unsaturated,[9] halogenated,[10] aromatic[11] and branched[12] monomers can be incorporated in PHAs. PHAs are synthesized by the PHA synthase(s) inside various microorganisms or plants when they encounter nutrient-limited condition.[13] Depending on species, carbon source, nutrients, and culture conditions, PHA polymers, with average molecular weight ranging from 200,000 to 3,000,000 g/mol,[14] can reach levels as high as 90 % of their cell dry mass.[15] Additionally, not only polyesters of β-hydroxyalkanoate, but variation of the position of the hydroxyl group is also possible, and accumulation of polymers containing γ-,[16] δ-[17] and ω-[18] hydroxyalkanoates have been reported. The structure of PHAs derived from short chain length (3-5 carbon atoms) and medium chain length (6-16 carbon atoms) hydroxyalkanoate can be depicted.

PHAs are accumulated in the cells as intracellular storage materials, also referred to as discrete granule 0.2-0.6 μm in diameter (see illustrated Figure 1-1).[19] The hydrophobic inclusions, suspended in cell cytoplasm, contain about 5-10 wt% of water and are largely in amorphous state.[20] Each granule is surrounded by a phospholipid monolayer membrane in which proteins including PHA synthase and

depolymerase are located.[21] The membrane also contains other proteins (phasins) that are presumed to be involved in stabilization of the amorphous granules. To date, more than 300 different microorganisms are known to synthesize PHAs, exhibiting diversity in monomer size, polymer length, co-polymer composition and molecular weight, which depends on the species type and the growth conditions.[22] Among them, only a few bacteria have been employed for the production because they can be cultivated efficiently to high cell densities with high PHA content in a relatively short period of time.

Recently, Taguchi's group succeeded in construction of biosynthetic system of copolymers consisting of (*R*)-lactate ((*R*)-2-hydroxypropionate; 2HP) and (*R*)-3HB units (P[(*R*)-3HB-*co*-(*R*)-2HP]), and the copolymers with a wide range of composition have been produced.[23] Among the microbial PHAs containing (*R*)-3HB units, P[(*R*)-3HB-*co*-(*R*)-2HP] copolymers are quite interesting due to their glass transition temperatures ranging from below room temperature to above body temperature. By applying the relaxation phenomenon of glass-transition, it is expected that the P[(*R*)-3HB-*co*-(*R*)-2HP] copolymers have a potential to be an intelligent material, e.g., matrixes for controlled release of drug or fertilizer in response to temperature.

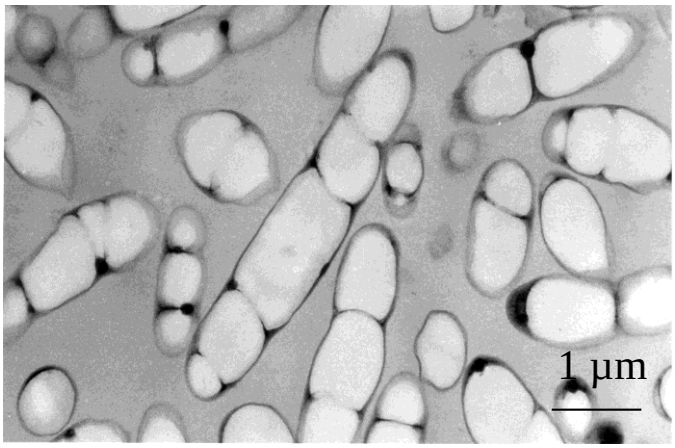

Figure 1-1. Transmission electron micrograph of thin section of recombinant *Ralstonia eutropha* cells accumulated PHA. Bar represents 1 μm.[19]

1-2-2-2 Chemical synthesis of PHAs

There are two routes by which PHAs may be manufactured from the α- and β-hydroxyalkanoate monomers.

The first route is direct condensation polymerization.[24] The molecular weight of polymer have obtained by this method was low about 50,000 g/mol due to equilibrium reaction.[25] In addition, it was known that this reaction included side reactions such as backbiting.

The second route is by ring-opening polymerization (ROP) of cyclic esters intermediate as lactones. Homopolymers and copolymers of *α*-hydroxyalkanoates, such as PGA and LA are prepared by ROP of their cyclic dimmers, glycolide (GA) and lactide (LA), respectively. On the other hand, homopolymer of *β*-hydroxyalkanoate, such as 3-hydroxybutyrate are prepared by ROP of their cyclic monomer of *β*-butyrolactone (BL). These reactions are generally carried out in bulk or in solution (THF, dioxane, toluene, etc), and most of lactones polymerize on room temperature or on heating in the presence of a catalyst.[26] ROP can be performed with various initiators to form high-molecular weight products (>100,000 g/mol). Many organometallic compounds, such oxides, carboxylates, and alkoxides, are effective initiators for the controlled polyester synthesis in ROP of lactones.[27] The highest yields and molecular weights have been obtained mainly by the anionic and coordinative ROP.

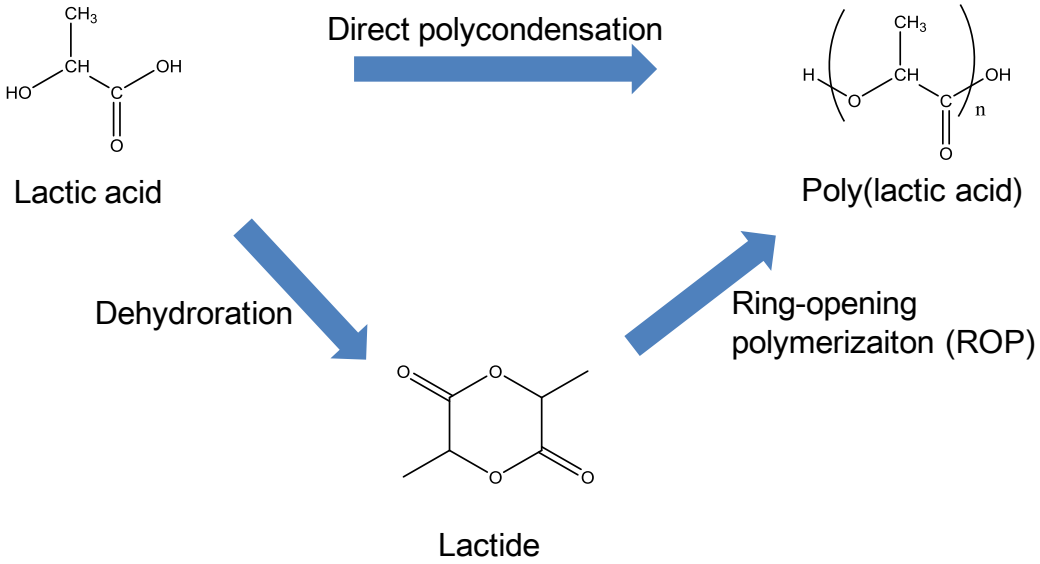

Figure 1-2. Schematic representation of polycondensation and dehydration of lactate, synthesis and ring-opening polymerization of lactide.

Effective initiators for anionic ROP of lactones include alkali metals, alkali metal alkoxides, etc. These polymerizations may proceed by living or non-living

mechanisms, depending on the reaction conditions, type of initiators and monomers. Chain propagation takes place by acyl-oxygen bond scission which leads to the formation of alkoxide end-groups. In order to obtain the high-molecular weight and/or high regularity products, side reactions, such as backbiting, alkyl-oxygen cleavage, intra- and inter-molecule transesterification, should be obviated.

Zn, Sn, and Al compounds, especially their alkoxides, have been generated much interest because of the versatility as initiator.[28] These polymerizations of lactones proceed according to a "coordination-insertion" mechanism, which involves the acryl-oxygen bond cleavage of monomer and insert on into the metal-oxygen bond. Transesterification reaction may also take place at elevated temperatures. These catalysts leading to coordinative ROP can produce the polyesters with narrow molecular weight distribution and/or high regularity (e.g., stereoregularity) by designing their ligands.

1-2-3 Physical properties and crystal structure of PHAs

The properties of PHAs can be tailor-made by blending, copolymerization, and molding process, or by a change in the macromolecular architecture (e.g. dendrimers, star-shaped, hyper-branched polymer). Table 1-3 lists the physical properties of various PHAs.

1-2-3-1 Poly(lactate) (PLA)

The melting temperature (T_m) and glass transition temperature (T_g) of PLLA homopolymers are 180 and 60 °C, respectively (see Table 1-3). The T_m becomes lower with decreasing crystallizable L- or D-lactyl unit sequence length in the LA homopolymers and copolymers, which can be caused by lowering the polymer molecular weight[29] and increasing the comonomer content.[30] The T_g of LA stereocopolymers is almost constant at about 60 °C, irrespective of L-lactide content, while the T_g of LA copolymers excluding stereocopolymers varies depending on the comonomer nature, its fraction, and the length of respective monomer sequences.[31] In addition, by blending PLLA and PDLA, stereocomplex PLA (Sc-PLA) formed, which had high thermal stability compared with homopolymers. The T_m and T_g of Sc-PLA are 230 and 72 °C, respectively.[32]

Depending on preparation condition, PLLA crystallizes in three forms (α, β, and γ). The stable α-form exhibits a well-defined diffraction pattern. The conformation is a helix characterized by ten monomer units in three turns. The α-form of PLLA has a pseudo-orthorhombic unit cell. The unit cell has the following

dimensions: a = 1.070 nm, b = 0.595 nm, c = 2.780 nm.[33] The β-form can be prepared at high draw ratio and high drawing temperature. The chain conformation is a left-handed three-fold helix. The β-form of PLLA has an orthomobic unit cell containg a 3_1 (3Å rise/1 monomeric unit) polymeric helix. The unit cell has the following dimensions: a = 1.031 nm, b = 1.821 nm, c = 0.900 nm.[34] The γ-form, found by epitaxial crystallization, contains two antiparallel s(3/2) helices in the orthorhombic unit cell (a = 0.995 nm, b = 0.625 nm, c = 0.880 nm.) and it assumes the known three-fold helix of PLA.[35]

1-2-3-2 P[(*R*)-3-hydroxybutyrate] (P[(*R*)-3HB])

P[(*R*)-3HB] has relatively high thermal stability but very stiff and brittle due to the high isotactic stereoregularity. P[(*R*)-3HB] has a glass transition temperature of 4 C and a high melting temperature around 180 °C. The melting temperature is closed the thermal degradation, which limiting the potential use of this homopolymer. Therefore, P[(*R*)-3HB] hasn't been considered to be well-suited for certain application as a commercial plastic. However, very strong fibers and films have been obtained by using drawing techniques (e.g. cold- and two-step drawing).[36] From the results of the regulation for working process, these characteristics of P[(*R*)-3HB], brittleness and stiffness, nowadays are not considered as defects for applications.

The crystal structure of P[(*R*)-3HB] has been determined using X-ray and computational analyses. The unit cell of P[(*R*)-3HB] is orthorhombic, $P2_12_12_1$, with a = 0.576 nm, b = 1.320 nm and c (fiber axis) = 0.596 nm, and two molecules of P[(*R*)-3HB] pass through the unit cell.[37] The conformation of the P[(*R*)-3HB] molecule has a compact, left-handed 2_1 helix with a two-fold screw axis.

Table 1-3. Thermal and mechanical properties of PHAs.

material	thermal properties		mechanical properties		
	T_g[a] (°C)	T_m[b] (°C)	young's modulus (GPa)	tensile strength (MPa)	elongation at break (%)
PGA	40	225-230	13.7	980	40
PLA	60	180	9.8	2200	20
Sc-PLA	65-72	220-230	8.6	880	30
P[(*R*)-3HB]	4	180	18.1	1320	35
P[(*R*)-3HB-*co*-7 mol%(*R*)-3HV]	-4	143	8.0	1065	40
P[(*R*)-3HB-*co*-10 mol%(*R*)-3HH]	-1	127		21	400
PCL	-60	60	-	780	120

[a] Glass transition temperature. [b] Melting temperature.

1-2-4 Sequential structure of copolymers

It has been reported that the bacterially produced PHA copolymers have broad distributions in randomness, resulting from various factors controlled by changing bacterial strains, carbon substrates, pH, in the fermentation medium, and so on during the cultivation. The sequence distribution of P[(*R*)-3HB-*co*-(*R*)-3HV] has been analyzed using ^{13}C-NMR spectroscopy. In the ^{13}C-NMR spectrum of P[(*R*)-3HB-*co*-(*R*)-3HV], the resonances are split into several peaks, which reflect comonomer sequence effects. Sequence distributions depending on diad and 3HV-centered triad were estimated.[38] Early studies on the sequence distribution indicated that the samples isolated from *R. eutropha* were random copolymers whose comonomer sequence distributions obeyed Bernoullian statistics.[39] However, Kamiya et al. performed the similar NMR analysis and reported that some P[(*R*)-3HB-*co*-(*R*)-3HV] samples extracted from the same bacterium were "blocky" copolymers, which contained more (*R*)-3HB-(*R*)-3HB and (*R*)-3HV-(*R*)-3HV sequences than would be predicted from Bernoullian statistics.[40] In order to estimate the extent of the deviation from Bernoullian statistics, a parameter D or randomness defined as:

$$D = \frac{F_{BB} F_{VV}}{F_{BV} F_{VB}} \qquad (1)$$

where F_{XY} indicates the fractional population of XY diad sequence. The *D* value of statistical random copolymers is 1.0. Block and alternating copolymers have *D* values much larger than 1 and very close to 0, respectively. A detailed statistical analysis showed that the P[(*R*)-3HB-*co*-(*R*)-3HV] samples with large *D* values had the sequence distribution which followed the model of a mixture of two random copolymers.

Further, these samples exhibited two or more melting peaks on the differential scanning calorimetry (DSC) curve. Thus, the authors concluded that the samples with large *D* values are mixtures of random copolymers. Every copolymer is considered to be a kind of polymer blend by nature, that is, a copolymer material consists of molecules with more or less a range of comonomer compositions. The range of composition distribution in chemically synthesized copolymers is generally believed to be very narrow. In contrast, some microbially produced copolyesters have complex composition distributions such as extremely broad compositional distributions and the various physical properties are substantially related to their composition distributions.[41] Recently, several researches have been studied to confirm the occurrence of the mixtures of bacterially produced PHA copolymers and broad distributions of comonomer composition by performing the compositional fractionation of different PHA copolymer.[42]

1-3 Sequential structure of polymer

Bio-polymers (e.g. proteins and nucleic acids) are sequence-regulated macromolecules with various properties originating from their perfectly sequenced primary structures. Nature makes the best use of sequence control using less than thirty monomers to assemble hundreds of thousands of precise. However, this level of exactness, a one-to-one structure-property relationship is rarely found, and the sequence regulation of synthetic polymers has not been achieved. In order to address the need for more sophisticated materials, sequence control is one of the ultimate goals in polymer chemistry.[43]

1-3-1 Current polymerization techniques

The scarcities of sequence specific synthetic polymers are due to the scarcity of polymerization techniques that are permit to complete sequential control. While the sequential control peptides and polypeptides is reported, at the current level of the synthetic polymerization techniques (i.e. living radical polymerization (CRP) and ring-opening polymerization (ROP)) are very far apart.[44] The design of sequential structure remains either stereosequence of homopolymer or sequence controlled copolymer (Figure 1-3). However, advances in catalysis design and use of directing group have enabled the preparation of more complex sequential structure.

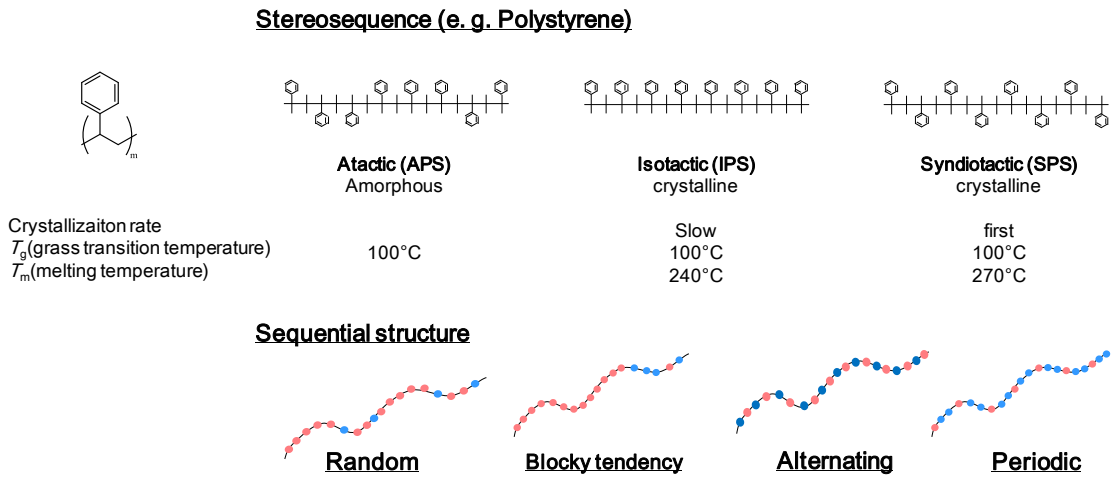

Figure 1-3. Type of stereosequence (e. g. polystyrene) and sequential structure.

Polymerization catalysts and catalyst design have advanced since the development of Ziegler-Natta catalysts.[45] The use of the Ru-based Grubbs catalysts has led to the development of sequence specific polymerization techniques of acyclic-diene metathesis (ADMET). Wagener et al. have developed the methodology

of aliphatic polymers with functional groups from α,ω-diolefins.[46] Grubbs et al. improved the methodology to generate alternating copolymers by incorporating a diacrylate moiety that slowly and irreversibly inserts into the olefinic polymer backbone.[47]

Some other polymerization technique has advanced due to design of catalyst in ROP. Recently, developments in coordination catalysts of ROP have made progress in control of stereosequence and regioselectivity. A large portion of study involves the preparations of stereosequence of PLA and P(3HB).[48] Coates et al. reported the isotactic, syndiotactic, and stereoblock PLA.[49] On the other hand, Carpentier et al. reported isotactic and syndiotactic P(3HB).[50] Recently, Coates et al. prepared the most complex stereosequence, an alternating syndiotactic P(3HB)[51]

The effect of catalysts on control of sequential structure reduces in radical polymerizations. In copolymerization of styrene with diphenylethylene[52] or maleic anhydride[53], the radical polymerizations were believed to be too fast to control except under specific conditions at first. Recent development of CRP techniques such as atom transfer radial polymerization (ATRP) and reversible addition-fragmentation transfer polymerization (RAFT) have slowed the polymerizations by shifting the equilibrium towards excess dormant but living chains.[54] These longer reaction times enable control of sequential structure by complex of directing groups.

It is known that the additive agent of Lewis acid to aid both stereo- and sequential structure controls in CRPs. Matyaszewski et al. reported that the 85 % isotactic stereosequences of Poly(dimethylacrylamide) were synthesized by both RAFT and ATRP using Y- and Yb- based Lewis acids.[55] Sawamoto et al. were able to be achieved 87 % isotactic stereosequences of poly(N-isopropylacrylamide) using a similar method.[56] Alternating architectural motifs of similarly reactive comonomers styrene and methylmethacrylate, were possible with the addition of diethylaluminium chloride.[57] Isobe et al. reported that predominately syndiotactic P(acrylates) was synthesized by both free radical and ATRP using bulky fluoroalcohol solvent.[58] Satoh et al. reported that predominately syndiotactic polymers were synthesized by RAFT using bulky side groups generated by hydrogen bonded moieties.[59]

Template-assisted polymerization techniques have been developed in an effort to assert complete sequential structure control.[60] Sawamoto et al. have created macroinitiator templates for chain-growth polymerizations.[61] These macroinitiators possess two polymerization sites: one for cationic polymerization and the second for radical polymerization. The ‘template’ copolymer was created by cationic polymerization followed by free radical polymerization of the sequenced copolymer.

The flaw in this method is that the 'template' copolymer has to be as complex as the desired sequenced copolymer. Avoiding the synthesis of a complex template, Datta et al. have modified DNA for the formation of sequenced polyaniline nanowires.[62]

1-3-2 Consequences of the sequential structure

The advantage of synthetic polymerization techniques such as CRP is the preparation of well-defined sequential structure such as di- and multiblock copolymers. The diblock copolymers by covalently linking different block types that would normally disassociate when blended, i.e. hydrophilic with hydrophobic and hard with soft, can generate organized macrostructures such as spherical, rod and lamellar.[63] RAFT and ATRP are tolerant to many monomer types and functional groups facilitating chemically active surfaces and stimuli responsive copolymer systems. ADMET polymerization as well, has been utilized to determine the effect of sequence length and substitution pattern on lamellar packing and crystal thickness in polyethylene and polypropylene.[64]

In order to synthetize polymers with more complex sequential structure and functions, similar to those found in nature, methodologies are need. The spider silk is protein fibers spun by spiders. The combination of stereo- and sequence-complexity of spider silk far exceeds the emerging technology of human work. Spider silk, a segmented natural material with hard β-sheet and soft α-helix segments, is tougher than many man-made materials including steel.[65]

1-4 Purpose of this thesis

Bio-based polyesters have attracted industrial attention and as environmentally friendly polymeric materials to be used for a wide range of applications to date. In order to fulfill the demands in practical and specialized applications, the research on synthesis of bio-polyesters has been established to obtain high-performance and specific functional bio-plastic materials. Thus, to achieve this target, the present thesis has focused on construct the methodology of molecular design for bio-plastics to predict their properties and functions, and efficient and precise bio-plastic synthesis technology.

Compared to chemical synthesized PHAs, biological PHAs has advantage of high molecular weight. However, it has been reported that the bacterially produced PHA copolymers have broad distributions in randomness, resulting from various factors controlled by changing bacterial strains, carbon substrates, pH, in the fermentation medium, and so on during the cultivation. On the other hand, it was reported that the obtained copolymers had a statistically random distribution of (*R*)-3HB unit and dimeric units of (*R*)-2HP since the (*R*)-2HP comonomers were inserted as in units of lactide into

the polymer chains. Chemosynthesis method can be used to make sequentical control polymer.

It has been suggested that the properties of polymers were influenced by sequential structure. Although, the relationships between sequential structure and properties has not been completely explained yet. It's important to explaining the relationships between sequential structure and properties, which can construct the methodology of molecular design for PHAs to predict their properties and functions, and new properties of PHAs.

This thesis, focused on the structure and physical properties of copolymers of 3-hydroxybutyrate (3HB) and lactate (2-hydroxypropionate: 2HP) units. The structure and physical properties of random, block tendency, and alternating were characterized. The relationships among the molecular structure, thermal property, crystalline structure and sequential structure in copolymers were investigated.

In Chapter 2, copolymers of (*R*)-3HB and (*R*)-2HP units ([(*R*)-3HB-*co*-(*R*)-2HP]) were synthesized by polycondensation reaction from methyl esters of (*R*)-3HB and (*R*)-2HP in the presence of titanium-based catalyst. Mixing of two monomers from the beginning of polymerization yielded random copolymers of (*R*)-3HB and (*R*)-2HP units. On the other hand, by controlling the time of mixing of two monomers, copolymers with blocking tendency were obtained. According to the results of physical properties of copolymer samples, the relationship between the compositional and sequential structure and the physical properties of copolymers are discussed.

In Chapter 3, alternating copolymers of (*R*)-3HB and 2HP were synthesized by the polycondensation reaction of pre-prepared dimeric monomers, (*R*)-3HB-(*R*)-2HP and (*R*)-3HB-(*S*)-2HP, in the presence of condensation agent. In contrast to random copolymers of (*R*)-3HB and 2HP units, the repeating sequence of alternately connected (*R*)-3HB and 2HP units formed crystalline region. The crystalline structure and thermal properties was different from each other between the alternating copolymers obtained from two types of stereoisomeric macromonomers. On the basis of the results of physical properties of alternating copolymer samples, the relationship between the stereocompositional and sequential structure and the properties of copolymers are discussed.

In Chapter 4, by means of transmission electron microscopy (TEM) and X-ray diffraction, crystalline structure of the alternating copolymer is examined. From the obtained results, the molecular conformation of alternating copolymer and the molecular packing arrangements with the unit cell are discussed.

Finally, results and knowledge obtained in the former chapters are summarized in Chapter 5.

Reference

[1] Sperling, L. H. *Introduction to Physical polymer Science* 4th Edition, John Wiley & Sons, Inc. **2006**.

[2] MacGregor, E. A.; Greenwood. C. T. *Polymer in nature*, John Wiley & Sons, Inc. **1980**, 391-397.

[3] (a) Potts, J. E.; Clendinnings, R.V.; Ackart, W. B.; Niegisch, W. D. *Polym Sci. Technol.* **1973**, 3, 61-79. (b) Diamond, M. J.; Freesman, B.; Galibaldi, J. A. *Int. Biodetn. Bull.* **1975**, 11, 127-132. (c) Fields, R. D.; Rodrigues, F.; Finn, R. K. J. *Appl. Polym. Sci.* **1974**, 18, 3571-3579. (d) Tokiwa, Y.; Suzuki, T. *J. Appl. Polym. Sci.* **1981**, 26, 441-448.

[4] Tokiwa, Y.; Suzuki, T. *Nature* **1977**, 270, 76-78.

[5] Auras, R.; Lim, L. K.; Selke, S. EK, Tsuji, H. *Poly(Lactic acid): Synthesis, Structures, Properties, Processingm and Applications.* John Wiley & Sons, Inc. **2010**.

[6] (a) Chiellini, E.; Solaro, R. *Adv. Mater.* **1996**, 29, 1375-1381. (b) Albertsson, A.-C.; Varma, I. K. *Biomacromolecules* **2003**, 4, 1466-1486. (c) Dechy-Cabaret, O.; Martin-Vaca, B.; Bourissou, D. *Chem. Rev.* **2004**, 104, 6147-6176. (d) Anderson AJ. Dawes EA. *Microbiol Rev* **1990**, 54, 450-472.

[7] Lemoigne, M. *Bull Soc. Chem. Biol.* **1926**, 8, 770-782.

[8] Griebel, R.; Smith, Z.; Merrick, J. M. *Biochemistry* **1968**, *7*, 3676-3681.

[9] Fritzsche, K.; Lenz, R. W.; Fuller, R. C. *Int. J. Biol. Macromol.* **1990**, *12*, 92-101.

[10] (a) Abe, C.; Taima, Y.; Nakamura, Y.; Doi, Y. *Polym. Commun.* **1990**, *31*, 404-406. (b) Doi, Y.; Abe, C. *Macromolecules* **1990**, 23, *15*, 3705-3707.

[11] (a) Kim, Y. B., Lenz, R. W.; Fuller, R. C. *Macromolecules* **1991**, *24*, 5256-5260. (b) Curley, J. M.; Hazer, B.; Lenz R. W.; Fuller, R. C. *Macromolecules* **1996**, *29*, 1762-1766.

[12] (a) Choi, M. H.; Yoon, S. C. *Appl. Environ. Microbiol.* **1994**, *60*, 3245-3254. (b) Hazer, B.; Lenz, R. W.; Fuller, R. C. *Macromolecules* **1994**, 27, 45-49.

[13] (a) Doi, Y. Microbial Polyesters; VCH Publishers; New York, **1990**. (b) Anderson, A. J.; Dawes, E. A. Microbiol. Rev. 1990, 54, 450-472.

[14] Byrom D. *ed. Plastics from microbes*, **1994**, 5-33.

[15] (a) Brandl, H.; Gross, R. A.; Lenz, R. W.; Fuller, R. C. *Appl. Environ. Microbiol.* **1988**, *54*, 1977-1982. (b) Lee S.Y. *Biotechnol. Bioeng.* **1996**, 49, 1-14. (c)

Steinbüchel, A.; Füchtenbusch B. *Trend. Biotech.* **1998**, 16, 419-427.

[16] (a) Kunioka, M.; Kawaguchi, Y.; Doi, Y. *Appl. Microbiol. Biotechnol.* **1989,** *30*, 569-573. (b) Valentin, H. E.; Schönebaum A.; and Steinbüchel, A. *Appl. Microbiol. Biotechnol.* **1992,** *36*, 507-514.

[17] Valentin, H. E.; Schönebaum A.; and Steinbüchel, A. *Appl. Microbiol. Biotechnol.* **1996,** *46*, 261-267.

[18] Eggink, G.; de Waard, P.; Huijberts, G. N. M. *Can. J. Microbiol.* **1995,** *41*, 14-21.

[19] Fuller, R. C. *Int. J. Biol. Macromol.* **1999**, *25*, 21-29.

[20] (a) De Koning, G. J. M.; Lemstra, P. J. *Polymer* **1992**, 33, *15*, 3292-3294. (b) McCool, G. J.; Fernandez, T.; Li, N.; Cannon, M. C. *FEMS Microbiol. Lett.* **1996**, *138*, 41-48.

[21] Stuart, E. S.; Tehrani, A.; Valentin, H. E.; Dennis, D.; Lenz, R. W.; Clinton Fuller, R. *J. Biotech.* **1998**, *64*, 137-144.

[22] (a) Steinbüchel, A.; Doi, Y. *Biotechnology of Biopolymers-From Synthesis to Patents*. Wiley-VCH: Weinheim, Germany, **2005**. (b) Lee, S. Y. *Nat. Biotechnol.* **2006,** 24, *10*, 1227-1229. (c) Steinbüchel, A.; Valentin, H. E. *FEMS Microbiol. Lett*. **1995**, *128*, 219-228. (d) Sudesh, K.; Abe, H.; Doi, Y. *Prog. Polym. Sci.* **2000**, *25*, 1503-1555.

[23] (a) Taguchi, S.; Yamada, M.; Matsumoto, K.; Tajima, K.; Satoh, Y.; Munekata, M.; Ohno, K.; Kohda, K.; Shimamura, T.; Kambe, H.; Obata, S. *Proc. Natl. Acad. Sci. U.S.A.* **2008**, 105, 17323-17327. (b) Yamada, M.; Matsumoto, K.; Nakai, T.; Taguchi, S. *Biomacromolecules* **2009**, 10, 677. (c) Yamada, M.; Matsumoto, K.; Shimizu, K.; Uramoto, S.; Nakai, T.; Shozui, F.; Taguchi, S. *Biomacromolecules* **2010**, 11, 815-819.

[24] Kim, S. H.; Kim, Y. H. *Macromol. Symp.* **1999**, 144, 277-287.

[25] Achmad, F.; Yamane, K.; Quan, S.; Kokugan, T. *Chem. Eng. J.* **2009**, 151, 342-350.

[26] Cerrai, P.; Tricoli, M.; Andruzzi, F.; Paci. M. *Polymer* **1989**, 30, 338-343.

[27] (a) Mecerreyes, D.; Jérome, R.; Dubois, P. *Adv Polym Sci* **1999**, 147, 1-59. (b) Mecerreyes, D.; Jérome, R. *Macromol. Chem. Phys.* **1999**, 200, 2581-2590. (c) Albertsson, A-C.; Varma, I.K. *Biomacromolecules* **2003**, 4, 1466-1486.

[28] (a) Kricheldorf, H. R.; Sumbel, M. V.; Kreiser-Saunders, I. *Macromolecules* **1991**, 24, 1944-1949. (b) Mecerreyes, D.; Miller, R. D.; Hedrick, J. L; Jerome, R. J. *Polym. Sci., Part A: Polym. Chem.* **2000**, 38, 870-875.

[29] Tsuji, H.; Ikada, Y. *Polymer* **1999**, 40, 6699-6708.

[30] Tsuji, H.; Ikada, Y. *Macromol. Chem. Phys* **1996**, 197, 3483-3499.

[31] Wada, R.; Hyon, S.-H.; Nakamura, T.; Ikada, Y.; *Pharm. Res.* **1991**, 8, 1292-1296.

[32] Tsuji. H.; Macromol. Biosci. **2005**, 5, 569-597.

[33] Desantis, P.; Kovacs, A. *J. Biopolymer* **1968**, 6, 299-306.

[34] Cartier, L.; Okihara, T.; Ikeda, Y.; Tsuji, H.; Puiggali, J.; Lotz, B. *Polymer* **2000**, 41, 8909-8919.

[35] Biopolymers, 4, Polyesters 3 Doi, Y.; Steinbuchel A. Eds.; Wiley-VCH: Weinheim, **2002**.

[36] (a) Iwata, T. *Macromol. Biosci.* **2005**, 5, 689-701. (b) Iwata, T.; Aoyagi, Y.; Fujita, M.; Yamane, H.; Doi, Y.; Suzuki, A. Takeuchi, A.; Uesugi, K. *Macromol. Rapid. Commun.* **2004**, 25, 1100-1104.

[37] (a) Okamura, K., Marchessault, R. H., *Conformation of Biopolymers*. In Ramachandran, G. N.; Ed, Academic Press: New York, **1967**; Vol. 2, p 709. (b) Cornitbert, J.; Marchessault, R. H. *J. Mol. Biol.* **1972**, *71*, 735-756. (c) Yokouchi, M.; Chatani, Y.; Tadokoro, H.; Teranishi, K.; Tani, H. *Polymer* **1973,** *14*, 267-272.

[38] (a) Bluhm, T. L.; Hamer, G. K.; Marchessault, R. H.; Fyfe, C. A.; Veregin, R. P. *Macromolecules* **1986**, *19*, 2871-2876. (b) Doi, Y.; Kunioka, M.; Nakamura, Y.; Soga, K. *Macromolecules* **1986**, 19, 2860-2864.

[39] Ballistreri, A.; Montaudo, G.; Garozzo, D.; Giuffrida, M.; Montaudo, M. S. *Macromolecules* **1991,** 24, 1231-1236.

[40] Kamiya, N.; Yamamoto, Y.; Inoue, Y.; Chujo, R.; Doi, Y. *Macromolecules* **1989**, *22*, 1676-1682.

[41] (a) Inoue, Y. *J. Mol. Struct.* **1998,** *441*, 119. (b) Yoshie, N.; Inoue, Y. *Int. J. Biol. Macromol.* **1999**, *25*, 193-200.

[42] (a) Feng, L.; Yoshie, N.; Asakawa, N.; Inoue, Y. *Macromol. Biosci.*, **2004**, *4*, 186-198. (b) Kazuki, I.; Naoki, A.; Yoshio, I. *Macromol. Symp.* **2005**, *224*, 47-57.

[43] (a) Stayshich, R. M.; Meyer, T. Y.; *J. Am. Chem. Soc.* **2010**, 132, 10920-10934. (b) Lutz, J.-F. *Polym. Chem.* **2010**, 1, 55-62. (c) Lutz, J.-F.; Boerner, H. G. *Macromol. Rapid Commun.* **2011**, 32, 113-114. (d) Jones, R. *Nat. Nanotechnol.* **2008**, 3, 699-700.

[44] (a) Cheng, R. P.; Gellman, S. H.; DeGrado, W. F. *Chem. Rev.* **2001**, 101, 3219-3232. (b) Hill, D. J.; Mio, M. J.; Prince, R. B.; Hughes, T. S.; Moore, J. S. *Chem. Rev.* **2001**, 101, 3893-4012. (c) Cui, H.; Webber, M. J.; Stupp, S. I. *Biopolymers* **2010**, 94, 1-18. (d) Ueda, M.; *Prog. Polym. Sci.* **1999**, 24, 699-730. (e) Yokota, K. *Prog. Polym. Sci.* **1999**, 24, 517-563. (f) Stewart, F. H. C. *Aust. J. Chem.* **1969**, 22, 1291-1298. (g) Kent, S. B. H. *Chem. Soc. Rev.* **2009**, 38, 338-351.

[45] Lin, S.; Waymouth, R. M. *Acc. Chem. Res*. **2002**, 35, 765-773.

[46] (a) Baughman, T. W.; Sworen, J. C.; Wagener, K. B. *Macromolecules* **2006**, 39, 5028-5036. (b) Hopkins, T. E.; Wagener, K. B. *Macromolecules* **2004**, 37, 1180-1189. (c) Leonard, J. K.; Turek, D.; Sloan, K. B.; Wagener, K. B. *Macromol. Chem. Phys.*

2010, 211, 154-165. (d) Mei, J.; Aitken, B. S.; Graham, K. R.; Wagener, K. B.; Reynolds, J. R.; *Macromolecules* **2010**, 43, 5909-5913.

[47] Choi, T.-L.; Rutenberg, I. M.; Grubbs, R. H. *Angew. Chem., Int. Ed.* **2002**, 41, 3839-3841.

[48] (a) Thomas, C. M. *Chem. Soc. Rev.* **2010**, 39, 165-173. (b) Dechy-Cabaret, O.; Martin-Vaca, B.; Bourissou, D. *Chem. Rev.* **2004**, 104, 6147-6176. (c) Dove, A. *P. Chem. Commun.* **2008**, 6446-6470. (d) Stanford, M. J.; Dove, A. *P. Chem. Soc. Rev.* **2010**, 39, 486-494.

[49] Amgoune, A.; Thomas, C. M.; Ilinca, S.; Roisnel, T.; Carpentier, J.-F. *Angew. Chem., Int. Ed.* **2006**, 45, 2782-2784.

[50] Ajellal, N.; Bouyahyi, M.; Amgoune, A.; Thomas, C. M.; Bondon, A.; Pillin, I.; Grohens, Y.; Carpentier, J.-F. *Macromolecules* **2009**, 42, 987-993.

[51] Kramer, J. W.; Treitler, D. S.; Dunn, E. W.; Castro, P. M.; Roisnel, T.; Thomas, C. M.; Coates, G. W. *J. Am. Chem. Soc.* **2009**, 131, 16042-16044.

[52] Natalello, A.; Hall, J. N.; Eccles, E. A. L.; Kimani, S. M.; Hutchings, L. R. *Macromol. Rapid Commun.* **2011**, 32, 233-237.

[53] Klumperman, B. *Polym. Chem.* **2010**, 1, 558-562.

[54] Matyjaszewski, K.; Xia, *J. Chem. Rev.* **2001**, 101, 2921-2990.

[55] Lutz, J.-F.; Neugebauer, D.; Matyjaszewski, K. *J. Am. Chem. Soc.* **2003**, 125, 6986-6993.

[56] Ray, B.; Isobe, Y.; Morioka, K.; Habaue, S.; Okamoto, Y.; Kamigaito, M.; Sawamoto, M. *Macromolecules* **2003**, 36, 543-545.

[57] Lutz, J.-F.; Kirci, B.; Matyjaszewski, K.; *Macromolecules* **2003**, 36, 3136-3145.

[58] Isobe, Y.; Yamada, K.; Nakano, T.; Okamoto, Y. *Macromolecules* **1999**, 32, 5979-5981.

[59] Tao, Y.; Satoh, K.; Kamigaito, M. *Macromol. Rapid Commun.* **2011**, 32, 226-232.

[60] (a) Brudno, Y.; Liu, D. R. Chem. Biol. (Cambridge, MA, U. S.) **2009**, 16, 265-276. (b) Ida, S.; Ouchi, M.; Sawamoto, M. *J. Am. Chem. Soc.* **2010**, 132, 14748-14750.

[61] (a) Ida, S.; Terashima, T.; Ouchi, M.; Sawamoto, M.; J. Am. Chem. Soc. 2009, 131, 10808-10809. (b) Ida, S.; Ouchi, M.; Sawamoto, M. *Macromol. Rapid Commun.* **2011**, 32, 209-214.

[62] (a) Datta, B.; Schuster, G. B. *J. Am. Chem. Soc.* **2008**, 130, 2965-2973. (b) Datta, B.; Schuster, G. B.; McCook, A.; Harvey, S. C.; Zakrzewska, K. *J. Am. Chem. Soc.* **2006**, 128, 14428-14429.

[63] (a) Matyjaszewski, K.; Tsarevsky, N. V. *Nat. Chem.* **2009**, 1, 276-288. (b) Smith, A.

E.; Xu, X.; McCormick, C. L. *Prog. Polym. Sci.* **2010**, 35, 45-93.

[64] Hosoda, S.; Nozue, Y.; Kawashima, Y.; Suita, K.; Seno, S.; Nagamatsu, T.; Wagener, K. B.; Inci, B.; Zuluaga, F.; Rojas, G.; Leonard, J. K.; *Macromolecules* **2011**, 44, 313-319.

[65] Vollrath, F.; Porter, D. *Polymer* **2009**, 50, 5623-5632.

Chapter 2

Effects of composition and sequential structure on thermal properties for copolymer of 3-hydroxybutyrate and lactate units

2-1 Introduction

Poly(hydroxyalkanoates) (PHAs) are naturally occurring polyesters synthesized by a wide variety of bacteria and accumulated as an intracellular carbon and energy storage material.[1] PHAs are biodegradable and biocompatible thermoplastics and have attracted industrial attention as an environmentally degradable material for a wide range of agricultural, marine and medical applications.[1d]

Poly[(*R*)-3-hydroxybutyrate], P[(*R*)-3HB], is the most studied polymer material in the family of PHAs. P[(*R*)-3HB] isolated from microorganisms has a melting temperature around 180 °C and a glass transition temperature around 4 °C.[1c] To meet a variety of demands for a usage of PHA materials in a wide range of application fields, copolymerization of P[(*R*)-3HB] with other PHA monomer units has been attempted. Copolymers containing (*R*)-3HB as a constituent and other PHA monomer units such as (*R*)-3-hydroxyvalerate ((*R*)-3HV),[2] 4-hydroxybutyrate (4HB),[3] and (*R*)-3-hydroxyhexanoate ((*R*)-3HHx)[4] have been produced from various carbon substrates by a variety of bacteria. The structure and properties of random copolymers containing (*R*)-3HB units have been examined, and it has been found that the physical and thermal properties of P[(*R*)-3HB]-based copolymers be regulated by varying their molecular structure and copolymer compositions.

Homopolymers of lactates (PLAs) are also known as biodegradable and biocompatible thermoplastics chemically synthesized from either lactates or its cyclic dimers.[5] PLAs have been investigated as a material for medical devices such as controlled drug release matrixes, degradable sutures, and implanted for bone fixation.[6] Optically pure PLA has a melting temperature around 180 °C and a glass transition temperature around 60 °C.

Recently, Taguchi's group succeeded in construction of biosynthetic system of

copolymers consisting of (*R*)-lactate ((*R*)-2-hydroxypropionate; (*R*)-2HP) and (*R*)-3HB units (P[(*R*)-3HB-*co*-(*R*)-2HP]), and the copolymers with a wide range of composition have been produced.[7] Among the microbial PHAs containing (*R*)-3HB units, P[(*R*)-3HB-*co*-(*R*)-2HP] copolymers are quite interesting due to their glass transition temperatures ranging from below room temperature to above body temperature. By applying the relaxation phenomenon of glass-transition, it is expected that the P[(*R*)-3HB-*co*-(*R*)-2HP] copolymers have a potential to be an intelligent material, e.g., matrixes for controlled release of drug or fertilizer in response to temperature.

It has been reported that the bacterially produced PHA copolymers have broad distributions in randomness, resulting from various factors controlled by changing bacterial strains, carbon substrates, pH, in the fermentation medium, and so on during the cultivation.[8] Most recently, Ochi et al. have succeeded in production of P[(*R*)-3HB-*co*-7 mol%(*R*)-2HP] copolymer with blocking tendency by using recombinant *Escherichia coli* harboring the point-mutated PHA synthase.[9] The variation in sequential distribution of monomeric units for copolymers will certainly expand the properties and functions of PHAs and their applications. In comparison with random copolymers containing (*R*)-3HB units, the investigation on the copolymers with blocking tendency is still few. Understanding the relationship between sequential distribution and properties is valuable to design the copolymer molecules with desirable properties. In this chapter, the effects of copolymer composition and sequential structure on thermal properties of P[(*R*)-3HB-*co*-(*R*)-2HP] copolymers were investigated. The P[(*R*)-3HB-*co*-(*R*)-2HP] copolymers with wide ranges of composition and sequential distributions were prepared by chemosynthetic methods, and their thermal properties and structure were examined.

Chemical syntheses of P[(*R*)-3HB] have been achieved by both the ring-opening polymerization of *β*-butyrolactone and the polycondensation reaction of 3HB derivatives.[10] In contrast to microbial syntheses of P[(*R*)-3HB], most cases of chemosynthetic methods hardly yielded P[(*R*)-3HB] polymers with high molecular weights. It has been merely found that the distannoxane catalysts were very active for the ring-opening polymerization of *β*-butyrolactone to afford P[(*R*)-3HB] with high molecular weights (M_n > 100,000 g/mol). By using the same tin-based catalyst, the copolymers of (*R*)-3HB and (*R*)-2HP units with relatively high molecular weights (M_n > 50,000 g/mol) were synthesized by ring-opening polymerization of a mixture of *β*-butyrolactone and lactide.[11] However, it was reported that the obtained copolymers had a statistically random distribution of (*R*)-3HB unit and dimeric units of (*R*)-2HP since the (*R*)-2HP comonomers were inserted as in units of lactide into the propagating

polymer chains. Although the molecular weights of products by polycondensation reaction are less than those by ring-opening polymerization, the polycondensation reaction yields the copolymers incorporating (*R*)-2HP comonomer as monomeric units and varies the composition and sequential distribution, extensively, by controlling the mixing conditions of two monomers. Therefore, I presumed to adopt the polycondensation reaction for preparation of P[(*R*)-3HB-*co*-(*R*)-2HP] copolymers in this chapter.

2-2 Experimental section

2-2-1 Materials

Basic chemicals were purchased from Kanto Chemical Co. (Japan). Methyl (*R*)-3-hydroxybutyrate ((*R*)-3HB-M) and methyl (*R*)-lactate (methyl (*R*)-2-hydroxypropionate; (*R*)-2HP-M) were used as received.

2-2-2 Synthesis of random copolymers

P[(*R*)-3HB-*co*-(*R*)-2HP] random copolymers were prepared by polycondensation reaction of (*R*)-3HB-M and (*R*)-2HP-M in the presence of titanium tetraisopropoxide ($Ti(O^iPr)_4$) as a catalyst. First, copolymerization of (*R*)-3HB-M and (*R*)-2HP-M with $Ti(O^iPr)_4$ was carried out at 140 °C under atmospheric pressure for 24 h. Then, the pressure was gradually reduced to less than 0.1 mbar, and the reaction was continuously progressed for 66 h. The product was dissolved into chloroform and precipitated in cold methanol. The precipitate was dried in vacuo at room temperature.

2-2-3 Synthesis of copolymers with blocking tendency

P[(*R*)-3HB-*co*-(*R*)-2HP] copolymers with blocking tendency were synthesized by two-step polycondensation reaction. (*R*)-3HB oligomers were prepared by pre-condensation reaction of (*R*)-3HB-M with $Ti(O^iPr)_4$ at 140 °C. The reaction was first carried out under atmospheric pressure for 24 h, and then the pressure was reduced to about 1 mbar. The degree of oligomerization of (*R*)-3HB was controlled by varying the reaction time for 1 to 6 h under the reduced pressure. Copolymerization was started by adding the (*R*)-2HP-M monomer into the (*R*)-3HB oligomers. After the initial copolymerization reaction at 140 °C for 12 h under atmospheric pressure, the pressure of reactor was gradually reduced to less than 0.1 mbar. After the additional polymerization reaction for 66 h, the product was cooled to room temperature and dissolved into chloroform. The copolymer precipitated in cold methanol was dried in vacuo at room temperature.

2-2-4 Analytical procedures

All molecular weight data were obtained by gel-permeation chromatography at 40 °C, using a Shimadzu 10A GPC system and 10A refractive index detector with Shodex K-806 M and K-802 columns. Chloroform was used as an eluent at a flow rate of 0.8 mL/min, and sample concentration of 1.0 mg/mL was applied. Polystyrene standards with a low polydispersity were used to make a calibration curve.

^{1}H and ^{13}C NMR analyses of copolymer samples were carried out on a Varian NMR System 500 spectrometer. The samples (2 mg/mL) were dissolved in $CDCl_3$ and the 500 MHz ^{1}H NMR spectra were recorded at 25 °C with a 5.45 μs pulse width (45° pulse angle), 3.2 s pulse repetition, 8,000 Hz spectral width, and 16 K data points. The 125 MHz ^{13}C NMR spectra were recorded at 25 °C in a $CDCl_3$ solution of polymer (30 mg/mL) with a 4.15 μs pulse width (45˚ pulse angle), 1.3 s pulse repetition, 30,000 Hz spectral width, 32 K data points. Data were analyzed by JEOL ALICE 2 software.

Differential scanning calorimetry (DSC) data of copolymer samples were recorded in the temperature range of –100 – +200 °C on a Perkin Elmer DSC 8500 equipped with a liquid nitrogen cooling accessory under a helium flow of 20 mL/min. Samples of 3 – 5 mg were encapsulated in aluminum pans and heated from –50 to +200 °C at a rate of 20 °C/min (first heating scan). The melting temperature (T_m) and enthalpy of fusion (ΔH_m) were determined from the DSC endotherms of first heating scan. The T_m was taken as the peak temperature of the main endothermal peak. For measurement of the glass-transition temperature (T_g), the samples were maintained at 200 °C for 1 min, and then rapidly quenched at –100 °C. They were then reheated from –100 to +200 °C at a heating rate of 20 °C/min (second heating scan). The T_g was taken as the midpoint of the heat capacity change.

The copolymer spherulitic morphologies were observed with an Olympus optical microscope equipped with crossed polarizers and a Linkham hot stage. The copolymer samples (2 mg) were first heated on a hot stage from room temperature to +200 °C at a rate of 30 °C/min. Samples were maintained at +200 °C for 30 s, and then the temperature was rapidly lowered to a given crystallization temperature (T_c). The samples were crystallized isothermally at a given T_c to monitor the growth of the spherulites as function of time. The radial growth rate of spherulites was calculated as the slope of the line obtained by plotting the spherulite radius against time with more than ten data points. For each crystallization measurement, the radial growth rates of different three spherulites were recorded under the same conditions, and the values were averaged. During the thermal treatment, the copolymer films were kept under nitrogen flow in order to limit the degradation of the polymer. In order to minimize the risk of

thermal degradation of copolymer, individual samples were used for each crystallization measurement.

Wide angle X-ray diffraction (WAXD) patterns of copolymer samples were recorded at 23 °C on a Rigaku RINT 2500 system using a nickel-filtered Cu Kα radiation (λ = 0.154 nm; 40 kV; 100 mA) in the 2θ range of 6 to 60 ° at a scanning speed of 2.0 °/min. The crystallinity of copolymer samples was calculated from diffracted intensity data according to Vonk's method.[12]

2-3 Results and discussion

2-3-1 Synthesis of random copolymers

Copolymerization of (*R*)-3HB and (*R*)-2HP methyl esters was carried out at different monomer feed ratios in the presence of titanium tetraisopropoxide as a catalyst. The composition of the copolymers was determined from the peak intensities of proton resonances of (*R*)-3HB and (*R*)-2HP units in the ^{1}H NMR spectra. Table 2-1 lists the monomer feed ratio, copolymer composition, weight-average molecular weight, and polydispersity of copolymers. Copolymers with molecular weights ranging from M_w=7,600 to 17,400 were obtained at various compositions. The compositions of the obtained copolymers were in good agreement with the monomer feed ratios.

Table 2-1. Compositions and molecular weights of P[(*R*)-3HB-*co*-(*R*)-2HP] random copolymers

sample no.	monomer feed ratio (mol%)		copolymer composition [a] (mol%)		molecular weight [b]	
	(*R*)-3HB-M	(*R*)-2HP-M	(*R*)-3HB	(*R*)-2HP	M_w	M_w/M_n
1	100	0	100	0	9,300	1.5
2	90	10	92	8	7,600	1.9
3	80	20	83	17	13,400	1.4
4	60	40	64	36	10,000	1.8
5	50	50	53	47	8,600	1.7
6	40	60	45	55	8,600	2.0
7	20	80	28	72	14,200	1.5
8	10	90	18	82	10,100	1.8
9	5	95	5	95	17,400	1.7
10	0	100	0	100	16,000	1.4

[a] Determined from ^{1}H NMR spectra. [b] Determined by GPC measurements.

Sequential distribution of P[(*R*)-3HB-*co*-(*R*)-2HP] copolymers was examined from ^{13}C NMR spectra. Figure 2-1 shows a typical ^{13}C NMR spectrum of P[(*R*)-3HB-*co*-47mol% (*R*)-2HP], together with the assignment of each carbon resonance. The majority of carbon resonances were split into several peaks due to diad or triad sequences of (*R*)-3HB (B) and (*R*)-2HP (P) units. The diad and triad fractions

were determined from the ratios of peak areas of resonances, and the results are given in Table 2-2. The diad and triad sequence distribution data for (*R*)-3HB and (*R*)-2HP units were compared with Bernoullian statistics applicable to a statistically random copolymerization. In the Bernoullian model, the mole fraction F_{ij} of diad sequence *ij* can be expressed in terms of the mole fractions F_i and F_j of *i* and *j* units as $F_{ij}=F_iF_j$ and the mole fraction F_{iji} of triad sequence *iji* as $F_{iji}=F_i^2F_j$. As shown in Table 2-2, the calculated diad and triad fractions were in agreement with the observed values for all samples. It has been applied the *D* parameter defined as $D=F_{ii}F_{jj}/F_{ij}F_{ji}$, to estimation of the randomness in sequential distribution.[8] However, as shown in Figure 2-1, several peaks arising from different sequence structure were overlapped, and it was difficult to separate into distinct peaks. Therefore, instead of the *D* parameter, the randomness of copolymers was conveniently evaluated by using the χ parameter defined as $\chi = F_{ij}/F_iF_j$. If a copolymer has completely random distribution, the χ value is equal to 1.0. For all samples, the calculated χ values were very close to 1.0, indicating that the sequence distributions of (*R*)-3HB and (*R*)-2HP units were statistically random.

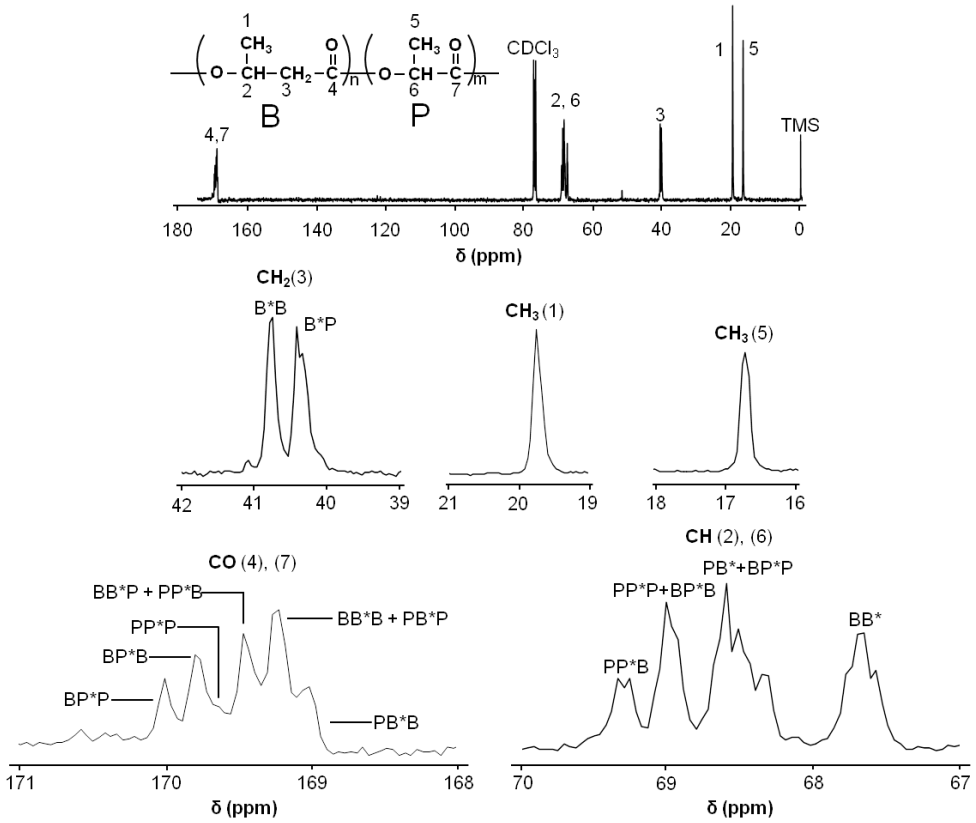

Figure 2-1. ^{13}C NMR spectrum of P[(*R*)-3HB-*co*-47mol% (*R*)-2HP] random copolymer (sample no. 5) in $CDCl_3$ at 25

Table 2-2. Chemical shifts and relative Intensities of ^{13}C resonances in P[(*R*)-3HB-*co*-(*R*)-2HP] random copolymers

carbon atoms	sequence	chemical shift (ppm)	relative intensities							
			sample no. 2 ((*R*)-2HP% = 8)	no. 3 (17)	no. 4 (36)	no. 5 (47)	no. 6 (55)	no. 7 (72)	no. 8 (82)	no. 9 (95)
CH(2)	BB*	67.6	0.85	0.69	0.40	0.31	0.23	0.10	0.01	0.00
			(0.85)	(0.69)	(0.41)	(0.28)	(0.20)	(0.08)	(0.03)	(0.00)
CH(6)	PB*+ BP*P	68.4	0.09	0.16	0.33	0.35	0.40	0.37	0.16	0.04
			(0.07)	(0.17)	(0.31)	(0.37)	(0.38)	(0.35)	(0.27)	(0.09)
	PP*P+BP*B	68.9	0.06	0.12	0.19	0.21	0.23	0.36	0.74	0.87
			(0.07)	(0.12)	(0.20)	(0.23)	(0.28)	(0.43)	(0.58)	(0.86)
	PP*B	69.2	0.00	0.03	0.08	0.12	0.14	0.17	0.09	0.09
			(0.01)	(0.02)	(0.08)	(0.12)	(0.14)	(0.14)	(0.12)	(0.05)
CO(4)	PB*B	169.0	0.06	0.11	0.15	0.12	0.10	0.04	0.03	0.00
			(0.07)	(0.12)	(0.15)	(0.13)	(0.11)	(0.05)	(0.03)	(0.00)
CO(7)	BB*B+PB*P	169.2	0.80	0.60	0.31	0.27	0.30	0.27	0.26	0.10
			(0.78)	(0.60)	(0.34)	(0.27)	(0.23)	(0.17)	(0.12)	(0.04)
	BB*P+PP*B	169.4	0.08	0.15	0.24	0.26	0.19	0.15	0.19	0.12
			(0.07)	(0.14)	(0.23)	(0.25)	(0.25)	(0.19)	(0.15)	(0.05)
	PP*P	169.6	0.00	0.00	0.04	0.07	0.13	0.31	0.35	0.75
			(0.00)	(0.00)	(0.05)	(0.10)	(0.16)	(0.40)	(0.55)	(0.86)
	BP*B	169.7	0.06	0.11	0.17	0.16	0.17	0.08	0.08	0.00
			(0.07)	(0.12)	(0.15)	(0.13)	(0.11)	(0.05)	(0.03)	(0.00)
	BP*P	169.9	0.00	0.03	0.09	0.12	0.11	0.15	0.09	0.03
			(0.01)	(0.02)	(0.08)	(0.12)	(0.14)	(0.14)	(0.12)	(0.05)

The values in parentheses were calculated by Bernoullian statistics with the mole fraction of monomers in copolymers.

2-3-2 Properties of random copolymers

Thermal properties of the random copolymer of (*R*)-3HB and (*R*)-2HP units were determined by DSC. Glass-transition temperatures (T_g) of P[(*R*)-3HB] and P[(*R*)-2HP] homopolymers were -8 and 47 °C, respectively. The molecular weights of the polymers prepared in this study ranged from M_w=7,600 to 17,400, and the values were quite small compared with the biosynthesized P[(*R*)-3HB] and chemosynthesized P[(*R*)-2HP] by ring-opening polymerization of lactide. As a result, the T_g values of the homopolymers prepared in this study were apparently lower than the typically reported values determined from those homopolymers with higher molecular weights. The T_g values of the random copolymers varied almost proportionally with the copolymer composition within the T_g values of each homopolymer. Melting temperatures (T_m) of the P[(*R*)-3HB] and P[(*R*)-2HP] samples were respectively detected at 139 and 153 °C, and the values were also lower than those of high-molecular weight polymers. The melting endotherms of random copolymers were very broad. In addition, some samples revealed the multiple endotherms. Therefore, the T_m of random copolymers was taken as a peak temperature of the main endothermal peak. The T_m of random copolymers decreased with an incorporation of the second monomer units in the polymer chains. The random copolymers with (*R*)-2HP units from 36 to 82 mol% hardly crystallized, and melting endotherm was undetectable in their DSC thermograms.

Table 2-3. Thermal properties and X-ray crystallinity of P[(*R*)-3HB-*co*-(*R*)-2HP] random copolymers

sample no.	(*R*)-2HP fraction (mol%)	thermal properties [a]			crystallinity [b] (%)
		T_g (°C)	T_m (°C)	ΔH_m (J/g)	
1	0	–8	139	82	74 ± 5
2	8	–6	101	56	53 ± 5
3	17	2	68	32	27 ± 5
4	36	8	n.d. [c]	0	
5	47	15	n.d.	0	
6	55	20	n.d.	0	
7	72	23	n.d.	0	
8	82	25	n.d.	0	
9	95	47	133	33	
10	100	44	153	39	

[a] Determined from DSC thermograms. T_g: glass-transition temperature, T_m: melting temperature, ΔH_m: heat of fusion. [b] Determined from X-ray diffraction patterns. [c] Not detected.

Morphologies and growth rate of spherulites for P[(*R*)-3HB-*co*-(*R*)-2HP] random copolymer were investigated with a polarized optical microscope. Figure 2-2 shows typical optical micrographs of spherulites formed under isothermal crystallization

from melt for P[(*R*)-3HB-*co*-(*R*)-2HP] copolymers with random distribution. After crystallization, uniform spherulites were well-developed throughout the copolymer samples. The spherulite growth rates (*G*) of P[(*R*)-3HB-*co*-(*R*)-2HP] random copolymers are also shown in Figure 2-2. The *G* values were dependent on both the crystallization temperature and the copolymer composition. A maximum *G* value of 2.6 μm/s was observed at around 80 °C for P[(*R*)-3HB] homopolymer, however, the growth rates remarkedly reduced as (*R*)-2HP composition increased. The *G* values for P[(*R*)-3HB-*co*-17mol% (*R*)-2HP] random copolymer were slower by two orders of magnitude than those for P[(*R*)-3HB], and the maximum growth rate was detected at around 50 °C.

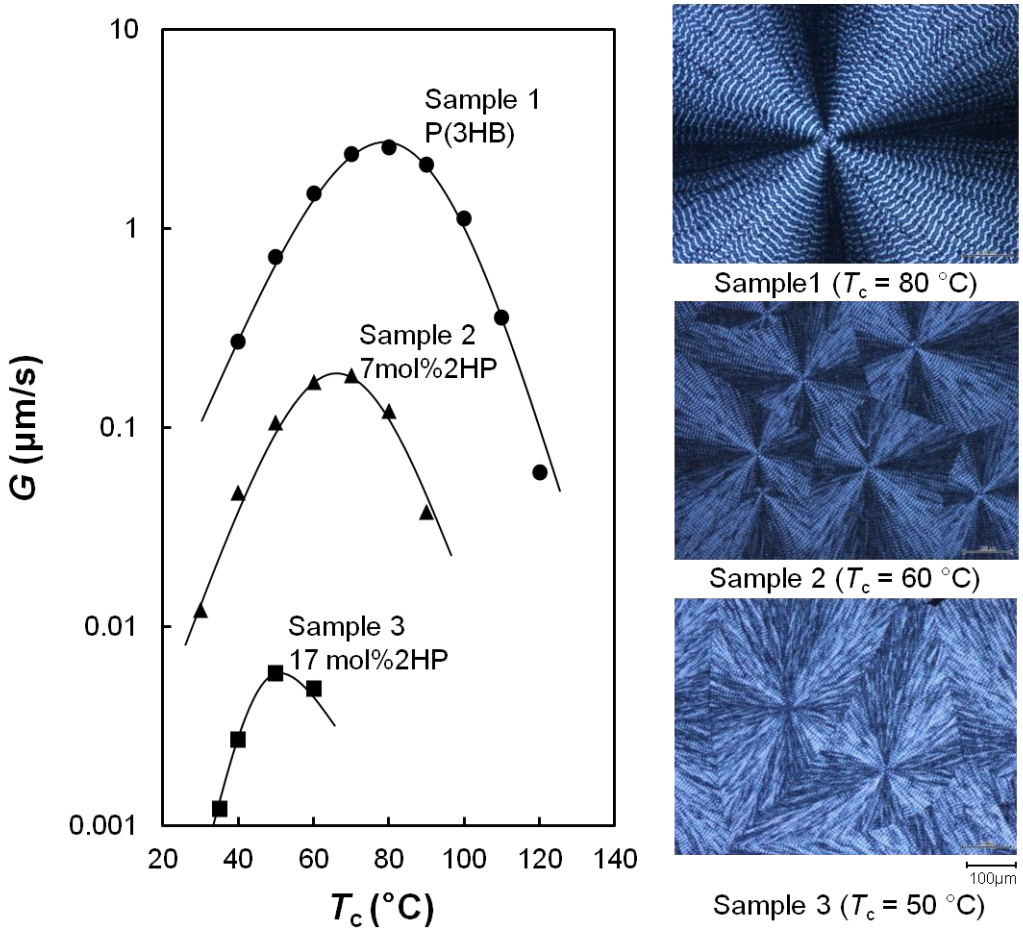

Figure 2-2. Typical optical micrographs of spherulites for P[(*R*)-3HB-*co*-(*R*)-2HP] random copolymers formed at a given crystallization temperature (T_c) and plots of radial growth rate (*G*) of spherulites against T_c.

2-3-3 Synthesis of copolymers with blocking tendency

Preparation of the copolymers with blocking tendency executed for the condition of compositionally (*R*)-3HB-rich region. Oligomers of (*R*)-3HB prepared in advance by condensation reaction were mixed with (*R*)-2HP methyl ester, and then the polycondensation reaction was carried out. By varying the average size of (*R*)-3HB oligomers as a macromonomer and feeding ratios of (*R*)-2HP monomer, several series of copolymers with different (*R*)-2HP compositions could be obtained. The copolymer composition and molecular weight data are given in Table 2-4. The ^{13}C NMR spectra revealed that the obtained copolymers had different distributions in the diad and triad sequences compared with the random copolymers with almost identical (*R*)-2HP content (see Figure 2-3). The resonances from (*R*)-3HB-(*R*)-3HB diad sequence apparently swelled compared with random copolymer. To characterize the sequential structure of the obtained copolymer, the χ values were determined from the ^{13}C NMR spectra of the samples. For all samples, the χ values (0.20 – 0.83) were smaller than 1.0, meaning that the copolymers had blocking tendency.

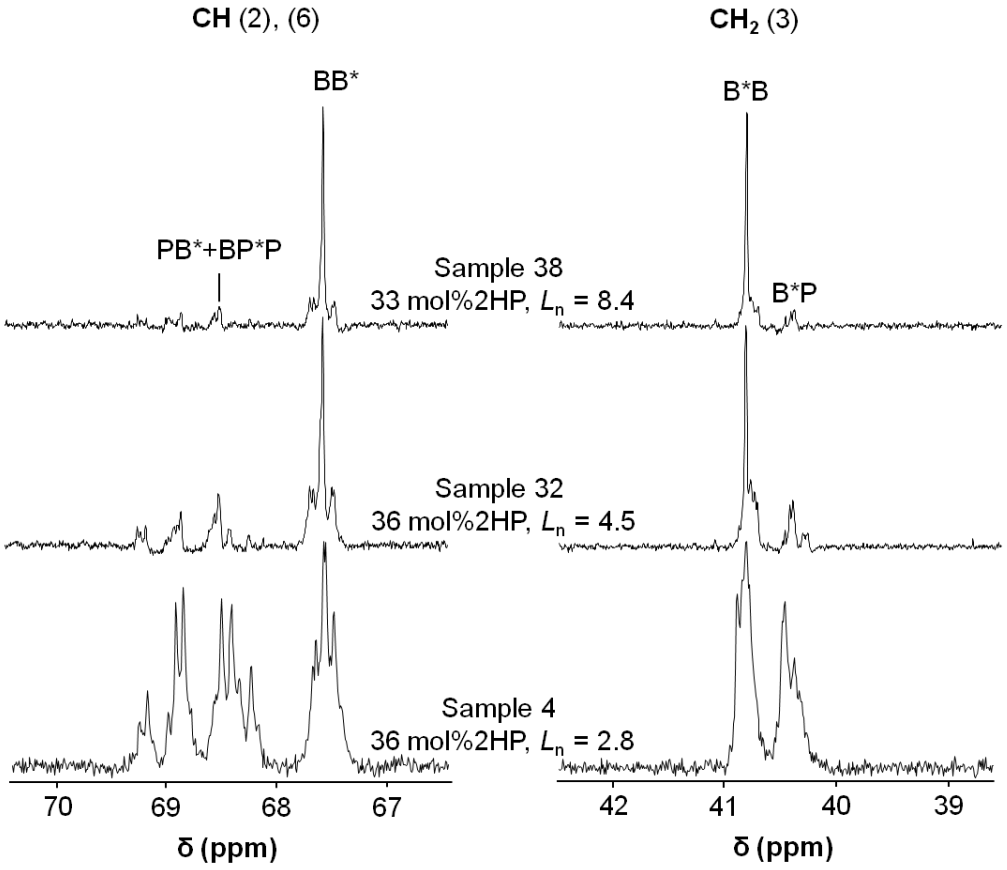

Figure 2-3. Expanded ^{13}C NMR spectra of methylene and methine carbon resonances for P[(*R*)-3HB-*co*-(*R*)-2HP] copolymers with different sequential structure.

Table 2-4. Compositions and molecular weights of P[(*R*)-3HB-*co*-(*R*)-2HP] copolymers with blocking tendency

sample no.	size of (*R*)-3HB oligomer [a] (units)	copolymer composition [b] (mol%)		molecular weight [c]		χ [d]	L_n [e] (units)
		(*R*)-3HB	(*R*)-2HP	M_w	M_w/M_n		
monomer feed ratio: (*R*)-3HB-M/(*R*)-2HP-M = 80 / 20 (mol/mol)							
11	5.0	88	12	8,500	1.5	0.54	15.5
12	4.5	85	15	12,500	1.6	0.73	9.1
13	6.2	85	15	11,700	1.4	0.33	20.2
14	4.8	84	16	11,300	1.7	0.57	11.0
15	8.7	83	17	12,400	1.5	0.81	7.3
16	7.0	83	17	12,100	1.5	0.59	10.0
17	6.5	83	17	12,100	1.5	0.47	12.6
18	4.1	83	17	12,500	1.5	0.55	10.7
(*R*)-3HB-M/(*R*)-2HP-M = 60 / 40 (mol/mol)							
19	27.1	86	14	9,200	1.8	0.56	12.7
20	7.8	79	21	12,400	1.5	0.61	7.8
21	15.1	79	21	12,000	1.6	0.39	12.2
22	6.7	75	25	13,000	1.6	0.68	5.9
23	9.4	75	25	12,200	1.4	0.58	6.9
24	6.7	72	28	11,100	1.3	0.55	6.5
25	4.1	70	30	13,000	1.4	0.78	4.3
26	4.8	61	39	14,300	1.5	0.83	3.1
(*R*)-3HB-M/(*R*)-2HP-M = 50 / 50 (mol/mol)							
27	20.1	82	18	8,400	1.6	0.35	15.8
28	23.3	73	27	11,200	1.4	0.36	10.4
29	25.4	72	28	8,300	1.6	0.26	13.8
30	17.9	69	31	12,600	1.4	0.53	6.1
31	5.3	68	32	14,300	1.8	0.68	4.6
32	6.4	64	36	13,700	1.7	0.62	4.5
33	8.2	61	39	13,800	1.7	0.67	3.8
34	9.9	59	41	11,200	1.4	0.57	4.3
35	11.7	50	50	12,600	1.3	0.74	2.7
(*R*)-3HB-M/(*R*)-2HP-M = 40 / 60 (mol/mol)							
36	15.8	78	22	8,100	1.7	0.20	22.3
37	26.3	71	29	10,700	1.4	0.35	9.9
38	31.6	67	33	9,500	1.5	0.36	8.4
39	6.1	55	45	13,100	1.4	0.74	3.0

[a] Degree of oligomerization of (*R*)-3HB macromonomer prepared by pre-condensation reaction. [b] Determined from ^{1}H NMR spectra. [c] Determined by GPC measurements. [d] Parameter for estimation of the randomness defined as $\chi = F_{ij}/F_iF_j$. [e] Number-averaged sequential length of (*R*)-3HB units.

2-3-4 Properties of copolymers with blocking tendency

Also, for the copolymers with blocking tendency, the T_g, T_m, and ΔH_m values were determined from DSC thermograms. Figure 2-4 shows the plots of T_g, T_m, and ΔH_m values against copolymer composition. As shown in Figure 2-4A, the plots of T_g values for P[(*R*)-3HB-*co*-(*R*)-2HP] copolymers with blocking tendency were fitted fairly well with the line obtained from plotting the T_g and composition of random copolymer samples. On the other hand, the plots of T_m and ΔH_m values against composition for the copolymers with blocking tendency deviated from the estimated lines for the random copolymers. The incorporation of 36 mol% of (*R*)-2HP units gave rise to be amorphous state for the random copolymer, whereas the copolymers with blocking tendency showed melting endotherms even for the samples with more large amount of (*R*)-2HP contents.

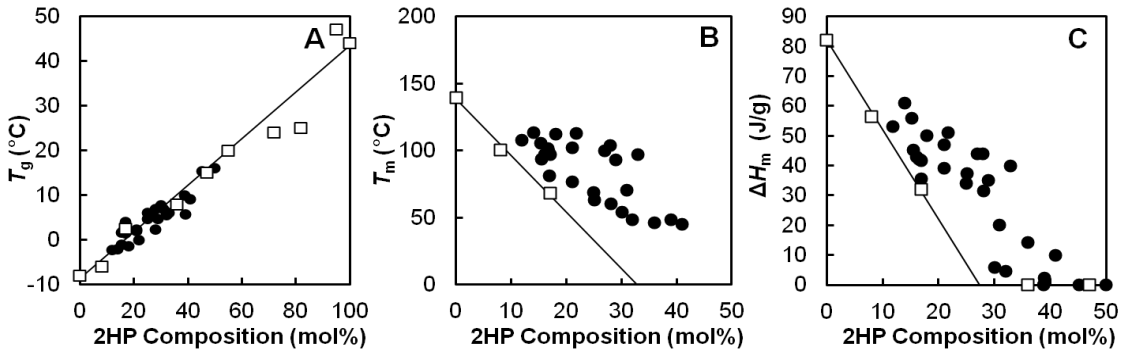

Figure 2-4. Effect of copolymer composition on the thermal properties of P[(*R*)-3HB-*co*-(*R*)-2HP] copolymers. (A) Glass transition temperature (T_g), (B) melting temperature (T_m), and (C) heat of fusion (ΔH_m). Symbols: Random copolymers (open square), copolymers with blocking tendency (closed circle).

Here, we introduce the number-average sequential length of crystallizable monomeric units to consider the relationship between the T_m and sequential structure of P[(*R*)-3HB-*co*-(*R*)-2HP] copolymers. The number-average sequential length (L_n) is defined as $L_n = 1/(1–p)$, where p is the probability of repeating the same monomeric unit. The p value can be estimated from the diad fraction data and is given as F_{ii}/F_i. Then, the L_n values were calculated by using following equation: $L_n = F_i/F_{ij}$. The L_n values of repeating (*R*)-3HB units were in the range from 2.7 to 20.2 units. When the T_m values plotted against the reciprocal value of L_n, the plots showed a linear relationship (see Figure 2-5A). It has been known that the melting temperature of polymers is strongly dependent on the lamellar thickness, and that the observed melting temperature

is inversely proportional to the lamellar thickness in accordance with the Gibbs-Thomson theory.

The probability of formation of N repeating (R)-3HB units in the copolymer can be theoretically expressed by using the probability of p as following equation: $f_n(N)=(1-p)\cdot p^{N-1}/\sum(1-p)\cdot p^{N-1}=(1-p)\cdot p^{N-1}$. The weight fraction of N repeating (R)-3HB units in the total (R)-3HB units of copolymer is given as $f_w(N)=N(1-p)\cdot p^{N-1}/\sum N(1-p)\cdot p^{N-1}=N(1-p)^2\cdot p^{N-1}$. Figure 2-6 shows the distributions of weight fraction of repeating (R)-3HB units. The repeating number of N has a wide distribution, and the weight fraction of repeating (R)-3HB units reveals a convex distribution against the repeating number of N, taking the major weight fraction at the repeating number of L_n. The number-average sequential length (L_n) of crystallizable (R)-3HB units may be the main factor to determine the lamellar thickness of the P[(R)-3HB-*co*-(R)-2HP] copolymers.

The ΔH_m values were obtained as the heat capacity per unit weight of copolymers. Since the (R)-2HP units in (R)-3HB-rich copolymers acted as the non-crystallizable units, the ΔH_m values were normalized by the weight fraction of (R)-3HB units (w_B) in the copolymer. It is of interest to note that the normalized ΔH_m ($\Delta H_m/w_B$) values of copolymers revealed a linear relationship with the reciprocal value of L_n (see Figure 2-5B). As mentioned above, it is suggested that the lamellar thickness of the copolymer is governed by the average sequential length of (R)-3HB units in the copolymer. In the copolymers, the distribution of repeating number of N is widespread. The fractions with shorter sequence than the lamellar thickness hardly participate the crystal formation, and are accumulated into the amorphous region. The integrated values of weight fractions with shorter sequence than the L_n value are around 34 wt% of the total (R)-3HB units for each copolymer with different sequential structure. On the other hand, the fractions with quite longer sequence than the lamellar thickness are incorporated into the crystalline regions forming the chain folding structure and/or penetrating the interlamellar regions. These chain-folding regions and the interlamellar regions are non-crystallized parts. It can be understood that the area of chain-folded surface of lamellar crystals in the unit volume of crystalline region is inversely proportional to the lamellar thickness. Accordingly, the amounts of (R)-3HB units trapped into such non-crystallized regions increase with a decrease in the lamellar thickness. Thus, it is concluded that the ΔH_m values are influenced by both the contents of (R)-3HB units in the copolymer and the number-average sequential length of crystallizable (R)-3HB units.

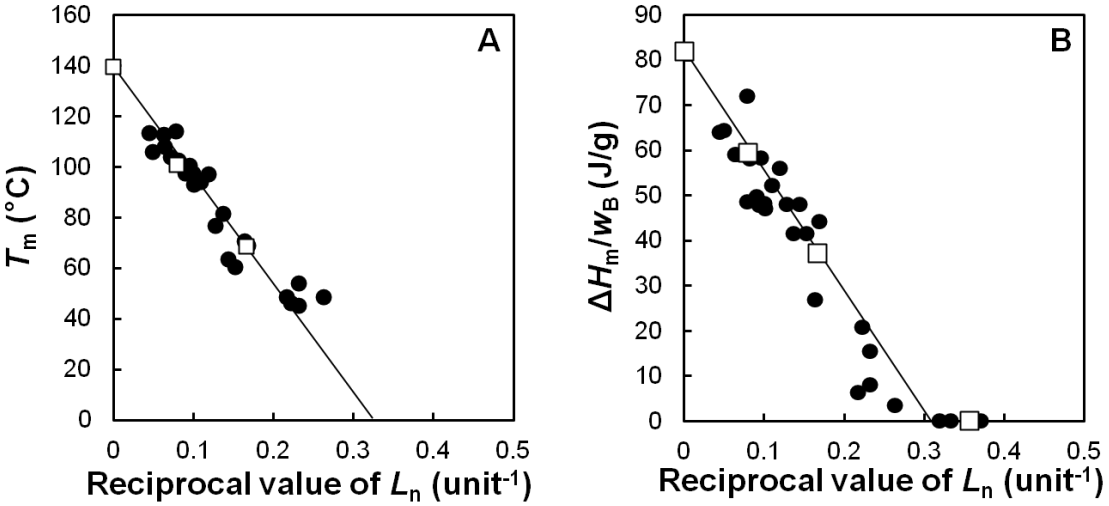

Figure 2-5. Relationships between the number-average sequential length (L_n) of crystallizable (*R*)-3HB units and (A) melting temperature (T_m) and (B) enthalpy of fusion normalized by weight fraction of (*R*)-3HB units ($\Delta H_m/w_B$).

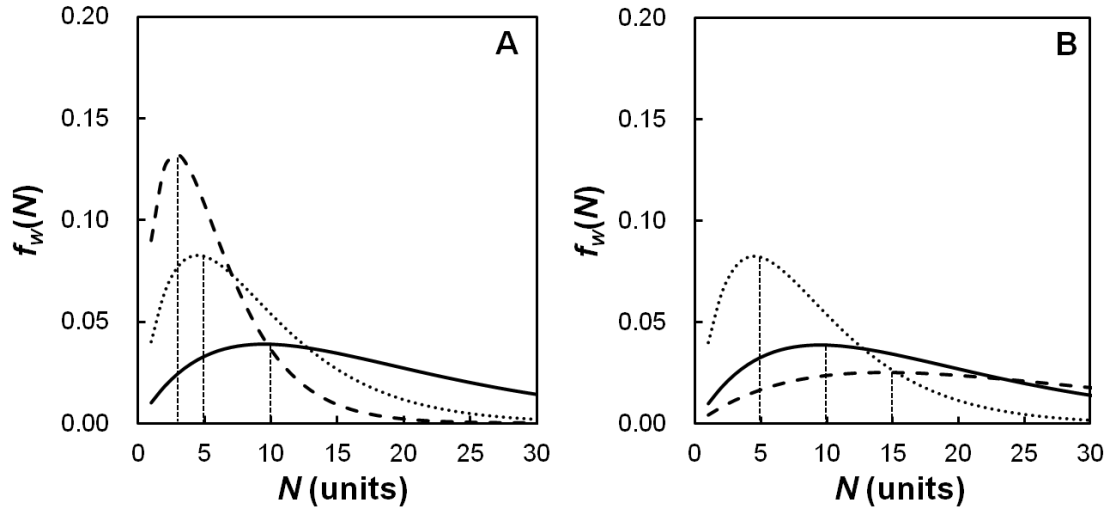

Figure 2-6. Theoretical distributions of weight fraction of repeating (*R*)-3HB units in copolymers with different composition and sequence structure. (A) Series of random copolymers with different (*R*)-2HP composition. 10 mol% (*R*)-2HP (solid line), 20 mol% (*R*)-2HP (dotted line), and 30 mol% (*R*)-2HP (dashed line). (B) Series of copolymers containing 20 mol% of (*R*)-2HP with different blocking tendency. Random; L_n = 5 (dotted line), blocking tendency; L_n = 10 (solid line) and L_n = 15 (dashed line).

Table 2-5. Thermal properties and X-ray crystallinity of P[(*R*)-3HB-*co*-(*R*)-2HP] copolymers with blocking tendency

sample no.	(*R*)-2HP fraction (mol%)	L_n (units)	thermal properties [a]			crystallinity [b] (%)
			T_g (°C)	T_m (°C)	ΔH_m (J/g)	
11	12	15.5	–2	94, **108** [c]	53	53
12	15	9.1	2	83, **94**	45	45
13	15	20.2	–1	88, **106**	56	49
14	16	11.0	2	80, **98**	43	
15	17	7.3	4	81	36	32
16	17	10.0	2	81, **97**	42	35
17	17	12.6	2	82, **101**	42	
18	17	10.7	2	83, **99**	42	
19	14	12.7	–2	85, **114**	61	54
20	21	7.8	2	77	39	36
21	21	12.2	2	83, **102**	47	37
22	25	5.9	6	69	34	23
23	25	6.9	5	63	37	23
24	28	6.5	7	60	32	20
25	30	4.3	8	54	6	
26	39	3.1	10	n.d. [d]	0	
27	18	15.8	–1	82, **113**	50	48
28	27	10.4	5	78, **100**	44	32
29	28	13.8	2	80, **104**	44	32
30	31	6.1	7	70	20	29
31	32	4.6	6	48	5	
32	36	4.5	8	46	14	
33	39	3.8	6	48	2	
34	41	4.3	9	45	10	
35	50	2.7	16	n.d.	0	
36	22	22.3	0	82, **114**	51	40
37	29	9.9	5	72, **93**	35	28
38	33	8.4	6	76, **97**	40	27
39	45	3.0	15	n.d.	0	

[a] Determined from DSC thermograms. T_g: glass-transition temperature, T_m: melting temperature, ΔH_m: heat of fusion. [b] Determined from X-ray diffraction patterns. [c] The T_m values in bold were a peak temperature of the main endothermal peak. [d] Not detected.

Figure 2-7 shows the spherulite growth rates (G) of P[(*R*)-3HB-*co*-(*R*)-2HP] copolymers with almost identical (*R*)-2HP composition of 17 mol% and different sequential structure plotted against crystallization temperature, together with typical micrographs of formed spherulites. Each plot of G against the crystallization temperature revealed a convex curve. The curves were shifted towards higher temperature region with an increase of the number-average sequential length (L_n). The maximum G value tended to increase with an increase of the L_n value, indicating that the spherulites growth rate of P[(*R*)-3HB-*co*-(*R*)-2HP] copolymers is affected by the sequential structure. Here, it is pointed out that the random copolymer with 8 mol% of (*R*)-2HP (sample no.2) showed more faster crystallization than the copolymer sample no. 27, which contained 18 mol% of 2HP, although the L_n value of sample no.2 (12.5 units) was shorter than that of sample no. 27 (L_n = 15.8 units). The incorporation of non-crystallizable (*R*)-2HP units causes the dilution of crystallizable (*R*)-3HB segments and leads to the decrease of the transportation rate of (*R*)-3HB segments at the growth front of crystalline lamellae. As a result, the spherulite growth rate of copolymers is also influenced by both the contents of (*R*)-3HB units in the copolymer and the number-average sequential length of crystallizable (*R*)-3HB units

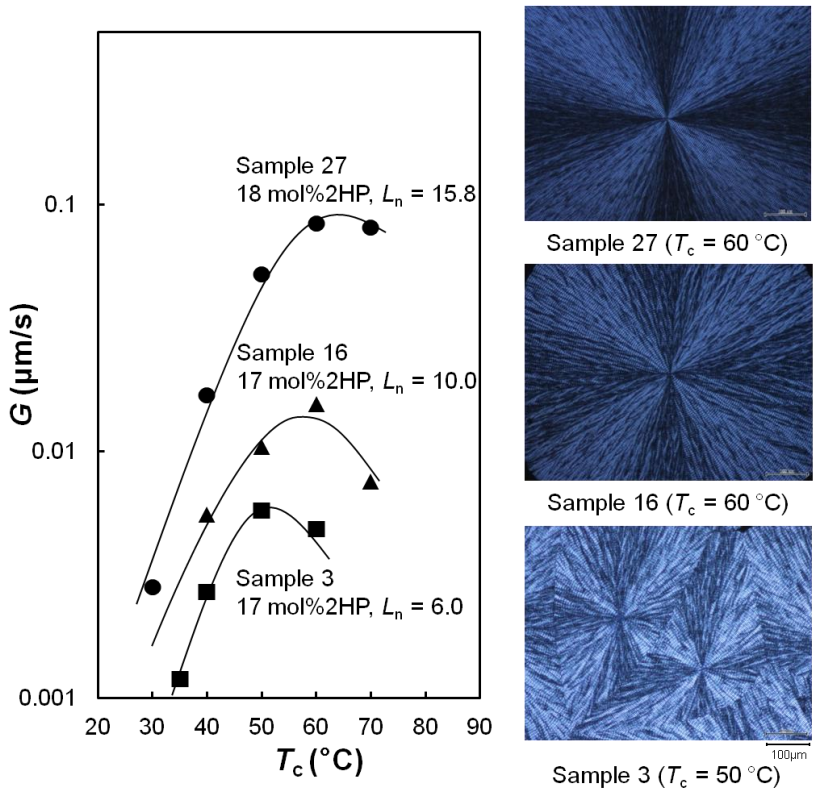

Figure 2-7. Typical optical micrographs and radial growth rate (G) of spherulites for P[(*R*)-3HB-*co*-(*R*)-2HP] copolymers with different sequential structure.

2-4 Conclusions

The effects of copolymer composition and sequential structure on the thermal properties of P[(*R*)-3HB-*co*-(*R*)-2HP] copolymers were investigated. The obtained results indicate that the T_g of copolymers varies in accordance with the copolymer composition, while that the T_m is predominantly determined by the averaged sequential length of crystallizable monomer units. It means that we can produce the copolymers with various T_m values and a constant T_g value by varying the sequential length of monomers at the fixed copolymer composition.

Unfortunately, since the synthesized copolymers had relatively low molecular weights, it is difficult to prepare films being subjected to biodegradation test. It has been demonstrated that the rate of biodegradation for PHA materials is strongly dependent both on the chemical structure of monomeric unit and on the solid-state structure of samples.[13] In the aspect of the solid-state structure of PHA materials, the crystallinity and lamellar crystal sizes play a decisive role in degradation process. The lamellar thickness of P[(*R*)-3HB-*co*-(*R*)-2HP] copolymers is regulated by the averaged sequential length of crystallizable monomer units, and the crystallinity is versatile with the combination of copolymer composition and averaged sequential length of monomers. Therefore, it is expectable that the biodegradation rate of P[(*R*)-3HB-*co*-(*R*)-2HP] copolymers is also controlled desirably by selecting the copolymer composition and averaged sequential length of monomers.

References

[1] (a) Doi, Y. *Microbial Polyesters, VCH Publishers, New York,* **1990**. (b) Sudesh, K.; Abe, H.; Doi, Y. *Prog. Polym. Sci.* **2000**, 25, 1503-1555. (c) Lenz, R. W.; Marchessault, R. H. *Biomacromolecules* **2005**, 6,1-8. (d) Chen, G-Q. *Chem. Soc. Rev.* **2009**, 38, 2434-2446.

[2] (a)Doi, Y.; Kunioka, M.; Nakamura, Y.; Soga, K. *Macromolecules* **1986**, 19, 2860-2864. (b) Bloembergen, S.; Holden, A. D.; Hamer, G. K.; Bluhm, T. L.; Marchessault, R. H. *Macromolecules* **1986**, 19, 2865-2871. (c) Doi, Y.; Tamaki, A.; Kunioka, M.; Soga, K. *Appl. Microbiol. Biotechnol.* **1988**, 28, 330-334. (d) Kamiya, N.; Yamamoto, Y.; Inoue, Y.; Chujo, R.; Doi, Y. *Macromolecules* **1989**, 22, 1676-1682. (e) Mitomo, H.; Morishita, N.; Doi, Y. *Macromolecules* **1993**, 26, 5809-5811.

[3] (a) Doi, Y.; Kunioka, M.; Nakamura, Y.; Soga, K. *Macromolecules* **1988**, 21, 2722-2727. (b) Doi, Y.; Segawa, A.; Kunioka, M. *Int. J. Biol. Macromol.* **1990**, 12, 106-111. (c) Nakamura, S.; Doi, Y.; Scandola, M. *Macromolecules* **1992**, 25,

4237-4241. (d) Shi, F.; Ashby, R. D.; Gross, R. A. *Macromolecules* **1997**, 30, 2521-2523. (e) Hein, S.; Sohling, B.; Gottschalk, G.; Steinbuchel, A. *FEMS Microbiolgy Lett.* **1997**, 153, 411-418.

[4] (a) Shimamura, E.; Kasuya, K.; Kobayashi, G.; Shiotani, T.; Shima, Y.; Doi, Y. *Macromolecules* **1994**, 27, 878-880. (b) Doi, Y.; Kitamura, S.; Abe, H. *Macromolecules* **1995**, 28, 4822-4828. (c) Asrar, J.; Valentin, H. E.; Berger, P. A.; Tran, M.; Padgette, S. R.; Garbow, J. R. *Biomacromolecules* **2002**, 3, 1006-1012.

[5] (a) Kricheldorf, H. R.; Berl, M.; Scharnagl, N. *Macromolecules* **1988**, 21, 286-293. (b) Dubois, P.; Jacobs, C.; Jérôme, R.; Teyssié, P. *Macromolecules* **1991**, 24, 2266-2270. (c) Libiszowski, J.; Kowalski, A.; Duda, A.; Penczek, S. *Macromol. Chem. Phys.* **2002**, 203, 1694-1701. (d) Tsuji, H. *Biopolymers, 4, Polyesters;* Doi Y. and Steinbüchel A., Eds.; WILLEY-VCH Verlag GmbH, Weinheilm, **2002**, p. 129-177. (d) Auras, R.; Harte, B.; Selke, S. *Macromol. Biosci.* **2004**, 4, 835-864.

[6] (a) Leenslag, J. W.; Pennings, A. J.; Bos, R. M.; Rozema, F. R.; Boering, G. *Biomaterials* **1987**, 8, 311-314. (b) Väinionpää, S.; Rokkanen, P.; Törmälä, P. *Prog. Polym. Sci.* **1989**, 14, 679-716. (c) Ikada, Y.; Shikinami, Y.; Hara, Y.; Tagawa, M.; Fukada, E. *J. Biomed. Mater. Res.* **1996**, 30, 553-558.

[7] (a) Taguchi, S.; Yamada, M.; Matsumoto, K.; Tajima, K.; Satoh, Y.; Munekata, M.; Ohno, K.; Kohda, K.; Shimamura, T.; Kambe, H.; Obata, S. *Proc. Natl. Acad. Sci. U.S.A.* **2008**, 105, 17323-17327. (b) Yamada, M.; Matsumoto, K.; Nakai, T.; Taguchi, S. *Biomacromolecules* **2009**, 10, 677-681. (c) Yamada, M.; Matsumoto, K.; Shimizu, K.; Uramoto, S.; Nakai, T.; Shozui, F.; Taguchi, S. *Biomacromolecules* **2010**, 11, 815-819. (d) Shozui, F.; Matsumoto, K.; Motohashi, R.; Sun, J.; Satoh, T.; Kakuchi, T.; Taguchi, S. *Polym Degrad Stab* **2011**, 95, 1340-1344.

[8] (a) Yoshie, N.; Inoue, Y. *Int. J. Biol. Macromol.* **1999**, 25, 193-200. (b) Feng, L.; Yoshie, N.; Asakawa, N.; Inoue, Y. *Macromol. Biosci.* **2004**, 4, 186-198. (c) Pederson, E. N.; McChalicher, C. W. J.; Srienc, F. *Biomacromolecules* **2006**, 7, 1904-1911.

[9] Ochi, A.; Matsumoto, K.; Ooba, T.; Sakai, K.; Tsuge, T.; Taguchi, S. *Appl Microbiol. Biotechnol.* **2013,** 97, 3441-3447.

[10] (a) Gross, RA.; Zhang, Y.; Konrad, G.; Lenz, RW. *Macromolecules* **1988**, 21, 2657-2668. (b) Hori, Y.; Suzuki, M.; Yamaguchi, A.; Nishishita, T. *Macromolecules* **1993**, 26, 5533-5534. (c) Kobayashi, T.; Hori, Y.; Kakimoto, M.; Imai, Y. *Makromol. Chem. Rapid Commum* **1993**, 14, 785-790. (d) Albertsson, AC.; Varma, IK. *Biomacromolecus* **2003**, 4, 1466-1486.

[11] Abe, H.; Doi, Y.; Hori, Y.; Hagiwara, T. *Polymer* **1997**, 39, 59-67.

[12] Vonk, CG. *J. Appl. Crystallogr* **1973**, 6, 148-152.

[13] Abe, H.; Doi, Y., Aoki, H.; Akehata, T. *Macromolecules* **1998**, 31, 1791-1797.

Chapter 3

Synthesis and properties of alternating copolymers of 3-hydroxybutyrate and lactate units with different stereocompositions

3-1 Introduction

Nowadays, aliphatic polyesters have attracted an industrial attention as environmentally degradable thermoplastics to be used for a wide range of applications. Among a family of aliphatic polyesters, poly[(*R*)-3-hydroxybutyrate] (P[(*R*)-3HB]),[1] poly(L-lactate) (PLLA, poly[(*S*)-2-hydroxypropionate]; P[(*S*)-2HP]), [2] and their copolymers [3] have been most extensively investigated. Bacterially synthesized P[(*R*)-3HB] has a melting temperature around 180 °C, and the value is very close to that of polypropylene which is a commodity plastic. The introduction of second monomer units into P[(*R*)-3HB] molecules by copolymerization varies their melting temperatures in the range from 50 to 180 °C, depending on both the chemical structure of second monomer and the composition, and P[(*R*)-3HB]-based copolymers offer a wide variety of polymeric materials in properties, from hard crystalline plastic to elastic rubber.[9-14] Optically pure PLLA also show a melting temperature at around 180 °C. Since the PLLA has a glass-transition temperature of 60 °C, the transparent materials can be provided. It has been found that the PLLA molecules form a stereocomplex crystalline structure in the presence of stereoisomeric poly(D-lactate) segments.[4] The melting temperature of the stereocomplex crystal reaches to 230 °C, and the value is the highest ones, along with poly(glycolate), in the aliphatic polyesters.[5]

For copolymerization, the regulation of sequential structure is powerful tool to design the polymeric materials with appropriate properties.[6] Various types of copolymers with statistically random,[7] blocking tendency,[8] or alternative distributions[9] have been produced, and the structure and physical properties were characterized.

In preceding chapter, I investigated the effects of sequential structure on the thermal properties by preparing the copolymers of (*R*)-3HB and 2HP units with various

sequential distributions from random to blocking tendency.[10] The obtained results indicate that the melting temperature of copolymers be tuned to the averaged sequential length of crystallizable monomer units. However, in each case, the second monomer units introduced with statistical regularity act as defects of crystalline state consisting of repeating crystallizable monomer units and induce the inhibition of crystallization and the depression of melting temperature.

With the progresses in polymer synthesis techniques, approaches to the precise regulation of monomer sequence in copolymer molecules have been attempted, instead of usual statistical regulation of sequential structure. For olefinic monomers, Wagener et al. synthesized the copolymers possessing an ethyl branch on every ninth, 15th and 21st carbon along the backbone of polyethylene via acyclic diene metathesis.[11] Satoh et al. succeeded in 1:2-sequence-regulated radical copolymerization of maleimide and terpenes in the presence of fluorinated alcohol.[12] In the case of polyesters, Meyer et al. synthesized the various types of copolymers with precise repeating sequence of lactate and glycolate units by condensation reactions of oligomeric precursors of two monomers. They investigated the effects of sequence structure in the copolymers containing both α-hydroxyl acid monomeric units on the physical properties and biodegradability.[13] Kramer et al. succeeded in syntheses of sequence-regulated copolymers consisted of *β*-hydroxyalkanoate monomeric units by polymerization of a mixture of enantiopure two *β*-lactone monomers as pairing the opposite configuration using syndiospecific catalysts.[14] They reported that the melting temperatures of the synthesized copolymers with alternating sequence structure were strongly influenced by characteristics of side-chain groups.

The simplest type of sequence-regulated copolymer is an alternating copolymer. In this chapter, I focused the structure and physical properties of alternating copolymers consisting of *α*-hydroxyalkanoate monomeric unit of lactate (2HP) and *β*-hydroxyalkanoate monomer unit of (*R*)-3HB. Taking into account the chiral structure of monomeric units, two types of stereoisomeric dimers ((*R*)-3HB-(*R*)-2HP and (*R*)-3HB-(*S*)-2HP) were respectively prepared, and the alternating copolymers with different stereocompositions were synthesized from the dimeric monomers by condensation reaction. The structure and physical properties of obtained copolymers were characterized by NMR, DSC, and WAXD. On the basis of the obtained results, the relationships among the molecular structure, thermal properties, and crystalline structure in the alternating copolymers were discussed.

3-2 Experimental section

3-2-1 Materials

Methyl (*R*)-3-hydroxybutyrate, methyl (*R*)-lactate, *tert*-butyldiphenylchlorosilane (TBDPSCl), benzyl bromide (BnBr), and *N*,*N*′-diisopropylcarbodiimide (DIC) were purchased from Tokyo Chemical Industry Co. (*S*)-Lactic acid, benzyl alcohol (BnOH), 1,8-diazobicycloundec-7-ene (DBU), and *N*,*N*-dimethyl-4-aminopyridine (DMAP) were purchased from Wako Chemical Industry Co. *p*-Toluenesulfonate (TsOH), dimethylformamide (DMF), triethylamine (TEA), lithium hydroxide monohydrate ($LiOH \cdot H_2O$), and *N*,*N*′-dicyclohexylcarbodiimide (DCC) were purchased from Kanto Chemical Co. The 5% Pd on silica sample was purchased from Strem Chemicals, Inc. All of these chemical reagents were used as supplied without further purification. 4-(Dimethylamino)pyridinium *p*-toluenesulfonate (DPTS) was prepared from TsOH and DMAP according to the reported procedure.[15] Dichloromethane (DCM) and THF (Kanto Chemical Co, super dehydrated grade) were passed through activated alumina using the SPS 800 (Innovative Technology).

3-2-2 Synthesis of dimeric monomers

Benzyl (*R*)-lactate (1: (*R*)-2HP-Bn)

Methyl (*R*)-lactate (22.6 mL, 20.8 g, 200.0 mmol) was added to a solution of benzyl alcohol (104.0 mL, 108.0 g, 1.0 mol) and *p*-toluenesultanate (0.2 g, 1.0 mmol). The reaction mixture was stirred at 80 °C for 2 h, and the pressure was reduced subsequently at 9 kPa for 10 h. Diethyl ether (400 mL) was added, and an organic extracts were successively washed with saturated sodium hydrogen carbonate (2 × 200 mL), 5% sodium carbonate (4 × 50 mL), saturated sodium chloride (6 × 50 mL), dried over anhydrous magnesium sulfate, and evaporated. The crude product was distilled, to give a colorless oil (bp 1 kPa, 125 – 130 °C, 25.2 g, yield = 70 %). ^{1}H NMR ($CDCl_3$, 500 MHz): δ 7.4–7.2 (m, 5H, Ar*H*), δ 5.21 (s, 2H, PhCH_2O), δ 4.31 (m, 1H, C*H*), δ 2.90 (d, *J* = 4.9 Hz, 1H, O*H*), δ 1.43 (d, *J* = 5.5 Hz, 3H, CH_3). Anal. CHN Calcd: $C_{10}H_{12}O_3$: C, 66.7; H, 6.7; N, 0.0. Found: C, 65.7; H, 6.7; N, 0.0.

Benzyl (*S*)-lactate (2: (*S*)-2HP-Bn)

Benzyl (*S*)-lactate was prepared following Wolfe et al. [16] 1,8-Diazobicyclo[5.4.0]undeca-7-ene (DBU) (90.0 mL, 94.5 g, 600.0 mmol) was added slowly with stirring to a solution of 90 % (*S*)-lactic acid (59.4 mL, 54.0 g, 600.0 mmol) in methanol (250 mL). The solvent was removed under reduced pressure at 70 – 80 °C,

and the resulting oil, in DMF (250 mL), was cooled to 15 °C. Benzyl bromide (59.5 mL, 85.5 g, 500.0 mmol) was added dropwise, and the reaction mixture was stirred at room temperature for 30 h. After removal of approximately 200 mL of solvent by vacuum distillation, ethyl acetate (500 mL) was added, followed by water (150 mL). The aqueous layer was washed with ethyl acetate (3 × 150 mL), and the combined organic extracts were washed successively with water (150 mL), 5% citric acid (150 mL), water (150 mL), saturated sodium chloride (2 × 150 mL), dried over anhydrous magnesium sulfate, and evaporated. The crude product was distilled, to give a colorless oil (bp 1 kPa, 125–130 °C, 91.8 g, yield = 85 %). ^{1}H NMR ($CDCl_3$, 500 MHz): δ 7.4–7.2 (m, 5H, Ar*H*), δ 5.21 (s, 2H, PhCH_2O), δ 4.32 (m, 1H, C*H*), δ 2.89 (d, *J* =5.9 Hz, 1H, O*H*), δ 1.43 (d, *J* = 7.1 Hz, 3H, CH_3). Anal. CHN Calcd: $C_{10}H_{12}O_3$: C, 66.7; H, 6.7; N, 0.0. Found: C, 65.5; H, 6.7; N, 0.0.

(*R*)-3-(*tert*-Butyldiphenylsilanyloxy)-butanoic acid (3: TBDPS-(*R*)-3HB)

Methyl (*R*)-3-hydroxybutyrate (11.8 g, 100.0 mmol), TEA (20.2 g, 200.0 mmol), DMAP (6.1g, 50.0 mmol), and DCM (400 mL) were added under nitrogen to 1 L oven-dried two neck eggplant-shaped flask. After cooling the reaction mixture to 0 °C, TBDPSCl (30.2 g, 110.0 mmol) was added by syringe. The ice bath was removed and the reaction was stirred at room temperature overnight (24 h). The reaction mixture was filtered, and the filtrate was washed with 2 × 300 mL 10% HCl, 2 × 200 mL H_2O, and dried with $MgSO_4$. Removal of the solvent under vacuum gave a colorless oil (37.4 g). The resultant oil (37.4 g) was dissolved in THF (1500 mL) and cooled in an ice bath. $LiOH{\cdot}H_2O$ (9.4 g, 200.0 mmol) in 600 mL of H_2O was added dropwise for over 15 min. The ice bath was removed, and the reaction was stirred for 10 min. Water (100 mL) was added and the THF was removed under vacuum. The aqueous phase was extracted with 2 × 150 mL of ether to remove starting material, acidified using 1.0 M HCl, and then extracted with 2 × 150 mL of ether. The second ethereal phase was dried with $MgSO_4$ and the solvent was removed to give a colorless oil, and recrystallized from hexane solution under isothermal condition at 4 °C (20.6 g, yield = 60 %). ^{1}H NMR ($CDCl_3$, 500 MHz): δ 7.7–7.6 (m, 4H, Ar*H*), δ 7.5–7.2 (m, 6H, Ar*H*), δ 4.27 (m, 1H, C*H*), δ 2.49 (m, 2H, CH_2), δ 1.13 (d, *J* = 6.4 Hz, 3H, CH_3), δ 1.03 (s, 9H, CH_3). Anal. CHN Calcd: $C_{20}H_{26}O_3Si$: C, 70.1, H, 7.7; N, 0.0. Found: C, 70.1; H, 7.7; N, 0.0.

(*R*)-2-[(*R*)-3-(*tert*-Butyldiphenylsilanyloxy)butoxy]propionic acid benzyl ester (4: TBDPS-(*R*)-3HB-(*R*)-2HP-Bn)

TBDPS-(*R*)-3HB (**3**) (34.3 g, 100.0 mmol), (*R*)-2HP-Bn (**1**) (18.0 g, 100 mmol), and DMAP (6.1 g, 50 mmol) were combined under nitrogen with 600 mL of DCM. DCC (20.6 g, 100 mmol) was added, and the reaction was stirred for 18 h. The reaction mixture was filtered to remove urea, and the filtrate was concentrated under vacuum. The crude oil was chromatographed over silica gel (5 % ethyl acetate in hexanes) to give a colorless oil (37.8 g, yield = 75 %). ^{1}H NMR ($CDCl_3$, 500 MHz): δ 7.7–7.6 (m, 4H, Ar*H*), δ 7.5–7.2 (m, 11H, Ar*H*), δ 5.14 (m, 2H, PhCH_2O), δ 5.03 (m, 1H, C*H*), δ 4.31 (m, 1H, C*H*), δ 2.55 (m, 2H, CH_2), δ 1.36 (d, *J* = 7.1 Hz, 3H, CH_3), δ 1.13 (d, *J* = 6.2 Hz, 3H, CH_3), δ 1.03 (s, 9H, CH_3). Anal. CHN Calcd: $C_{30}H_{36}O_5Si$: C, 71.4; H, 7.2; N, 0.0. Found: C, 71.3; H, 7.2; N, 0.0.

(*S*)-2-[(*R*)-3-(*tert*-Butyldiphenylsilanyloxy)butoxy]propionic acid benzyl ester (5: TBDPS-(*R*)-3HB-(*S*)-2HP-Bn)

In the same way as TBDPS-(*R*)-3HB-(*R*)-2HP-Bn (**4**), TBDPS-(*R*)-3HB-(*S*)-2HP-Bn (**5**) was prepared from TBDPS-(*R*)-3HB and (*S*)-2HP-Bn (2). The product was obtained as colorless oil (15.2 g, yield = 83 %). ^{1}H NMR ($CDCl_3$, 500 MHz): δ 7.7–7.6 (m, 4H, Ar*H*), δ 7.5–7.2 (m, 11H, Ar*H*), δ 5.14 (m, 2H, PhCH_2O), δ 5.06 (m, 1H, C*H*), δ 4.31 (m, 1H, C*H*), δ 2.55 (m, 2H, CH_2), δ 1.46 (d, *J* = 7.1 Hz, 3H, CH_3), δ 1.12 (d, *J* = 6.1 Hz, 3H, CH_3), δ 1.02 (s, 9H, CH_3). Anal. CHN Calcd: $C_{30}H_{36}O_5Si$: C, 71.4; H, 7.2; N, 0.0. Found: C, 71.3; H, 7.3; N, 0.0.

(*R*)-2-[(*R*)-3-(Hydroxybutoxy)]propionic acid benzyl ester (6: (*R*)-3HB-(*R*)-2HP-Bn)

The di-protected dimeric monomer (**4**) (4.0 g, 8.0 mmol) and acetic acid (1.5 g, 25.0 mmol) were combined under nitrogen with 60 mL of THF. TBAF (1M in THF) (12.0 mL) was added, and the reaction mixture was allowed to stir for 3 day at 50 - 60 °C. Brine (30 mL) was added and extracted with 2 × 40 mL with ether. The ethereal phase was washed with 3 × 30 mL sat. $NaHCO_3$, 2 × 30 mL H_2O, and dried with $MgSO_4$. The crude oil was chromatographed over silica gel (10 % ethyl acetate in hexanes) to give a colorless liquid (5.8 g, yield = 72 %). ^{1}H NMR ($CDCl_3$, 500 MHz): δ 7.4–7.2 (m, 5H, Ar*H*), δ 5.19 (m, 2H, PhCH_2O), δ 5.19 (m, 1H, C*H*), δ 4.19 (m, 1H, C*H*), δ 3.22 (s, 1H, O*H*), δ 2.52 (m, 2H, CH_2), δ 1.50 (d, *J* = 7.1 Hz, 3H, CH_3), δ 1.24 (d, *J* = 6.4 Hz, 3H, CH_3). Anal. CHN Calcd: $C_{14}H_{18}O_5$: C, 63.2; H, 6.8; N, 0.0. Found: C, 62.1; H, 6.8; N, 0.0.

(*S*)-2-[(*R*)-3-(Hydroxybutoxy)]propanoic acid benzyl ester (7: (*R*)-3HB-(*S*)-2HP-Bn)

In the same way as (*R*)-3HB-(*R*)-2HP-Bn (**6**), (*R*)-3HB-(*S*)-2HP-Bn (**7**) was prepared from TBDPS-(*R*)-3HB-(*S*)-2HP-Bn (5). The product was a clear liquid (4.6 g, yield = 89 %). ^{1}H NMR ($CDCl_3$, 500 MHz): δ 7.5–7.2 (m, 5H, Ar*H*), δ 5.20 (m, 2H, PhCH_2O), δ 5.17 (m, 1H, C*H*), δ 4.26 (m, 1H, C*H*), δ 3.03 (s, 1H, O*H*), δ 2.54 (m, 2H, CH_2), δ 1.52 (d, *J* = 13.5 Hz, 3H, CH_3), δ 1.24 (d, *J* = 12.0 Hz, 3H, CH_3). Anal. CHN Calcd: $C_{14}H_{18}O_5$: C, 63.2; H, 6.8; N, 0.0. Found, C, 62.4; H, 6.8; N, 0.0.

(*R*)-2-[(*R*)-3-(Hydroxybutoxy)]propanoic acid (8: (*R*)-3HB-(*R*)-2HP)

The benzyl dimeric monomer (**6**) (266.0 mg, 10.0 mmol) were hydrogenated by flow reactor, using an EYELA CCR-1000G system with 10 % Pd on silica and an Air-tech NM-H-100. Hydrogen gas was used at a flow rate of 10.0 mL/min, ethanol was used as an eluent at a flow rate of 0.5 mL/min, and concentration of 0.1 M was applied. After reaction, the solvent was removed to give a colorless oil (1.75 g, yield = 99 %). ^{1}H NMR ($CDCl_3$, 500 MHz): δ 5.19 (m, 1H, C*H*), δ 4.27 (m, 1H, C*H*), δ 2.56 (m, 2H, CH_2), δ 1.56 (d, *J* = 7.0 Hz, 3H, CH_3), δ 1.28 (d, *J* = 6.5 Hz, 3H, CH_3). Anal. CHN Calcd: $C_7H_{12}O_5$: C, 47.7; H, 6.9; N, 0.0. Found: C, 45.5; H, 6.9; N, 0.0.

(*S*)-2-[(*R*)-3-(Hydroxybutoxy)]propanoic acid (9: (*R*)-3HB-(*S*)-2HP)

In the same way as (*R*)-3HB-(*R*)-2HP (**8**), (*R*)-3HB-(*S*)-2HP (**9**) was prepared from (*R*)-3HB-(*S*)-2HP-Bn (**7**). The product was colorless oil (2.29 g, yield = 100 %). ^{1}H NMR ($CDCl_3$, 500 MHz): δ 5.19 (m, 1H, C*H*), δ 4.28 (m, 1H, C*H*), δ 2.54 (m, 2H, CH_2), δ 1.52 (d, *J* = 7.5 Hz, 3H, CH_3), δ 1.24 (d, *J* = 4.0 Hz, 3H, CH_3). Anal. CHN Calcd: $C_7H_{12}O_5$: C, 47.7; H, 6.9; N, 0.0. Found: C, 46.8; H, 6.9; N, 0.0.

3-2-3 Condensation of dimeric monomers

(*R*)-3HB-2HP dimeric monomer (176.0 mg, 1.0 mmol) was added to 1 mL of DCM. DPTS (64.7 mg, 0.2 mmol) was added, and the reaction mixture cooled to 0 °C. Then, DIC (189.3 mg, 232 μL, 1.5 mmol) was added slowly for over 1 min. The reaction mixture was allowed to stir for 5 h at room temperature (25 °C). The urea was removed by filter, then taken up in DCM and precipitated in cool 2-propanol (IPA).

3-2-4 Analytical procedures

Gel-permeation chromatography, ^{1}H and ^{13}C NMR analyses, Differential scanning calorimetry (DSC), and Wide angle X-ray diffraction (WAXD) measurement

were carried out by the same way as described in article 2-2-4 in chapter 2.

High-resolution solid-state ^{13}C NMR measurements were carried out by using a Chemagnetics CMX Infinity 400 spectrometer in under a static magnetic field of 9.4 T. Both the ^{1}H and ^{13}C radio field strength $\gamma B1/2\pi$ were 52.0 kHz. The magic angle spinning (MAS) rate was set to 9.0 kHz to avoid the overlapping of spinning side bands on other resonance lines. The contact time for the cross- polarization (CP) process was 3.0 ms throughout this work. ^{13}C chemical shifts were expressed as values relative to tetramethylsilane (TMS) by using the CH_3 line at 17.36 ppm of hexamethylbenzene as an external reference.

Thermogravimetric (TG) analysis was performed on a Seiko instruments TG/DTA 220U using nitrogen as a purge gas. About 3.0 mg of each sample was heated from room temperature to +500 °C at 20 °C/min. T_{dmax} is the temperature corresponding to the inflection point of the thermodegradation curves that corresponds to the maximum reaction rate.

3-3 Results and discussion

3-3-1 Synthesis of alternating copolymers of P[(*R*)-3HB-*alt*-2HP]

The dimeric monomers of (*R*)-3HB and 2HP were synthesized by coupling reaction of benzyl lactate with silyl protected 3-hydroxybutanoic acid in the presence of DCC and DMAP, according to the method reported by Meyer et al.,[13] with modification of the conditions as necessary (see Scheme 3-1). Two types of stereoisomeric dimers ((*R*)-3HB-(*R*)-2HP and (*R*)-3HB-(*S*)-2HP) were obtained by selecting enantiomer of lactate monomer. By mixing the stereoisomers, the dimeric monomers with different stereocomposition were prepared.

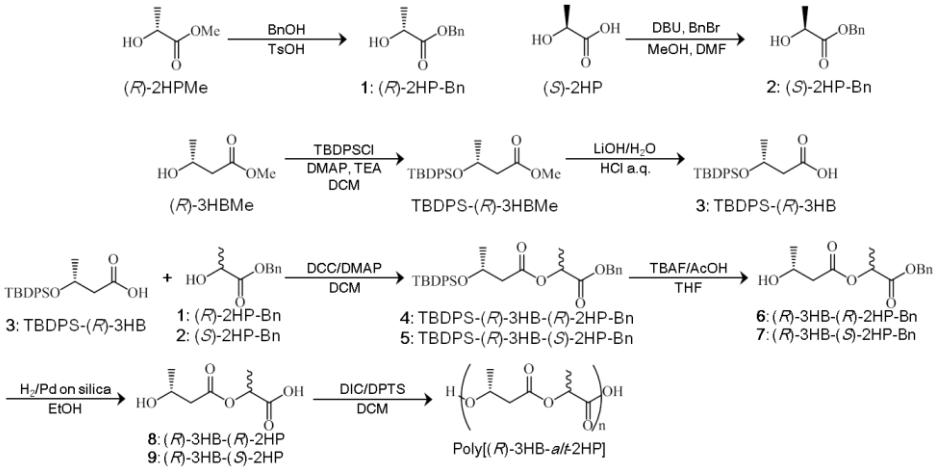

Scheme 3-1. Synthetic Procedures of Dimeric Monomers and Polymers with Alternating Sequence of (*R*)-3HB and 2HP Units

Polymerization of dimeric monomers was carried out by using condensation reaction in the presence of DIC/DPTS as a condensation agent.[15] As the condensation reaction progressed, solidified urea was generated in the reaction mixture. The polymer products were still soluble in methylene chloride after the removal of urea by filtration. The polymer solution was poured into cold 2-propanol to precipitate as a solid product. Table 3-1 lists the polymerization results of stereoisomeric (*R*)-3HB-2HP dimeric monomers. Polymer yields were varied from 37 to 78 %. Except for the product from (*R*)-3HB-(*R*)-2HP dimeric monomer, the obtained polymers were soluble in methylene chloride or chloroform. However, the polymer from (*R*)-3HB-(*R*)-2HP dimeric monomer became to be insoluble in methylene chloride or chloroform once it was solidified. The solidified polymer of (*R*)-3HB-(*R*)-2HP was dissolved in a mixture solution of chloroform with 7.5 % HFIP. The number-average molecular weights (M_n) and polydispersities (M_w/M_n) of the samples were determined from GPC analysis and ranged from 7,000 to 72,400 g/mol and from 1.3 to 2.0 by using a polystyrene calibration, respectively. For the polymer obtained from (*R*)-3HB-(*S*)-2HP dimeric monomer, the sample was subjected to GPC analysis without precipitation treatment in cool 2-propanol. Both the M_n and M_w/M_n values of crude sample were almost identical with those of purified sample by precipitation. This result indicates that the polymerization of (*R*)-3HB-(*S*)-2HP dimeric monomer facilely gives product with higher molecular weight than that of (*R*)-3HB-(*R*)-2HP dimeric monomer. The M_n values of samples tended to decrease with an increase of feed ratio of (*R*)-3HB-(*R*)-2HP dimeric monomer.

Table 3-1. Molecular weights of alternating copolymers of (*R*)-3HB and 2HP Units.

sample	dimeric monomer feed ratio (mol%)		dimeric monomer composition (mol%) [a]		Yield (%)	molecular weight ($\times 10^3$ g/mol) [b]	
	(*R*)-3HB-(*R*)-2HP	(*R*)-3HB-(*S*)-2HP	(*R*)-3HB-(*R*)-2HP	(*R*)-3HB-(*S*)-2HP		M_n	M_w/M_n
P[(*R*)-3HB-*alt*-(*S*)-2HP] (*R/S*=0/100)	0	100	0	100	41	72	1.5
P[(*R*)-3HB-*alt*-(*R,S*)-2HP] (*R/S*=33/67)	33	67	37	63	42	54	1.3
P[(*R*)-3HB-*alt*-(*R,S*)-2HP] (*R/S*=50/50)	50	50	54	46	37	46	1.5
P[(*R*)-3HB-*alt*-(*R,S*)-2HP] (*R/S*=67/33)	67	33	64	36	78	32	1.8
P[(*R*)-3HB-*alt*-(*R,S*)-2HP] (*R/S*=75/25)	75	25	72	28	57	20	1.7
P[(*R*)-3HB-*alt*-(*R*)-2HP] (*R/S*=100/0)	100	0	100	0	77	7	2.0

[a] Determined from ^{1}H NMR spectra. [b] Determined by GPC measurements.

Sequence structure of the obtained copolymers was examined by ^{1}H and ^{13}C NMR analyses. Figures 3-1 and 3-2 show ^{1}H and ^{13}C NMR spectra of the polymers obtained from (*R*)-3HB-2HP dimeric monomers, respectively. As previously reported,[32] the majority of both proton and carbon resonances for the random copolymers of (*R*)-3HB and (*S*)-2HP units were split into multiple peaks due to diad or triad sequences of (*R*)-3HB and (*S*)-2HP units (see Figures 3-3 and 3-4). On the other hand, the polymers obtained from (*R*)-3HB-(*S*)-2HP dimeric monomers in this paper exhibited the simple signals in each resonance. This result indicates that the polymers have an alternating sequence of (*R*)-3HB and 2HP units. Here, it is of important to note that the chemical shifts of signals arising from the identical functional group were different between the polymers obtained from (*R*)-3HB-(*R*)-2HP and (*R*)-3HB-(*S*)-2HP dimeric monomers. Especially, significant differences in the chemical shifts were detected at the signals from methyl group of 2HP units in proton resonance and signals from methylene group of (*R*)-3HB units in carbon resonance, and the gaps between chemical shifts of two stereoisomeric polymers were 0.04 ppm in proton resonance of methyl group of 2HP units and 0.25 ppm in carbon resonance of methylene group of (*R*)-3HB units, respectively. In the NMR spectra for the polymers obtained from a mixture of (*R*)-3HB-(*R*)-2HP and (*R*)-3HB-(*S*)-2HP dimeric monomers, the characteristic signals from both stereoisomers were detected. From the peak intensities of the signals, it was confirmed that the stereoisomeric compositions of the obtained polymers were in good agreement with the dimeric monomer feed ratios. The signals from methylene group of (*R*)-3HB units in carbon resonance were split into totally four peaks, and it was attributed to the difference in stereosequence of 2HP units adjoining both sides of (*R*)-3HB unit.

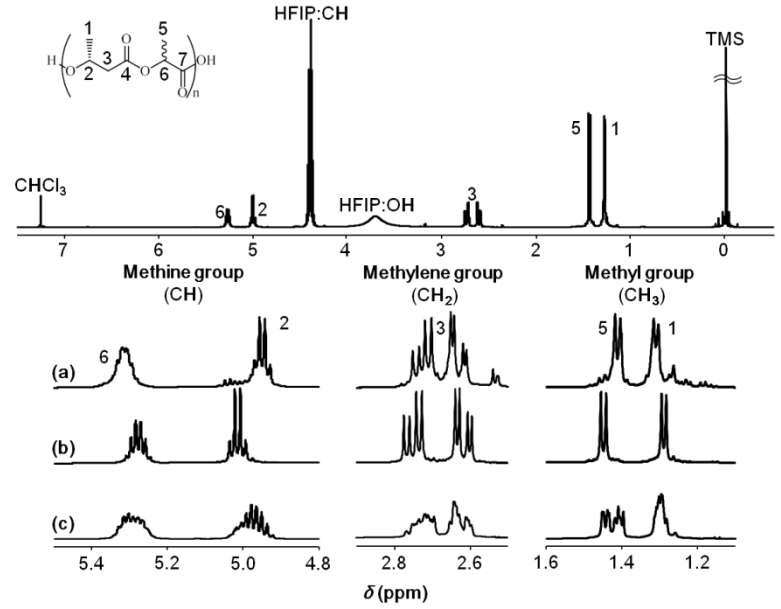

Figure 3-1. 500 MHz ^{1}H NMR spectra of P[(*R*)-3HB-*alt*-2HP] alternating copolymer in $CDCl_3$ containing 7.5 % HFIP at 25 °C. Key: (a) P[(*R*)-3HB-*alt*-(*R*)-2HP], (b) P[(*R*)-3HB-*alt*-(*S*)-2HP], and (c) P[(*R*)-3HB-*alt*-(*R*,*S*)-2HP] (*R*/*S*=50/50).

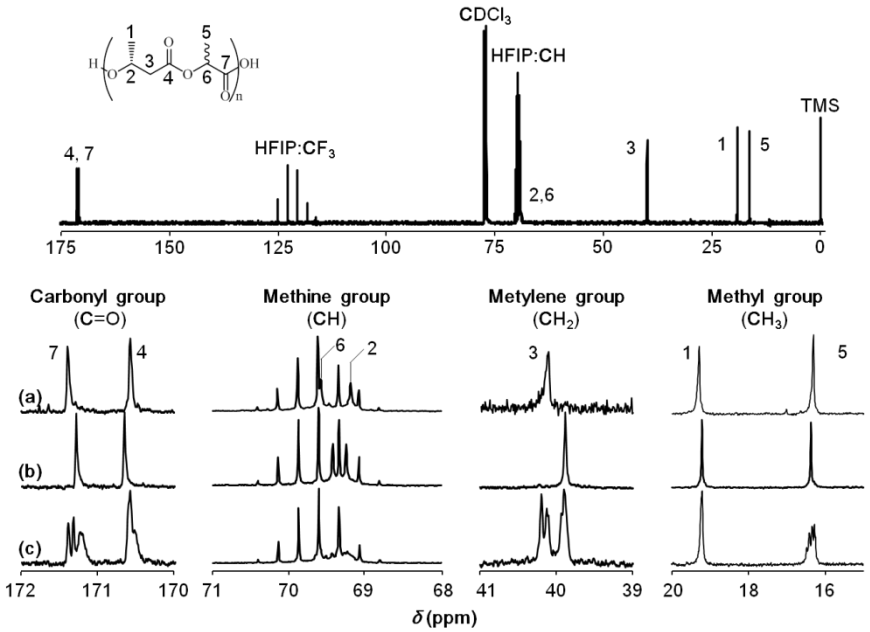

Figure 3-2. 125 MHz ^{13}C NMR spectra of P[(*R*)-3HB-*alt*-2HP] alternating copolymer in $CDCl_3$ containing 7.5 % HFIP at 25 °C. Key: (a) P[(*R*)-3HB-*alt*-(*R*)-2HP], (b) P[(*R*)-3HB-*alt*-(*S*)-2HP], and (c) P[(*R*)-3HB-*alt*-(*R*,*S*)-2HP] (*R*/*S*=50/50).

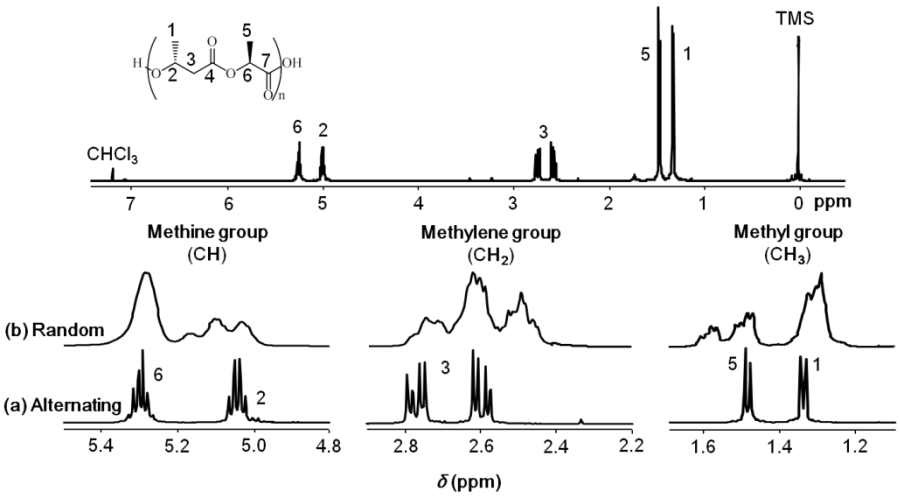

Figure 3-3. 500 MHz ^{1}H NMR spectra of P[(*R*)-3HB-*alt*-(*S*)-2HP] alternating copolymer (a) and P[(*R*)-3HB-*co*-47 mol%(*S*)-2HP] random copolymer (b) in $CDCl_3$ at 25 °C.

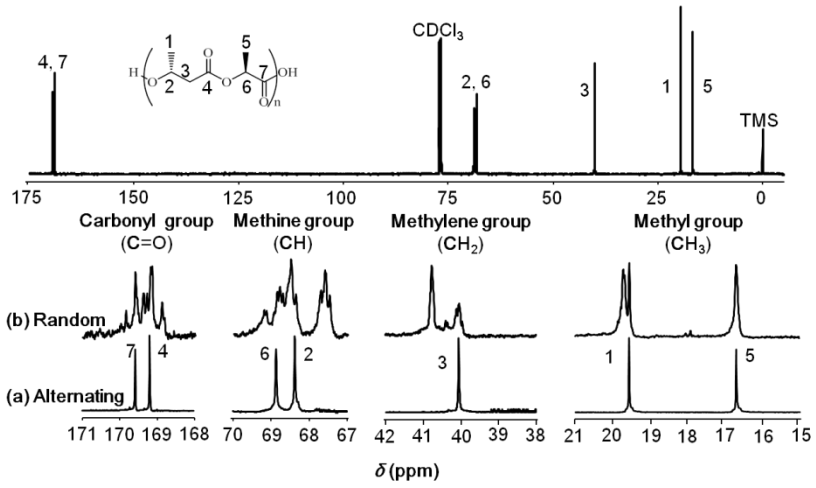

Figure 3-4. 125 MHz ^{13}C NMR spectra of P[(*R*)-3HB-*alt*-(*S*)-2HP] alternating copolymer (a) and P[(*R*)-3HB-*co*-47 mol%(*S*)-2HP] random copolymer (b) in $CDCl_3$ at 25 °C.

Table 3-2. Chemical shifts of alternating copolymers of (*R*)-3HB and 2HP units.

species	solution NMR in $CDCl_3$ counting 7.5 % HFIP				solid-state ^{13}C NMR	
	P[(*R*)-3HB-*alt*-(*R*)-2HP] (*R/S*=100/0)	P[(*R*)-3HB-*alt*-(*S*)-2HP] (*R/S*= 0/100)	P[(*R*)-3HB-*alt*-(*R*)-2HP] (*R/S*= 100/0)	P[(*R*)-3HB-*alt*-(*S*)-2HP] (*R/S*= 0/100)	P[(*R*)-3HB-*alt*-(*R*)-2HP] (*R/S*= 100/0)	P[(*R*)-3HB-*alt*-(*S*)-2HP] (*R/S*= 0/100)
CH_3 (1)	1.31	1.29 (1.33)[a]	16.32	16.38 (16.74)	16.7	15.8
CH_3 (5)	1.41	1.45 (1.46)	19.30	19.22 (19.61)	20.5	20.5
CH_2 (3)	2.64 2.70	2.63 (2.60) 2.74 (2.75)	40.15	39.90 (40.10)	38.6	41.4
CH (2)	4.95	5.02 (5.05)	69.20	69.25 (68.42)	69.9	69.1
CH (6)	5.32	5.28 (5.30)	69.59	69.43 (68.91)		70.8
CO (4)			170.59	170.68 (169.24)	171.5	169.5
CO (7)			171.41	171.31 (169.63)		

[a] The chemical shifts in parentheses were obtained in $CDCl_3$ at 25 °C.

3-3-2 Thermal properties of alternating copolymers of P[(*R*)-3HB-*alt*-2HP]

Thermal properties of alternating copolymers of (*R*)-3HB and 2HP units were determined by DSC. Figure 3-5 shows typical DSC thermograms of P[(*R*)-3HB-*alt*-2HP] samples. All of the copolymers with alternating sequence structure showed melting behavior during the first heating scan. The values of melting temperatures (T_m) and heat of fusion (ΔH_m) are summarized in Table 3-3. The T_m value of P[(*R*)-3HB-*alt*-(*S*)-2HP] was detected at 83 °C. On the other hand, the P[(*R*)-3HB-*alt*-(*R*)-2HP] had the T_m at 233 °C, and the value was much higher than those of homopolymers of (*R*)-3HB and 2HP and was comparable to those of poly(glycolate) and stereocomplex poly(lactate). It was found that the random copolymers of (*R*)-3HB and 2HP units with almost equimolar composition were completely amorphous. Therefore, the precise regulation of sequential structure as alternating manner brought about the crystallization of copolymer chains. For the samples prepared from a mixture of (*R*)-3HB-(*R*)-2HP and (*R*)-3HB-(*S*)-2HP dimeric monomers, the T_m values increased linearly from 53 to 174 °C as the (*R*)-3HB-(*R*)-2HP dimeric monomer feed ratio was increased from 33 to 75 mol% (see Figure 3-6A). The ΔH_m values also increased with an increase in the (*R*)-3HB-(*R*)-2HP dimeric monomer feed ratio (Figure 3-6B). These results indicate that the incorporation of stereoisomeric dimer inhibits the formation of crystalline state composed of the repeating sequences of the other stereoisomeric dimers. Thus, by selecting the combinations of the enantiomeric 3HB and 2HP monomers, the melting temperatures of the copolymers with alternating sequence structure varied in the wide range.

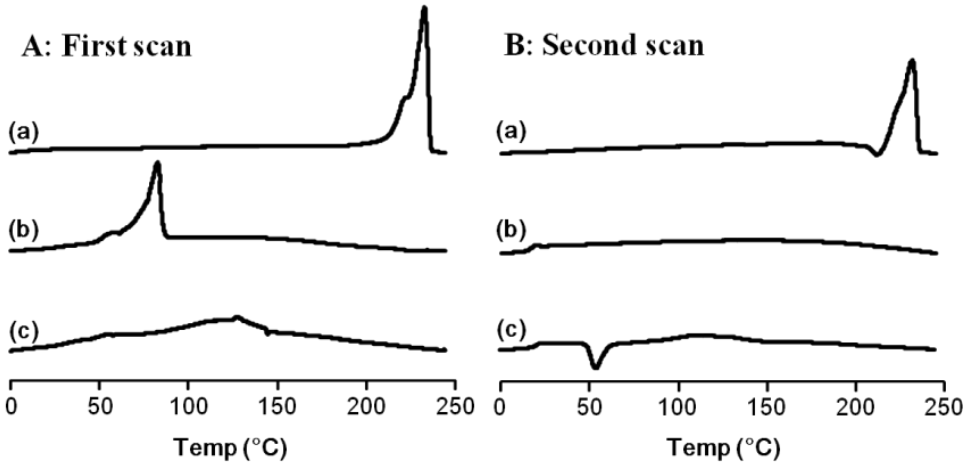

Figure 3-5. DSC thermograms of alternating copolymer samples at a heating rate of 20 °C: (A) first heating scans and (B) second heating scans after rapid quenching from the melt at 250 °C. Key: (**a**) P[(*R*)-3HB-*alt*-(*R*)-2HP], (**b**) P[(*R*)-3HB-*alt*-(*S*)-2HP], and (**c**) P[(*R*)-3HB-*alt*-(*R*,*S*)-2HP] (*R*/*S*=50/50).

Table 3-3 Thermal properties and X-ray crystallinities of alternating copolymer samples.

sample	thermal properties				crystallinity, X_c[e] (%)
	T_g[a] (°C)	T_m[b] (°C)	ΔH_m[c] (J/g)	T_{dmax}[d] (°C)	
P[(*R*)-3HB-*alt*-(*S*)-2HP] (*R*/*S*=0/100)	18	84	41	300	57 ± 5
P[(*R*)-3HB-*alt*-(*R*,*S*)-2HP] (*R*/*S*=33/67)	14	53	2	296	7 ± 5
P[(*R*)-3HB-*alt*-(*R*,*S*)-2HP] (*R*/*S*=50/50)	19	126	14	298	24 ± 5
P[(*R*)-3HB-*alt*-(*R*,*S*)-2HP] (*R*/*S*=67/33)	21	151	42	299	37 ± 5
P[(*R*)-3HB-*alt*-(*R*,*S*)-2HP] (*R*/*S*=75/25)	n.d.[f]	174	78	301	48 ± 5
P[(*R*)-3HB-*alt*-(*R*)-2HP] (*R*/*S*=100/0)	n.d.	233	116	304	78 ± 5
P[(*R*)-3HB-*co*-47mol%(*R*)-2HP]	15	n.d.	0	300	n.m.[g]
P[(*R*)-3HB]	4	176	96	299	74 ± 5
P[(*S*)-2HP]	60	176	43	378	47 ± 5

[a] Glass-transition temperature; measured by DSC (second scan) from 100 to +250 °C at a rate of 20 °C /min. [b] Melting temperature; measured by DSC (first scan) from 0 to +250 °C at a rate of 20 °C /min. [c] Enthalpy of fusion; measured by DSC (first scan). [d] Thermal degradation; measured by TG analysis from 25 to +500 °C at a rate of 20 °C/min. [e] Degree of crystallinity; determined from X-ray diffraction patterns. [f] Not detected. [g] Not measured.

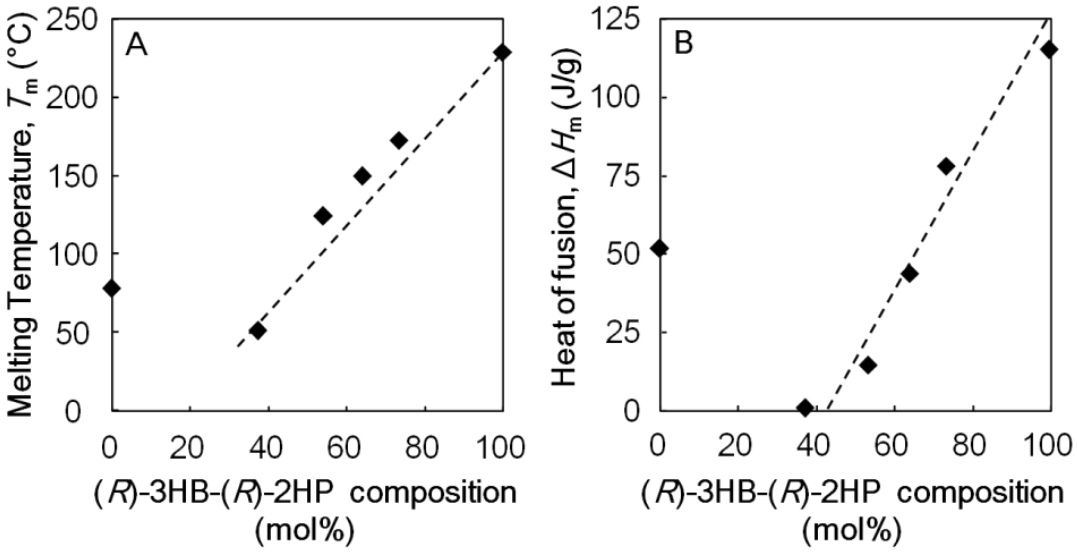

Figure 3-6. Effect of stereocomposition of dimeric monomer on the melting temperature (A) and the heat of fusion (B) of alternating copolymer samples.

For the samples with (*R*)-3HB-(*R*)-2HP dimeric monomer contents less than 67 mol%, the change in heat capacity corresponding to the glass transition phenomenon could be detected in the DSC endotherms of second heating scan. The T_g values of copolymers were in the range from 14 to 21 °C. However, the T_g could not be detected in the DSC thermograms for the samples with (*R*)-3HB-(*R*)-2HP dimeric monomer contents over than 75 mol%, since the crystallization took place during the cooling process from the melt state at 250 °C.

As well as the random copolymers of (*R*)-3HB and 2HP units mentioned above, the most of copolymers with a random sequence of almost equimolar two monomeric units become to be amorphous. However, the polymer obtained from the equimolar mixture of (*R*)-3HB-(*R*)-2HP and (*R*)-3HB-(*S*)-2HP dimeric monomers formed crystalline state and showed relative high melting temperature. As shown in Figure 3-2, in the ^{13}C NMR spectrum for the polymer obtained from the equimolar mixture of (*R*)-3HB-(*R*)-2HP and (*R*)-3HB-(*S*)-2HP dimeric monomers, the methylene carbon signals of (*R*)-3HB units were split into four peaks corresponding to the different stereo-sequence of 2HP units adjoining both sides of (*R*)-3HB unit. Since the peak intensities of each sequence were not equivalent, the obtained polymer rather had blocking tendency repeating the identical stereoisomeric dimers than random sequence. Taking account of the difference in solubility of precipitated polymers in methylene chloride, it was expected that the dispersibility of resultant oligomers in the reaction mixture changed during the polymerization dependent on both the degree of condensation and the sequence of stereoisomeric dimers. As a result, the sequential distribution of the polymers from a mixture of (*R*)-3HB-(*R*)-2HP and (*R*)-3HB-(*S*)-2HP dimeric monomers was inclined to have blocking tendency.

The thermal degradation profiles of alternating copolymers of P[(*R*)-3HB-*alt*-2HP] were examined by TG analysis. The temperatures of maximum degradation rate (T_{dmax}) were in the range from 296 to 304 °C for the alternating copolymers of P[(*R*)-3HB-*alt*-2HP]. It is well-known that the degradation of P[(*R*)-3HB] occurs exclusively via random chain scission reaction (*cis*-elimination), which has a six-membered ring ester intermediate.[17] On the other hand, the dominant thermal decomposition of PLLA (P[(*S*)-2HP]) progresses via cyclic rupture of polymer molecules by unzipping reaction from the hydroxyl chain-end or/and random intramolecular transesterification at the main-chain.[18] The T_{dmax} values of the alternating copolymers of P[(*R*)-3HB-*alt*-2HP] were very close to that of P[(*R*)-3HB] (299 °C), rather than P[(*S*)-2HP] (374 °C). Therefore, it was expected that the chain

scission by *cis*-elimination occurred at the (*R*)-3HB units in the alternating copolymers molecules during thermal degradation.

3-3-3 Crystal structure of alternating copolymers of P[(*R*)-3HB-*alt*-2HP]

Figure 3-7 shows the X-ray diffraction patterns of alternating copolymer samples, together with those of P[(*R*)-3HB] and P[(*S*)-2HP]. The diffraction patterns of P[(*R*)-3HB] and P[(*S*)-2HP] showed typical reflections arising from the α-forms of the P[(*R*)-3HB] and P[(*S*)-2HP] crystalline lattice, respectively. The alternating copolymer samples revealed different patterns from neither P[(*R*)-3HB] nor P[(*S*)-2HP]. In addition, the diffraction patterns were quite different between the two types of copolymers composed of (*R*)-3HB-(*R*)-2HP and (*R*)-3HB-(*S*)-2HP dimeric monomers (see the calculated *d*-spacing values listed in Table 3-4). Since the crystalline structure of these alternating copolymers have not been characterized, further investigation on the relationship between the thermal properties and crystalline structure of these samples is necessary. However, it is concluded that both the (*R*)-3HB and 2HP units participate into the formation of crystalline region by repeating the alternating sequence. The degrees of X-ray crystallinity (X_c) of alternating copolymers samples are also listed in Table 3-2. The X_c values of P[(*R*)-3HB-*alt*-2HP] samples decreased from 78 to 7 % as the fraction of (*R*)-3HB-(*S*)-2HP dimeric monomers was increased from 0 to 67 mol%. The X_c value of P[(*R*)-3HB-*alt*-(*S*)-2HP] sample was 73 %.

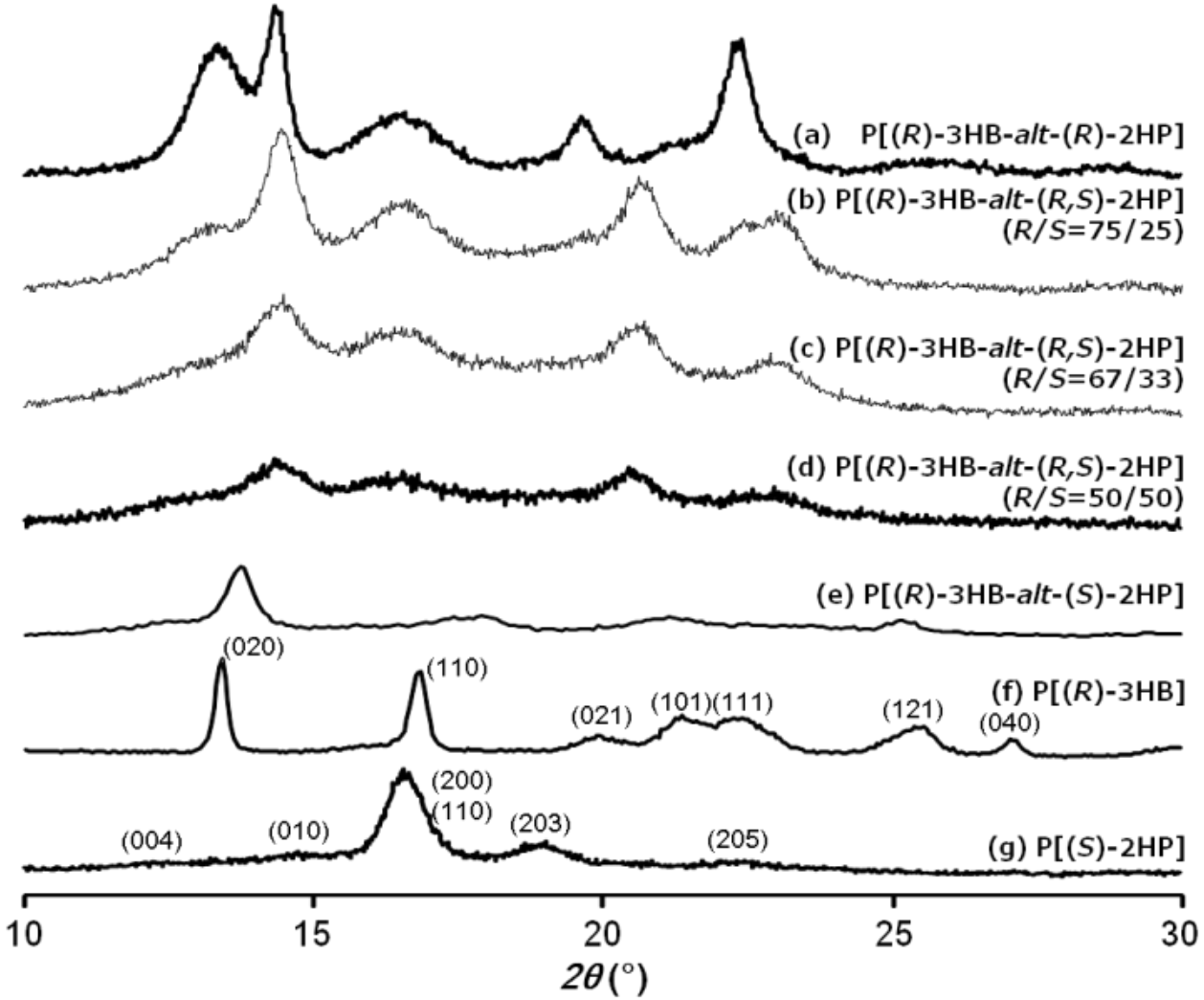

Figure 3-7. Wide-angle X-ray diffraction patterns of alternating copolymers.

Table 3-4. Interplannar *d*-spacing values measured from X-ray diffraction patterns of copolymer samples.

P[3HB-*alt*-(*R*)-2HP] (*R*/*S*=100/0)		P[3HB-*alt*-(*R*,*S*)-2HP] (*R*/*S*=75/25)		P[3HB-*alt*-(*R*,*S*)-2HP] (*R*/*S*=67/33)		P[3HB-*alt*-(*R*,*S*)-2HP] (*R*/*S*=50/50)		P[3HB-*alt*-(*S*)-2HP] (*R*/*S*=0/100)		P[(*R*)-3HB]		P[(*S*)-2HP]	
d-spacing (nm)	intensity	*d*-spacing (nm)	intensity	*d*-spacing (nm)	intensity	*d*-spacing (nm)	intensity	*d*-spacing (nm)	intensity	*d*-spacing (nm)	intensity	*d*-spacing (nm)	intensity
												0.709	w
								0.703	w				
0.665	s	0.669	m	0.681	w	0.681	w						
										0.662	s		
								0.645	s				
0.617	s	0.613	s	0.611	m	0.615	m						
												0.603	w
								0.558	w				
0.536	m	0.534	m	0.537	m	0.544	w						
												0.533	s
										0.528	s		
								0.498	w				
												0.469	m
										0.444	w		
0.451	m	0.451	w	0.451	w	0.451	w						
		0.428	m	0.429	m	0.431	m						
								0.419	w				
0.417	s												
										0.417	m		
										0.397	m		
												0.397	w
0.397	s	0.396	m	0.392	w	0.388	w						
		0.383	m	0.385	m	0.385	w						
								0.354	w				
										0.351	m		
0.344	w	0.340	w										
										0.329	m		
0.309	w	0.307	w	0.307	w	0.311	w						
								0.303	w				
										0.300	w		

Figure 3-8 shows high-resolution solid-state CP/MAS ^{13}C NMR spectra of P[(*R*)-3HB-*alt*-(*R*)-2HP] and P[(*R*)-3HB-*alt*-(*S*)-2HP]. In both of the P[(*R*)-3HB-*alt*-(*R*)-2HP] and P[(*R*)-3HB-*alt*-(*S*)-2HP], the carbonyl signals from (*R*)-3HB and 2HP units were overlapped, and the single peak was detected. The chemical shifts of carbonyl resonances were differed P[(*R*)-3HB-*alt*-(*R*)-2HP] and P[(*R*)-3HB-*alt*-(*S*)-2HP] samples. The carbonyl signal of P[(*R*)-3HB-*alt*-(*R*)-2HP] was shifted around 2 ppm toward lower magnetic field, compared with that of P[(*R*)-3HB-*alt*-(*S*)-2HP]. The peak of methylene group of (*R*)-3HB units also appeared at different chemical shifts between the P[(*R*)-3HB-*alt*-(*R*)-2HP] and P[(*R*)-3HB-*alt*-(*S*)-2HP]. In contrast to the carbonyl groups, the chemical shifts of methylene group were shifted 3 ppm toward higher magnetic field as changing from connecting with (*R*)-2HP to with (*S*)-2HP units. The differences in chemical shifts of resonance from the identical functional groups were also detected in the ^{13}C NMR spectra of solution dependent on configuration of 2HP units (see Figure 3-8), however, the gaps in the chemical shifts in the solution state were quite smaller than those in the solid-state. This result suggests that the differences in the chemical shifts in the solid-state CP/MAS ^{13}C NMR spectra are predominantly attributed to the conformational structure of monomeric units in the crystalline states.

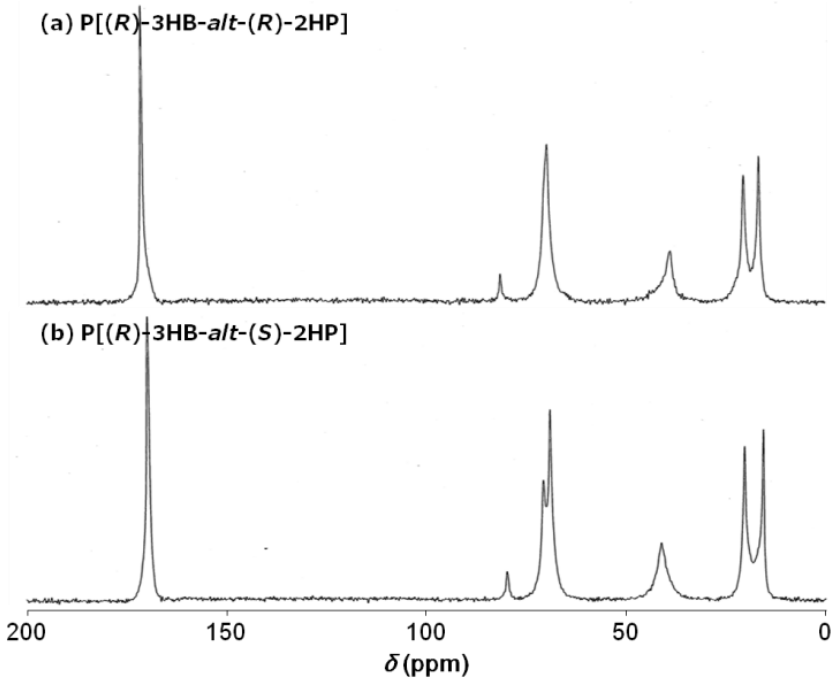

Figure 3-8. Cross-polarization magic-angle spinning ^{13}C NMR spectra of alternating copolymers of P[(*R*)-3HB-*alt*-(*R*)-2HP] (**a**) and P[(*R*)-3HB-*alt*-(*S*)-2HP] (**b**).

3-4 Conclusions

Novel alternating copolymers of (*R*)-3HB and 2HP units were synthesized by condensation reaction of stereoisomeric dimers of (*R*)-3HB-(*R*)-2HP and (*R*)-3HB-(*S*)-2HP. The effects of enantiomeric structure of 2HP units and stereocomposition of dimeric monomers on the thermal properties and crystalline structure of alternating copolymers were investigated. Precisely regulated alternating sequence of (*R*)-3HB and 2HP units were crystallizable, and the formed crystals had different structure from both P[(*R*)-3HB] and P[(*S*)-2HP] crystals. The melting of the crystalline region for alternating copolymers varied in the wide range of temperatures depending on both the enantiomeric structure of 2HP units and stereocomposition of dimeric monomers. In particular, the melting temperature of P[(*R*)-3HB-*alt*-(*R*)-2HP] was reached to 233 °C, and the copolymers was one of the aliphatic polyesters with highest melting temperature.

References

[1] (a) Doi, Y. *Microbial Polyesters;* VCH Publishers: New York, 1990. (b) Sudesh, K.; Abe, H.; Doi, Y. *Prog. Polym. Sci.* **2000**, *25*, 1503–1555. (c) Lenz, R. W.; Marchessault, R. H. *Biomacromolecules* **2005**, *6*, 1–8. (d) Chen, G-Q. *Chem. Soc. Rev.* **2009**, *38*, 2434–2446.

[2] (a) Kulkarni, R. K.; Moore, E. G.; Hegyeli, A. F.; Leonard, F. *J. Biomed. Mater. Res.* **1971**, *5*, 169–181. (b) Kricheldorf, H. R.; Berl, M.; Scharnagl, N. *Macromolecules* **1988**, *21*, 286–293. (c) Dubois, P.; Jacobs, C.; Jerome, R.; Teyssie, P. *Macromolecules* **1991**, 24, 2266–2270. (d) Auras, R.; Harte, B.; Selke, S. *Macromol. Biosci.* **2004**, *4*, 835–864.

[3] (a) Findlay, R. H.; White, D. C. *Appl. Environ. Microbiol.* **1983**, *45*, 71–78. (b) Doi, Y.; Kunioka, M.; Nakamura, Y.; Soga, K. *Macromolecules* **1986**, *19*, 2860–2864. (c) Nakamura, S.; Doi, Y.; Scandola, M. *Macromolecules* **1992**, *25*, 4237–4241. (d) Saito, Y.; Doi, Y. *Int. J Biol. Macromol.* **1994**, *16*, 99–104. (e) Doi, Y.; Abe, C. *Macromolecules* **1990**, *23*, 3705–3707. (f) Doi, Y.; Kitamura, S.; Abe, H. *Macromolecules* **1995**, *28*, 4822–4828. (g) Taguchi, S.; Yamada, M.; Matsumoto, K.; Tajima, K.; Satoh, Y.; Munekata, M.; Ohno, K.; Kohda, K.; Shimamura, T.; Kambe, H.; Obata, S. *Proc. Natl. Acad. Sci. U.S.A.* **2008**, 105, 17323–17327. (h) Shozui, F.; Matsumoto, K.; Motohashi, R.; Sun, J.; Satoh, T.; Kakuchi, T.; Taguchi, S. *Polym. Degrad. Stab.* **2011**, *96*, 499–504. (i) Sodergarda, A.; Stolt, M. *Prog. Polym. Sci.* **2002**, *27*, 1123–1163. (j) Abe, H.; Doi, Y.; Hori, Y.; Hagiwara, T. *Polymer* **1997**, *39*, 59–67.

[4] (a) Ikada, Y.; Jamshidi, K.; H. Tsuji, K; Hyon, S. H. *Macromolecules* **1987**, 20, 904. (b) Tsuji, H. *Macromol. Biosci.* **2005**, 5, 569.

[5] Tsuji, H. *in Biopolymers. Vol. 4. Polyesters III: Applications and Commercial Products,* ed.; Doi, Y. and Steinbuchel, A. Eds.; VCH, Weinheim, 2002; 129.

[6] (a) Ueda, M. *Prog. Polym. Sci.* **1999**, *24*, 699–730. (b) Badi, N.; Lutz, J. F. *Chem. Soc. Rev.* **2009**, *38*, 3383–3390. (c) Thomas, C. M. *Chem. Soc. Rev.* **2010**, *39*, 165–172. (d) Ouchi, M.; Badi, N.; Lutz, J. F.; Sawamoto, M. *Nat. Chem.* **2011**, *3*, 917–924.

[7] (a) Wu, T. K. *J. Phys. Chem.* **1969**, *73*, 1801–1805. (b) Bluhm, T. L.; Hamer, G. K.; Marchessault, R. H.; Fyfe, C. A.; Vergin, R. P. *Macromolecules* **1986**, *19*, 2871–2876.

[8] (a) Lenz, R. W.; Go, S. *J. Polym. Sci. Polym. Chem. Ed.* **1974**, *12*, 1–10. (b)Fernández, J; Meaurio, E; Chaos, A; Etxeberria, A.; Alonso-Varona, A.; Sarasua, J. R. *Polymer* **2013**, *54*, 2621–2631.

[9] (a) Hirooka, M.; Yabuuchi, H.; Iseki, J.; Nakai, Y. *J. Polym. Sci., Part A-1* **1968**, *6*, 1381–1396. (b) Shirota, Y.; Yoshimura, M.; Matsumoto, A.; Mikawa, H. *Macromolecules* **1974**, 7, 4.

[10] Tabata, Y.; Abe, H.; *Polym. Degrad. Stab.* **2013**, *98*, 1796–1803.

[11] Sworen, J. C.; Smith J. A.; Berg. J. M.; Wagener, K. B. *J. Am. Chem. Soc.* **2004**, *126*, 11238–11246.

[12] (a) Satoh, K.; Matsuda, M.; Nagai, K.; Kamigaito, M. *J. Am. Chem. Soc.* **2010**, *132*, 10003–10005. (b) Satoh, K.; Ozawa, S.; Mizutani, M.; Nagai, K.; Kamigaito, M. *Nat. Commun.* **2010**, *1*, 1–6. (c) Matsuda, M.; Satoh, K.; Kamigaito, M. *J. Polym. Sci. Part A. Polym. Chem.* **2013**, *51*, 1774–1785.

[13] (a) Stayshich, R.; Meyer, T. *J. Polym. Sci., Part A: Polym. Chem.* **2008**, *46*, 4704–4711. (b) Stayshich, R.; Meyer, T. *J. Am. Chem. Soc.* **2010**, *132*, 10920–10934. (c) Li, J.; Stayshich, R.; Meyer, T. *J. Am. Chem. Soc.* **2011**, *133*, 6910–6913.

[14] Kramer, J. W.; Treitler, D. S.; Dunn, E. W.; Castro, P. M.; Roisnel, T.; Thomas, C. H.; Coates, G. W. *J. Am. Chem. Soc.* **2009**, *131*, 16042–16044.

[15] Moore, J. S.; Stupp, S. I. *Macromolecules* **1990**, *23*, 65–70.

[16] Wolfe, S.; Wilson, M. C.; Cheng, M. H.; Chustov, G.V.; Akuche, C. I. *Can. J. Chem.* **2003**, *81*, 937–961.

[17] Aoyagi, Y.; Yamashita, K.; Doi, Y. *Polym. Degrad. Stab.* **2002**, *76*, 53–59.

[18] Kopinke, F. D.; Remmler, M.; Mackenzie, K.; Moder, M.; Wachsen, O. *Polym. Degrad. Stab.* **1996**, *53*, 329–342.

Chapter 4

Crystal structure of alternating copolymer of 3-hydorxybutyrate and lactate units

4-1 Introduction

In the former chapter, novel aliphatic copolyesters with defined alternating sequence composed of *α*- and β-hydroxyalkanoates as lactate (2-hydroxypropionate; 2HP) and (*R*)-3-hydroxybutyrate ((*R*)-3HB) units were synthesized by condensation reaction of dimeric monomers using polycondensation agent. Then, sequential structure and physical properties were investigated. Precisely regulated alternating sequence of (*R*)-3HB and (*R*)-2HP units were crystallizable, and the formed crystals had different structure from both P[(*R*)-3HB] and P[(*R*)-2HP] crystals. The melting temperature of P[(*R*)-3HB-*alt*-(*R*)-2HP] copolymer was detected at 233 °C, which was higher than those of homopolymers (about 180 °C).

Study on the relationships between structure and physical properties can lead to the design and synthesis of a great variety of polymers with superior properties to fulfill the demand in practical applications. Especially, investigation on crystal structure and their structural changes during thermal and mechanical treatment provide the fundamental understandings of chain mobility, directly relating to the performances of polymer materials. Thus, many types of poly(hydroxyalkanoates) (PHAs) have been studied on solid-state structure and physical properties. Among, the PHAs, the polyesters of consisting of *α*- and *β*-hydroxyalkanoates were extensively investigated on their crystal and molecular structures by X-ray diffraction of oriented films and electron diffraction of solution-grown single crystals.

The crystal structure of *α*-hydroxyalkanoates such as poly(glycolate) (PGA) and poly(lactate) (PLA) exhibits several types of crystalline structure. The crystal structure of PGA were determined by Chatani et al., and two molecular chains pass thorough the orthorhombic unit cell of dimensions a = 0.522 nm, b = 0.619 nm, and c (chain axis) = 0.702 nm. The planar zigzag chain molecules form a sheet structure parallel to the ac plane and do not have the polyethylene type arrangement. High density of the crystalline, 1.69 g/cm^3, namely the tight molecular packing and the close approach of the ester groups might stabilize the crystal lattice and contributions to the high melting temperature of this polymer. [1] On the other hands, three different

crystalline structure (α, β, and γ) of PLA have been identified upon changing the preparation condition. The α form is believed to grow upon melt or cold crystallization and has a 10_3 helical chain conformation.[2] The β form is prepared at a high draw ration and high drawing temperature and is known to take a handed 3_1 helical conformations.[3] The γ form is produced thorough epitaxial crystallization was described by Cartier et al.[4] For example, the α-form of PLA has a pseudo-orthorhombic unit cell. The unit cell has the following dimensional paramerters: a = 1.070 nm, b = 0.595 nm, c = 2.780 nm. The density of PLA crystalline is 1.29 g/cm^3. In addition, the stereocomplex PLA (Sc-PLA) is found to possess a racemic crystalline structure, where PDLA and PLLA chains are packed side by side with a D monomer unit to L monomer unit ration of 1:1.[5] The Sc-PLA crystal forms a triclinic system (P_1) with the following cell dimensions: a = 0.916 nm, b = 0.916 nm, c (fiber axis) = 0.870 nm, $\alpha = 109.2°$, $\beta = 109.2°$, and $\gamma = 109.8°$. PLLA and PDLA segments, each with a 3_1-helic conformation, are packed laterally in a parallel fashion as a pair in a unit cell.[6] This PLA stereocomplex shows a strikingly high melting temperature at 230 °C, which is 50 °C higher than that of the homocrystal, and the density is 1.27 g/cm^3.

The crystal structure of β-hydroxyalkanoate such as P[(*R*)-3HB] has been also investigated. In general, the P[(*R*)-3HB] is crystallized in an orthorhombic unit cell with a 2_1 helical conformation. However, the P[(*R*)-3HB] with highly oriented films and fibers indicated two types of molecular conformation: the 2_1 helix conformation (α-form) and the planar zigzag conformation (β-form).[7] The unit cell of α-form is orthorhombic with dimensions, a = 0.576 nm, b = 1.320 nm, c (fiber axis) = 0.596 nm. Two anti-parallel chains are paled in a unit cell, and the molecule has a left handed 2_1-helix conformation. On the other hand, the β-form of P[(*R*)-3HB] was first suggested by Yokouchi et al. from the X-ray diffraction measurement of a further drawn, uniaxially stretched P[(*R*)-3HB] film. The X-ray diffraction pattern of the sample revealed a sharp reflection on the equator and streaks on the layer lines. This suggested formation of a twisted planar zigzag conformation with a fiber period of 0.460 nm. Finally, the crystallographic parameter of PHA crystals was listed in Table 4-1.[8]

Table 4-1. Crystallographic parameter of PHA crystals, adapted from Tsuji.[9]

polymer			conformation	unit-cell dimensions(nm)			density
				a	*b*	*c*	(g/cm^3)
α-PHA	PGA		planar zigzag	0.522	0.619	0.702	1.69
	PLA	α	10_3 helix	1.070	0.595	2.780	1.29
		β	3_1 helix	1.031	1.821	0.900	1.20
		γ	3_1 helix	0.995	0.625	0.880	
	Sc-PLA		3_1 helix	0.916	0.916	0.870	1.27
β-PHA	P[(*R*)-3HB]	α	2_1 helix	0.576	1.320	0.596	1.26
		β	planar zigzag			0.460	

The sequentical control and selectivity stereosequence of alternating copolymers hides the possibility of causing polymers with superior properties and novel crystalline structure. Although, the crystal structure that is the high order structure of polymer changes by sequential structure, the relationship between sequential structure and crystal structure has not become clear. To clear relationship between physical properties and sequential structure, understanding of crystalline structure is indispensable.

In this chapter, the crystal structure of P[(*R*)-3HB-*alt*-(*R*)-2HP] alternating copolymer were investigated by means of wide angle X-ray diffraction (WAXD), and transmission electron microscopy (TEM) using solution grown single crystal. Furthermore, from the results of electron diffraction and X-ray diffraction, the lattice parameters and molecular packing arrangement with unit cell and density of alternating copolymer was determined. The relationships among the crystal structure and molecular structure were discussed.

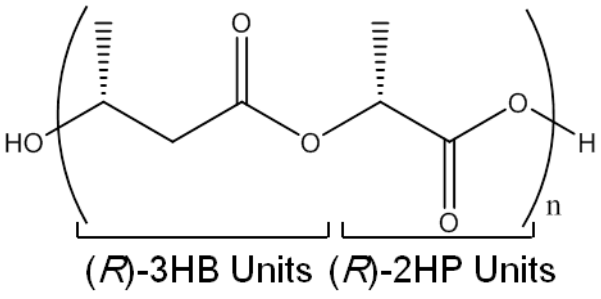

Figure 4-1. Chemical structure of alternating copolymer of (*R*)-3HB and (*R*)-2HP units (P[(*R*)-3HB-*alt*-(*R*)-2HP]).

4-2 Experimental section

4-2-1 Materials

P[(*R*)-3HB-*alt*-(*R*)-2HP] copolymer sample was employed for the structure analysis of the single crystal. The molecular weight and properties were listed in Table 3-1 and 3-2 in chapter 3.

4-2-2 Preparation of single crystals

P[(*R*)-3HB-*alt*-(*R*)-2HP] copolymer single crystals have been prepared from many kind of solvents, MeOH/HFIP, EtOH/HFIP, and Chroloform/HFIP. In addition, temperature and time were examined at a wide range of 50 to 130 °C and 3 to 168 h, respectively. The number of samples was above a hundred. The most suitable condition was described below. A 2 mg of P[(*R*)-3HB-*alt*-(*R*)-2HP] sample was dissolved in to 10 mL of mixing solution of HFIP and MeOH (HFIP : MeOH = 60:40) at 129 °C and maintained at this temperature for 30 min. The slow cooling was then applied until the crystallization temperature, 99 °C and the solution was kept there for 12 h. Then, the solution was cooled slowly room temperature. The slow cooling process was performed by cutting off heating element of a silicone oil bath. The single crystal of this method was used in analyzed crystalline structure.

4-2-3 Analytical procedures

Wide angle X-ray diffraction (WAXD) measurement were carried out by the same way as described in article 2-2-4 in chapter 2. Oriented single crystal mats suitable for X-ray diffraction were prepared by sucking the crystal suspension through a 0.2 μm P(Tetrafluoroethylene) filter. Oriented crystal mat was recorded in a flat plate camera on Fuji imaging plates, using Nickel-filtered CuKα radiation (λ = 0.15418 nm; 40 kV; 100 mA) with CaF_2 powder. The X-ray beam was directed perpendicular to the oriented direction for oriented crystal mats. All measurements were carried out in ambient conditions at room temperature.

Morphology and lamellar thickness of obtained single crystal was observed by atomic force microscopy (AFM). AFM observations were performed with an SPA400/SPI3800N ((Seiko Instruments Inc.) operating in a dynamic force microscope (DFM) mode. A 20 μm scanner (maximum scan range: ca.24 μm) and rectangular silicon cantilever (Si-DF20, Seiko instruments Inc.; 200 μm in length, resonant frequency of ca. 134 kHz, stiffness of ca. 16 N/m) was applied in all experiments. All measurements were carried out in ambient conditions at room temperature. The resulting images were flattened and plane-fit using Seiko Instruments software.

Drops of the crystal suspension were deposited on carbon-coated grids and dried under vacuum. The grids were observed with a JEM-2100F/SP (JEOL) electron microscope operated at an acceleration voltage 200 kV for both electron diffraction and imaging of crystals. The electron diffraction patterns were recorded with a charge-coupled-decide (CCD) camera. The resulting diffractions were analyzed by Rigaku Display software.

4-3 Results and discussion

4-3-1 X-ray diffraction

The powder sample of P[(*R*)-3HB-*alt*-(*R*)-2HP] copolymer was prepared by reprecipitation. The melt-crystallized sample of P[(*R*)-3HB-*alt*-(*R*)-2HP] copolymer was isothermally crystallized at 210 °C after melt at 250 °C. Figure 4-2 shows the WAXD patterns of powder and melt-crystallized samples of alternating copolymer of P[(*R*)-3HB-*alt*-(*R*)-2HP]. The diffraction pattern contains 16 independent diffraction peaks, and the diffraction peaks of melt-crystallized sample were sharper than powder sample. In addition, the crystallinity was increased from 78 to 82 % by thermal treatment. Table 4-1 lists the *d*-spacing values of determined from diffraction data of samples.

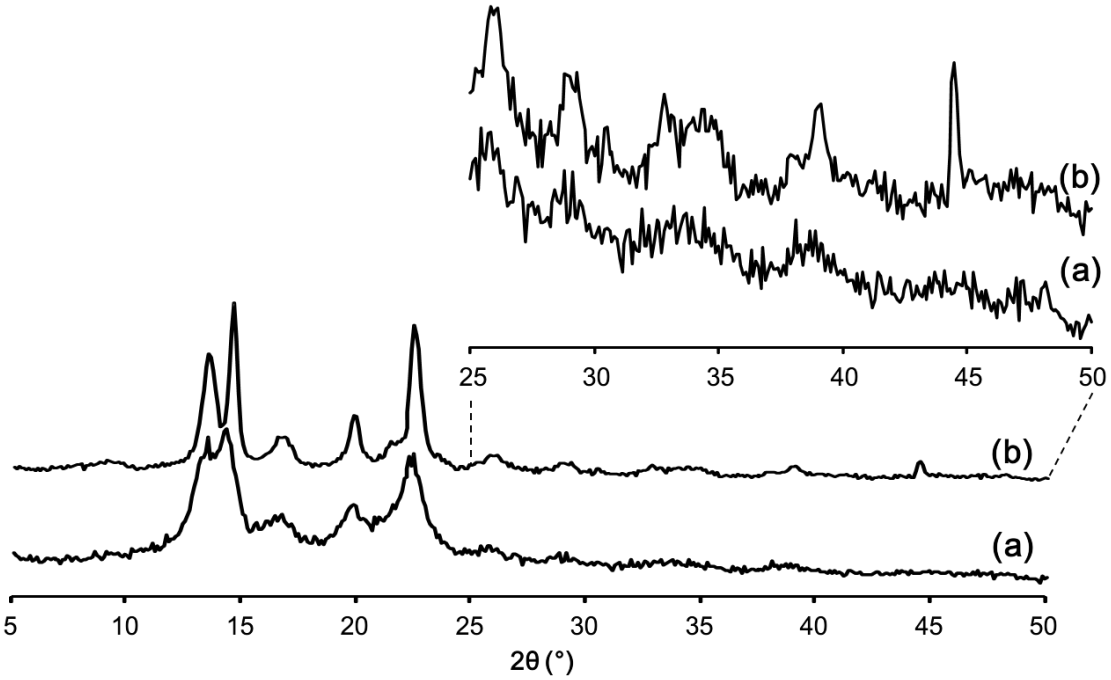

Figure 4-2. Wide angle X-ray diffractions of P[(*R*)-3HB-*alt*-(*R*)-2HP] copolymer. Key: (a) powder sample. (b) melt-crystallized sample.

Table 4-1. *d*-Spacings of P[(*R*)-3HB-*alt*-(*R*)-2HP] copolymer prepared by different condition.

powder	melt-crystallized
d-spacing (nm)	*d*-spacing (nm)
	0.946
0.665	0.652
0.617	0.607
0.536	0.529
0.451	0.448
0.417	0.413
0.397	0.394
	0.355
0.344	0.343
0.309	0.307
	0.293
0.273	0.272
0.262	0.260
	0.237
0.232	0.230
0.206	0.203

4-3-2 Morphology of single crystal

The single crystal of P[(*R*)-3HB-*alt*-(*R*)-2HP] copolymer was prepared from dilute solution of powder sample in a mixture of HFIP and methanol. The lamellar single crystals were deposited on silicon substrates, and the crystalline morphology was characterized by using AFM. The crystals revealed rhombus-shaped morphology. The rhombus-shaped crystals with dimensions of approximately 2 and 4 μm along the short and long axes, respectively, were observed for each sample, and the thickness of an individual single-crystal ranged from 5 to 7.0 nm as shown in Figure 4-3.

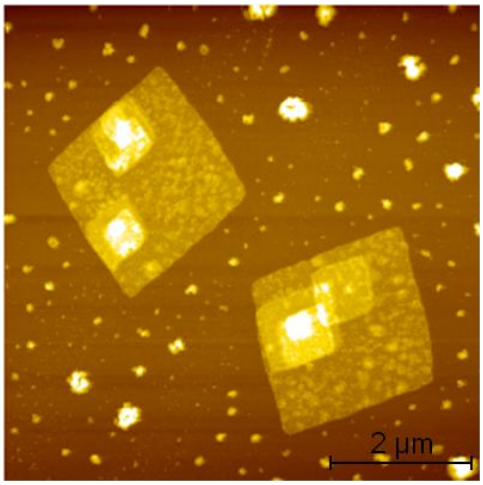

Figure 4-3. AFM image of P[(*R*)-3HB-*alt*-(*R*)-2HP] copolymer single crystals.

4-3-3 Unit cell determination

Figure 4-4 shows the electron micrograph and selected-area electron diffraction patterns of the obtained P[(*R*)-3HB-*alt*-(*R*)-2HP] copolymer solution-grown lamellar single crystals prepared from mixing solution of HFIP and MeOH. For the electron diffraction patterns in Figures 4-4 B and C, it is apparent that all the diffraction spots corresponding to equatorial *hk0* reflections, implying a flat-on structure of the crystal with the molecular chains oriented parallel to the lamellar thickness direction. The electron diffraction diagram contains 48 independent diffraction spots mirrored in the four quadrants, defined by the orthogonal axes a^* and b^*. On calibration of the electron diffraction spots, all of the reflections are accounted by the rectangular reciprocal lattice with the parameters: $a^* = 2.100$ nm^{-1}, $b^* = 1.133$ nm^{-1}, and $\gamma = 90°$. Table 4-2 lists the measured and calculated electron diffraction *d*-spacings for P[(*R*)-3HB-*alt*-(*R*)-2HP] copolymer.

Although electron diffraction spots of the orthorhombic crystal lattice shows strong intensity at long *d*-spacing (e. g. 110 or 1-10), the electron diffraction spots of P[(*R*)-3HB-*alt*-(*R*)-2HP] copolymer revealed the strongest spots at short *d*-spacing of 060 or 0-60. This result suggests that the fiber direction of P[(*R*)-3HB-*alt*-(*R*)-2HP] alternating copolymer in crystal state is slightly tilted against the lamellar thickness direction.

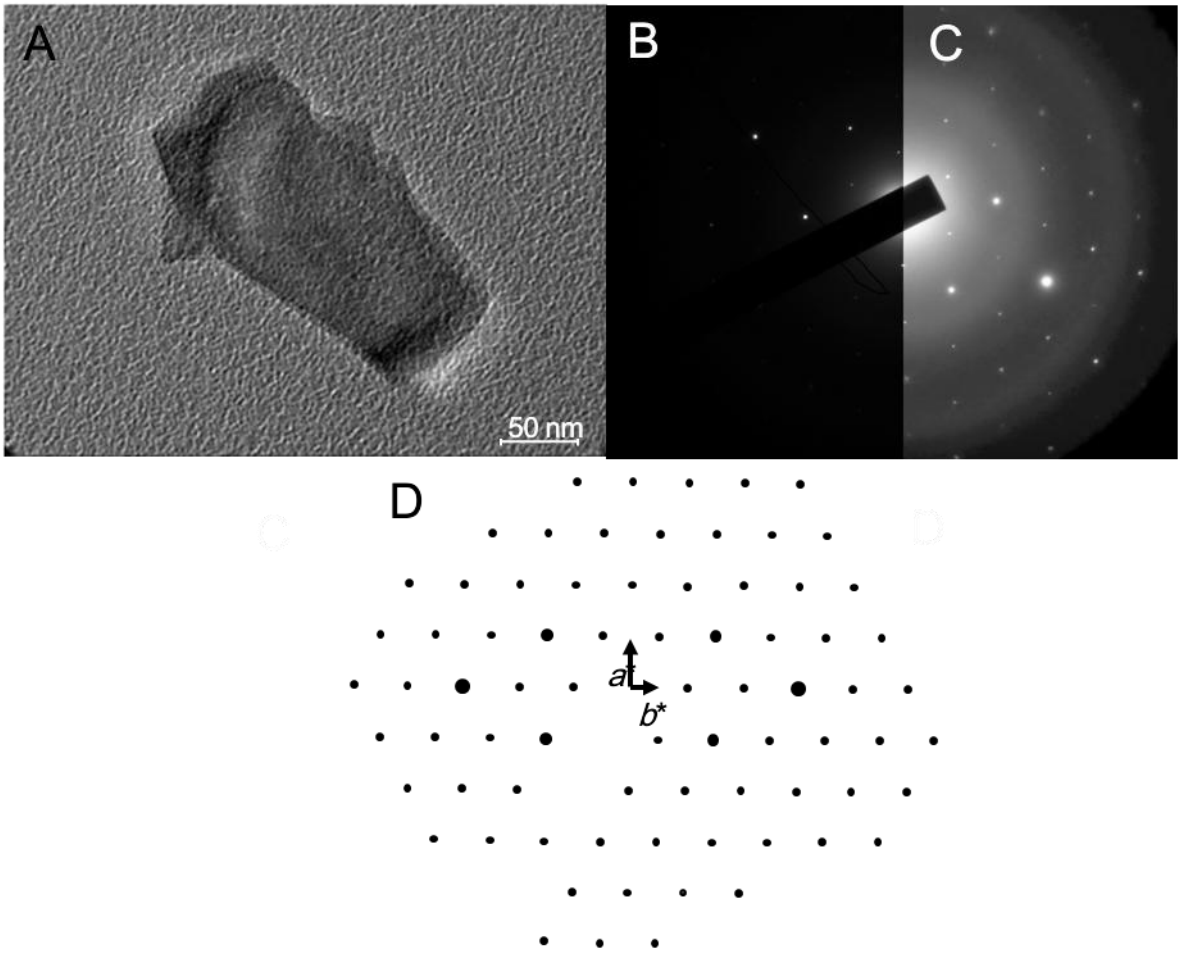

Figure 4-4. Electron micrograph of single crystal of P[(*R*)-3HB-*alt*-(*R*)-2HP] copolymer. Electron diffraction diagram: (B) underexposed, showing the strong diffraction spots; (C) overexposed, showing the weak diffraction spots; (D) summary of the observed diffraction spots with their relative intensities.

Table 4-2. Crystallographic data of P[(*R*)-3HB-*alt*-(*R*)-2HP] copolymer deduced from electron diffraction diagram of single crystal.

index [a]	d_{obs}	d_{calc}
020	0.440	0.442
110	0.423	0.419
130	0.249	0.250
200	0.241	0.238
040	0.221	0.221
220	0.211	0.210
150	0.166	0.166
240	0.162	0.162
310	0.157	0.156
060	0.147	0.147
330	0.141	0.140
260	0.126	0.125
170	0.122	0.122
350	0.119	0.118
400	0.119	0.119
420	0.116	0.115
080	0.110	0.110
440	0.106	0.105
280	0.101	0.100
370	0.099	0.099
190	0.096	0.096
510	0.096	0.095
460	0.094	0.093
390	0.085	0.083

[a]Indexed in terms of an orthorhombic unit cell with reciprocal lattice parameters $a^* = 2.100\ nm^{-1}$, $b^* = 1.133\ nm^{-1}$, and $\gamma = 90°$.

Figure 4-5 shows the WAXD patterns obtained from different directions of single crystal mats (*c* axis and *a*, *b*-plane) and non-oriented sample, and the main observed reflections are summarized in Table 4-3. In stacked for *c* axis of single crystal mats shows 00l reflections, but stacked for *a*, *b*-plane of that not showed. On the other hands, non-oriented sample shows diffraction ring of both *c* axis and *a*, *b* axes of single crystal mat.

From the diffraction data, all reflections were assigned, and lattice parameters were estimated. At first, applying the orthorhombic, unit cell the lattice parameters were estimated as a = 0.476 nm, b = 0.883 nm, c = 1.588 nm, and β = 90°. However, the *d*-spacing data between the calculated and observed values were not in good agreement, and the value of residual sum of squares (RSS) was 0.307.

In addition, several refractions could not be assigned by the in the electron diffraction section. As maintained, it is expected that the fiber axis be tilted against the lamellar thickness direction. Therefore, it is speculated that the monoclinic unit cell can be applied for the alternating copolymer. When the monoclinic unit cell unit applied, the lattice parameters were estimated as a = 0.645 nm, b = 0.896 nm, c = 1.727 nm, and β = 49°. The *d*-spacing data were in good agreement, and the value of RSS is 0.041. However, the characteristic reflection with *d*-spacing of 0.517 nm could not be explained by the given mirror index according to the proposed unit cell system. Then, taking account of the indexing for the characteristic reflection, the lattice parameters were estimated as a = 0.933 nm, b = 0.904 nm, c = 2.138 nm, and β = 82 °. The *d*-spacing data were more in good agreement, and value of RSS is reached to 0.037. The slight differences between the values of *a*, *b* axes obtained from the electron and X-ray diffractions may be ascribed to the crystal systems, orthorhombic or monoclinic.

Table 4-3. Crystallographic data of P[(*R*)-3HB-*alt*-(*R*)-2HP] alternating copolymer deduced from X-ray diffraction patterns.

	stacked				orthorhombic		monoclinic			
	single crystal mat			*a* (nm)	0.476		0.645		0.933	
				b (nm)	0.883		0.896		0.904	
melt-crystallized				*c* (nm)	1.313		1.727		2.138	
sample	*c*-axis	*a*, *b*-axes		*α* (°)	90		90		90	
(non-oriented)				*β* (°)	90		49		82	
				γ (°)	90		90		90	
	d_{obs} (nm)	d_{obs} (nm)			*hkl*	d_{calc} (nm)	*hkl*	d_{calc} (nm)	*hkl*	d_{calc} (nm)
0.652	0.652 w	0.660 w			011		002	0.656	-102	0.652
0.607	0.604 s	0.604 sv			012	0.590	101	0.606	-111	0.602
0.529	0.517 vs				003	0.529	012	0.530	004	0.529
0.448	0.441 vw	0.441 vw			020	0.442	020	0.448	020	0.452
0.413					110	0.419	110	0.430	211	0.414
0.394	0.389 s	0.387 s			102	0.408	114	0.389	-121	0.394
0.355					112	0.371	121	0.360	214	0.347
0.343	0.339 vw	0.343 vw			023	0.339	004	0.328	124	0.332
0.307							124	0.311	206	0.302
0.293	0.288 vw				122	0.300	214	0.301	216	0.286
0.272							212	0.287	126	0.275
0.260	0.262 vw	0.253 vw			123	0.276	224	0.260	-224	0.264
0.237					200	0.238	200	0.245	400	0.231
0.230	0.226 vw	0.227 vw			040	0.221	040	0.224	040	0.226
0.203					220	0.210	220	0.215	420	0.206

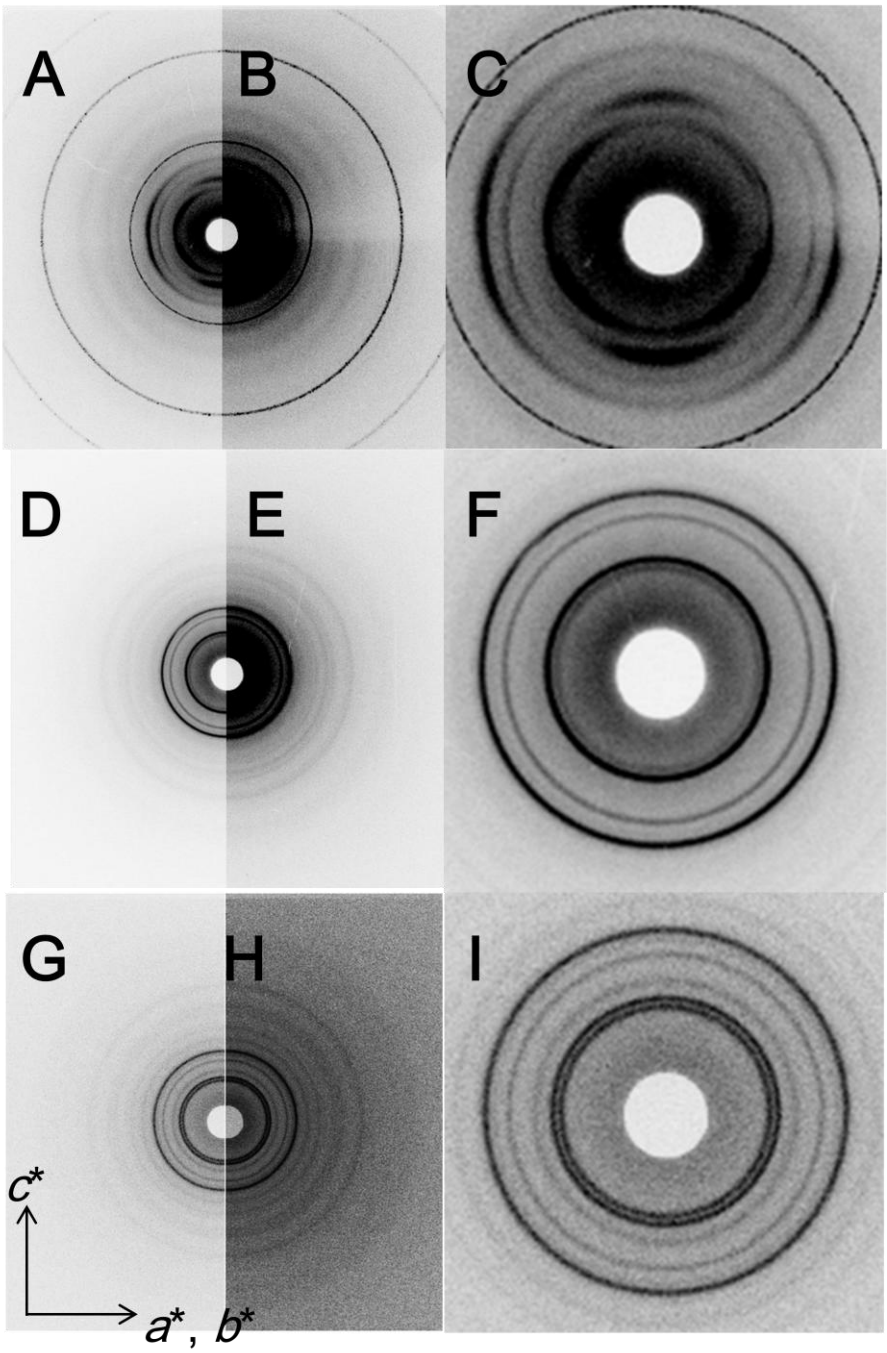

Figure 4-5. WAXD patterns of P[(*R*)-3HB-*alt*-(*R*)-2HP] copolymer. The oriented single crystal mats for *c* axis (A-C), the oriented single crystal mats for *a*,*b* axes (D-F), and non-oriented sample (G-I); underexposed showing the strong diffraction(A, D, G), overexposed showing the week diffraction(B, E, H), and magnified diagrams(C, F, I).

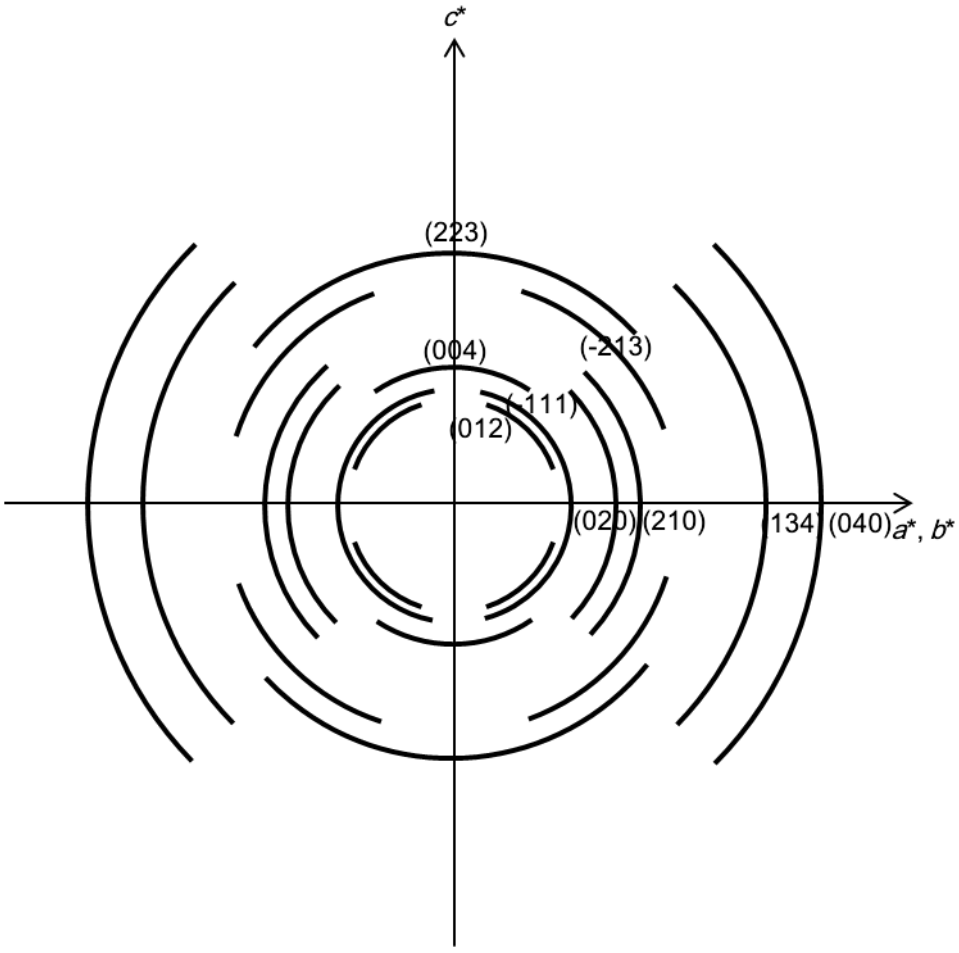

Figure 4-6. The schematic diagrams of WAXD patterns of the oriented single crystal mats for *c* axis.

4-3-2 Chain-Packing Analysis into Unit Cell

As shown in Figure 4-1, P[(*R*)-3HB-*alt*-(*R*)-2HP] alternating copolymer has the defined alternating sequence of 3HB and 2HP units. On the basis of the diffraction patterns and the unit cell parameters, the following possible model is proposed for the number of chain in unit cell (Figure 4-7). The solid-state CP/MAS ^{13}C NMR of P[(*R*)-3HB-*alt*-(*R*)-2HP] alternating copolymer was investigated in chapter 3. From the result of peak shifts, it was indicated that the (*R*)-3HB unit of P[(*R*)-3HB-*alt*-(*R*)-2HP] alternating copolymer was trans state. It was reported that conformation was gauche state in α-form of P[(*R*)-3HB], while was trans state in β-form of P[(*R*)-3HB].[6] It was suggested that the P[(*R*)-3HB-*alt*-(*R*)-2HP] alternating copolymer was containg helical form (*R*)-2HP and extended (*R*)-3HB units. The helical form (*R*)-2HP unit calculated by structure from 3_1 helix and *c* axis; 0.900 nm, that is about 0.300 nm. On the other hand, extended (*R*)-3HB units were reported, that

is about 0.460 nm. In total, chain length of (*R*)-3HB-(*R*)-2HP unit was calculated, that is about 0.760 nm. This value is corresponding to that one third of calculated c axis of 2.138 nm. In other words, *c*-axis was containing three units of 3HB-2HP unit.

In addition, a monomeric unit cell containing twelve 3HB-2HP units would give a predicted density of 1.77 g/cm^3. For instance, the density of α-hydroxyalkanoate such as PLA and *β*-hydroxyalkanoate such as P[(*R*)-3HB] were about 1.3 g/cm^3, which has melting point about 180 °C. On the other hands, the density of α-hydroxyalkanoate such as PGA was about 1.69 g/cm^3, which has melting temperature about 230 °C. ΔH_m^0 of PLA and P[(*R*)-3HB] were about 140 J/g, while ΔH_m^0 of PGA was 207 J/g. ΔH_m was increases with increase of density of polymer due to increase of intermolecular force.

In general, it was known that the melting temperature of polymer correlate closely with enthalpy. The free energy of fusion per a repeating unit of polymer, Δ*G*, is expressed by using the first law of thermodynamics:

$$\Delta G=\Delta H-T\Delta S$$

where ΔH is the enthalpy of fusion and Δ*S* is the entropy of fusion per repeating unit. The free energy is zero at the equilibrium temperature ($T = T_m^0$), the melting temperature (T_m^0) can be determined by the following relation between melting enthalpy (ΔH_m^0) and melt entropy (Δ*S*):

$$T_m^0 = \frac{\Delta H_m^0}{\Delta S}$$

The melting enthalpy ΔH_m^0 is an intermolecular force, which increase with hydrogen bonds, while the melting entropy Δ*S* decreases when main chains have symmetrical structures, are cross linked, or have higher rigidity. In other words, T_m was increases with increases of ΔH_m^0. In this case, P[(*R*)-3HB-*alt*-(*R*)-2HP] alternating copolymer has high melting temperature about 230 °C. In addition, density of alternating copolymer is 1.77 g/cm^3. It was suggest that intermolecular force of in each other chain was increased by alternating sequence of 3HB and 2HP units. As a result, it was caused high density and high melting temperature of P[(*R*)-3HB-*alt*-(*R*)-2HP] alternating copolymer.

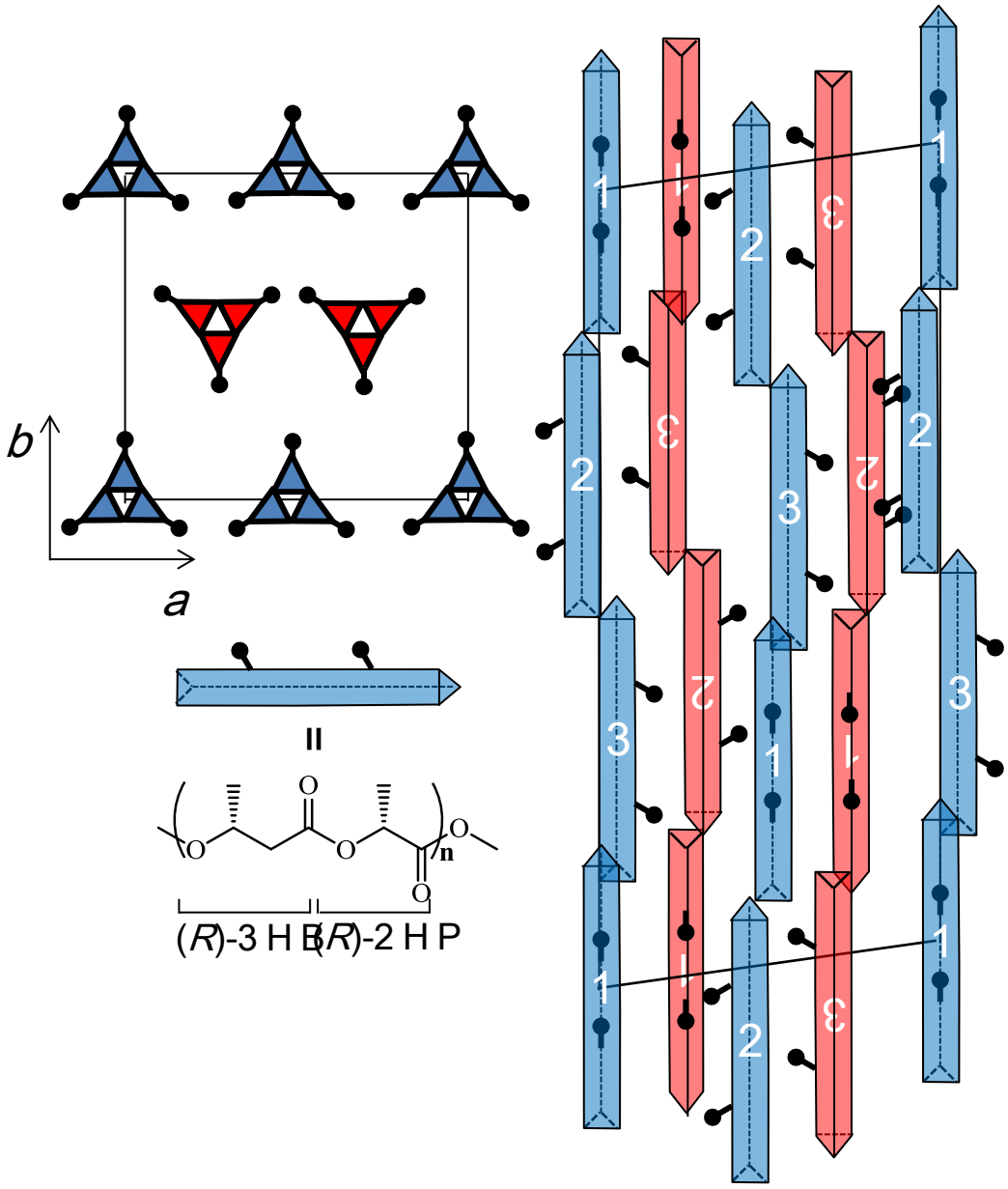

Figure 4-7. Schematic illustration of speculated cell structure for alternating copolymer crystal. (Blue chain is up chain. Red chain is down chain)

4-4 Conclusions

The single crystal and melt-crystallized sample of alternating copolymer of (*R*)-3HB and (*R*)-2HP units was successfully prepared, and the crystalline structure was investigated. The crystal structure of alternating copolymer of (*R*)-3HB and (*R*)-2HP units has been determined by the analysis of X-ray and electron diffraction patterns of single crystal specimens. The unit cell of alternating copolymer was determined as a monoclinic form with the lattice constants of a = 0.933 nm, b = 0.904 nm, c (chain axis) = 2.138 nm, and β = 82 °. The calculated density is 1.77 g/cm^3, which have comparable to PGA with high melting temperature. It was concluded that the density of alternating polymer was increased by sequential control of alternating, as a result, melting temperature of alternating polymer higher than homopolymer of 3HB and 2HP.

References

[1] (a) Fuller, C. S.; Erickson, C. L. *J. Am. Chem. Soc.* **1937**, 59, 344-351. (b) Hirono, H.; Wasai, G.; Saegusa, T.; Furukawa, J. *J. chem. Soc. Jan. Ind. Chem. Sect.* **1964**, 67, 604. (c) Chatani,Y.; Suehiro, K.; Okita, Y.; Tadokoro,; K. Chujo, H. *Dei Macro Chem* **1968**, 113, 215-229. (d) Singh, V.; Tiwari, M. *Int. J. Polym. Sci.* **2010**, 1-23.

[2] (a) De. Santis, P.; Kovacs, J. *Biopolymers* **1968**, 6, 299-306. (b) Hoogsteen, W.; Postema, A. R.; Pennings, A. J.; Ten Brinke, G. *Macromolecules* **1990**, 23, 634-642.

[3] (a) Eling, B.; Gogolewski, S.; Pennigs, A. J. *Polymer* **1982**, 23, 1587-1593. (b) Puiggali, J.; ikeda, Y.; Tsuji, H.; Puiggali, J.; Lotz, B. *Polymer* **2000**, 41, 8921-8930.

[4] (a) Carter, L.; Okihara, T.; Ikeda, Y.; Tsuji, H.; Puggali, J.; Lotz, B. *Polymer* **2000**, 41, 8909-8919.

[5] (a) Ikeda, Y.; Jamshidi, H.; Tsuji, H.; Hyon, S. H. *Macromolecules* **1987**, 20, 904-906. (b) Tsuji, H, in; Research Advances in Macromolecules, R. M. Mohan, Ed., Global Research Network, Trivandrum, India, Vol.1 **2000**, 25-48.

[6] (a) Okihara, T.; Tsuji, M.; kawahuchi, A.; Katayama, K.; Tsuji, H.; Hyon, S. H. *J. Macromol. Sci. phys.* **1991**, B30, 119-140. (b) Brizzolara, D.; Cantow, H. J.; Deiderichs, K.; Keller, E.; Domb, A. J. *Macromolecules*, **1996**, 29, 191-197. (c) Okihara, T.; Kawaguchi, A.; Tsuji, H.; Hyon, S. H. Ikeda, Y.; Katayama, K. *Bull. Inst. Chem. Res. Kyoto Univ.* **1988**, 66, 271. (d) Brizzolara, D.; Cantow, H.J.; Mulhaupt, R.; Domb, A. J. *J. Computer-Aided Mater. Design* **1996**. 3. 341-344.

[7] (a) Okihara, K.; Marchessault, R. H. "conformation of Bio-polymers", G. N. Ramachandran, Ed., Academic Press, New York Vol, 2. **1967**, 709-720. (b) Cornibert, J.; Marchessault, R. H. J. Mol. Biol. **1972**, 71, 735-756. (c) Yokouchi, M.; Chatani, Y.;

Tadokoro, H.; Teranishi, K.; Tani, H. Polymer 1973, 14, 267-272.

[8] (a) Iwata, T. *Macromol. Biosci.* **2005**, 5, 689-701. (b) Iwata, T.; Aoyagi, Y.; Fujita, M.; Yamane, H.; Doi, Y.; Suzuki, A. Takeuchi, A.; Uesugi, K. *Macromol. Rapid. Commun.* **2004**, 25, 1100-1104.

[9] (a) Tsuji, H. *Biopolymers, 4, Polyesters;* Doi Y. and Steinbüchel A., Eds.; WILLEY-VCH Verlag GmbH, Weinheilm, **2002**, p. 129-177. Auras, R.; Harte, B.; Selke, S. *Macromol. Biosci.* **2004**, 4, 835-864.

Chapter 5

Summary

In Chapter 1, the general introduction about the significance of bio-based polymer, aliphatic polyesters, polyhydroxyalkanoates (PHAs), and current polymerization techniques were described. From the viewpoint of environmental protection, bio-based polymers have attracted considerable attention. In addition, the two important classes, α- and β-hydroxyalkanoate in their polymers were taken, and the aim of this study, including methodology about the polymer design, was presented.

In chapter 2, copolymers of (*R*)-3HB and (*R*)-2HP units ([(*R*)-3HB-*co*-(*R*)-2HP]) were synthesized by polycondensation reaction from methyl esters of (*R*)-3HB and (*R*)-2HP in the presence of titanium-based catalyst. Mixing of two monomers from the beginning of polymerization yielded random copolymers of (*R*)-3HB and (*R*)-2HP units. On the other hand, by controlling the time of mixing of two monomers, copolymers with blocking tendency were obtained. According to the results of physical properties of copolymer samples, the relationship between the compositional and sequential structure and the physical properties of copolymers are discussed. The effects of copolymer composition and sequential structure on the thermal properties of P[(*R*)-3HB-*co*-(*R*)-2HP] copolymers were investigated. The obtained results indicate that the T_g of copolymers varies in accordance with the copolymer composition, while that the T_m is predominantly determined by the averaged sequential length of crystallizable monomer units. It means that we can produce the copolymers with various T_m values and a constant T_g value by varying the sequential length of monomers at the fixed copolymer composition. Unfortunately, since the synthesized copolymers had relatively low molecular weights, it is difficult to prepare films being subjected to biodegradation test. It has been demonstrated that the rate of biodegradation for PHA materials is strongly dependent both on the chemical structure of monomeric unit and on the solid-state structure of samples. In the aspect of the solid-state structure of PHA materials, the crystallinity and lamellar crystal sizes play a decisive role in degradation process. The lamellar thickness of P[(*R*)-3HB-*co*-(*R*)-2HP] copolymers is regulated by the averaged sequential length of

crystallizable monomer units, and the crystallinity is versatile with the combination of copolymer composition and averaged sequential length of monomers. Therefore, it is expectable that the biodegradation rate of P[(*R*)-3HB-*co*-(*R*)-2HP] copolymers is also controlled desirably by selecting the copolymer composition and averaged sequential length of monomers.

In chapter 3, novel alternating copolymers of (*R*)-3HB and 2HP units (P[(*R*)-3HB-*alt*-2HP]) were synthesized by the polycondensation reaction of pre-prepared dimeric monomers, (*R*)-3HB-(*R*)-2HP and (*R*)-3HB-(*S*)-2HP, in the presence of condensation agent. On the basis of the results of physical properties of alternating copolymer samples, the relationship between the stereocompositional and sequential structure and the properties of copolymers are discussed. The effects of enantiomeric structure of 2HP units and stereocomposition of dimeric monomers on the thermal properties and crystalline structure of alternating copolymers were investigated. In contrast to random copolymers of (*R*)-3HB and 2HP units, the repeating sequence of alternately connected (*R*)-3HB and 2HP units formed crystalline region. The crystalline structure and thermal properties was different from each other between the alternating copolymers obtained from two types of stereoisomeric macromonomers. The melting of the crystalline region for alternating copolymers varied in the wide range of temperatures depending on both the enantiomeric structure of 2HP units and stereocomposition of dimeric monomers. In particular, the melting temperature of P[(*R*)-3HB-*alt*-(*R*)-2HP] was reached to 233 °C, and the copolymers was one of the aliphatic polyesters with highest melting temperature.

In chapter 4, by means of transmission electron microscopy (TEM), single crystal for the alternating copolymer is resolved. The unit cell of P[(*R*)-3HB-*alt*-(*R*)-2HP] alternating copolymer was determined as a monoclinic form with the lattice constants of a = 0.933 nm, b = 0.904 nm, c (chain axis) = 2.138 nm, and β = 82 °. It was concluded that the density of P[(*R*)-3HB-*alt*-(*R*)-2HP] alternating polymer was increased by sequential control of alternating, as a result, melting temperature of P[(*R*)-3HB-*alt*-(*R*)-2HP] alternating polymer higher than homopolymer of 3HB and 2HP.

On the basis of the above results, it may be concluded that the thermal properties of polyesters can be improved by sequential structure and stereosequence, which can be lead to a variety of useful properties. This study would provide an alternative way for polyesters applications and industrial production, and a platform for material design.

List of publications for this thesis

(1) Y. Tabata, H. Abe

"Effects of composition and sequential structure on thermal properties for copolymer of 3-hydroxybutyrate and lactate units"

Polym. Degrad. Stab. **2013**, 98, 1796-1803. (Chapter 2)

(2) Y. Tabata, H. Abe

"Synthesis and properties of alternating copolymers of 3-Hydroxybutyrate and Lactate units with Different Stereocompositions"

Macromolecules **2014**, 47, 7354-7361. (Chapter 3)

(3) Y. Tabata, H. Abe.

"Crystal Structure of Alternating Copolymer of 3-Hydroxybutyrate and Lactate units"

(In preparation) (Chapter 4)

Acknowledgements

First of all, I would like to express sincerely thanks to the supervisors Professor Dr. Hideki Abe and Associate Professor Dr. Takeharu Tsuge, Department of Innovative and Engineered Materials, Interdisciplinary Graduate School of Science and Engineering, Tokyo Institute of Technology for their pertinent guidance, encouragement and valuable comments throughout this work.

I really appreciate to Professor Tomokazu Iyoda, Chemical Resources Laboratory, Professor Michikazu Hara, Department of Innovative and Engineered Materials, Interdisciplinary Graduate School of Science and Engineering, Tokyo Institute of Technology, and Professor Toshiaki Fukui, Depeartment of Biomolecular Engineering, Graduate School of Bioscience and Biotechnology, Tokyo Institute of Technology, for serving the dissertation committee.

I would like to thank to RIKEN Institute to provide the Riken “Junior research Associate” program for financial support during education period.

I especially would like to thank the entire Bio plastic research term, present and past members, I am thankful for all the help you have given to me. I wish the best of luck for all of you.

I should thank Mr. Kazunori Ushimaru, Student of Doctoral Program, Tokyo Institute of Technology. He provided me many events to enjoy my college life during five years. I am so lucky to have him as a dear friend.

Finally, I would like to thank my family for offering a lot of supports in many ways.

Yuta Tabata

March, 2015